

國立交通大學

電信工程研究所

博士論文

高效率之球型解碼演算法及其應用

Highly Efficient Sphere Decoding
Algorithm and Its Applications

研究生：黃崇榮

指導教授：李大嵩 博士

中華民國一百零二年九月

高效率之球型解碼演算法及其應用

Highly Efficient Sphere Decoding Algorithm and Its Applications

研究生：黃崇榮

Student: Chung-Jung Huang

指導教授：李大嵩 博士

Advisor: Dr. Ta-Sung Lee

國立交通大學

電信工程研究所

博士論文

A Dissertation

Submitted to Institute of Communication Engineering
College of Electrical and Computer Engineering
National Chiao Tung University
in Partial Fulfillment of the Requirements
for the Degree of Doctor of Philosophy
in
Communication Engineering

September 2013

Hsinchu, Taiwan, R.O.C.

中華民國一百零二年九月

高效率之球型解碼演算法及其應用

學生：黃崇榮

指導教授：李大嵩 博士

國立交通大學電信工程研究所

摘要

多輸入多輸出系統中，高效率且低功率消耗之接收機的設計為關鍵議題之一。在本論文中，吾人首先以 K -Best 解碼器為基礎，提出一個適用於大型積體電路架構的高性能球型解碼器。利用複數平面星座圖的規律特性來簡化路徑長度計算及排序，達到省卻大量資料排序動作及路徑值的運算需求，進而實現一個高效率且具有固定吞吐量的解碼器；更進一步針對傳統 K -Best 解碼性能的缺失，藉由所提出的一種新型搜尋策略可提供接近於最大似然搜尋之解碼性能。接著，吾人針對廣義之多天線之欠定系統，提出具有低解碼複雜度的解碼器。該解碼器包含了兩個步驟：1. 藉由所提出的高效率的平面候選點搜尋器將所有所需的候選點一一找出。2. 針對這些候選點集合進行平面交集的動作並配合動態半徑調整機制來快速地找出該問題的解。接著，一個可與所提出解碼器結合之通道矩陣行向量的排序策略亦被提出。進而提供低運算需求及近似最大似然搜尋的解碼性能。吾人亦針對排序策略所對應的運算降低率提出一套系統化的數學分析分法。最後，吾人針對上傳鏈結系統之多點協同傳輸系統中的碼簿搜尋問題，提出具有極低運算複雜度之演算法。首先，吾人根據矩陣運算理論，提出一個塊狀 QR 分解程序，能順利將原搜尋問題轉化成尋找最長路徑之命題。接著，運用所提出的修正 K -Best 解碼器便能以極低的運算量完成碼簿搜尋且仍保有極佳的系統性能。經由電腦模擬驗證本論文所提出的演算法及架構皆能提供優越的解碼性能及較低的運算需求，極適用於下世代之寬頻無線通訊系統。

Highly Efficient Sphere Decoding Algorithm and Its Applications

Student: Chung-Jung Huang

Advisor: Dr. Ta-Sung Lee

Institute of Communications Engineering
National Chiao Tung University

Abstract

In this dissertation, a low complexity near-ML K -Best sphere decoder is proposed as the first part. The development of the proposed K -Best sphere decoding algorithm (SDA) involves two stages. First, a new candidate sequence generator (CSG) is proposed. The CSG directly operates in the complex plane and efficiently generates sorted candidate sequences with precise path weights. Using the CSG and an associated parallel comparator, the proposed K -Best SDA can avoid the computational complexities in the large amount of path weight evaluations and sorting. Then a new search strategy based on a derived cumulative distribution function (cdf) and an associated efficient procedure is proposed. With the above features, the proposed SDA can provide near ML performance with the lower complexity than conventional K -Best SDAs. Afterwards, a novel decoder with low decoding complexity is proposed for underdetermined MIMO systems. The proposed decoder consists of two stages. First, an improved slab decoding algorithm is adopted to efficiently obtain valid candidate points within a given slab. Next, a multi-slab based decoding algorithm finds the

optimal solution by conducting intersections on the obtained candidate set with dynamic radius adaptation. Furthermore, an optimal preprocessing technique is proposed from the geometrical perspective and the comprehensive analysis on the complexity reduction is also provided. The proposed decoder incorporating preprocessing scheme offers a low (non-exponential) computational complexity and near-ML decoding performance for underdetermined MIMO systems, particularly with large number of antennas and/or high-order constellations. Finally, a tree based codebook search algorithm for uplink (UL) coordinated multipoint (CoMP) systems is proposed. The codebook search issue can be reformulated as a tree search form and the solution can be obtained efficiently using a modified K -Best enumeration strategy. The proposed approach provides the advantage of low computational complexity and nearly the same performance of the exhaustive search algorithm, especially when the CoMP size is significant. Simulation results show that these proposed algorithms can significantly reduce the computational complexity and maintain system performance, which provide a promising solution for future wireless communication systems.

Acknowledgement

I wish to express my deepest gratitude for the guidance, support and constructive criticism to my advisor Dr. Ta Sung Lee, whose elegant way of approaching problems has considerably influenced my research and working style. I especially want to thank Dr. Wei-Ho Chung from Academia Sinica for many helpful suggestions, valuable comments and writing improvement.

I want to thank the all members of the Communication System Design and Signal Processing (CSDSP) Lab for sharing their knowledge and inspiring discussion.

I also thank my mother, parents-in-law, brothers and friends for their encouragement and continual support. Finally, I thank my adorable children CoCo and Jim and my lovely wife Amy, who always stood by me during frustrating and hard times, and without whom this work would not have been completed.

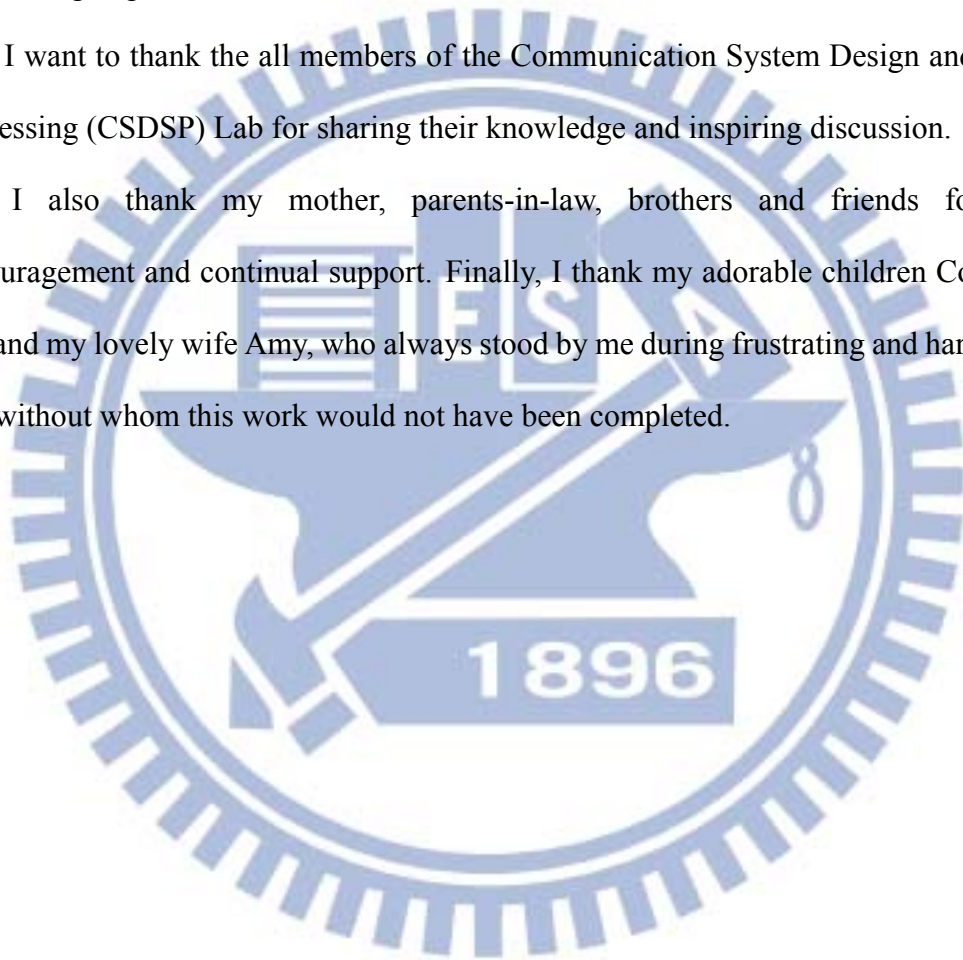
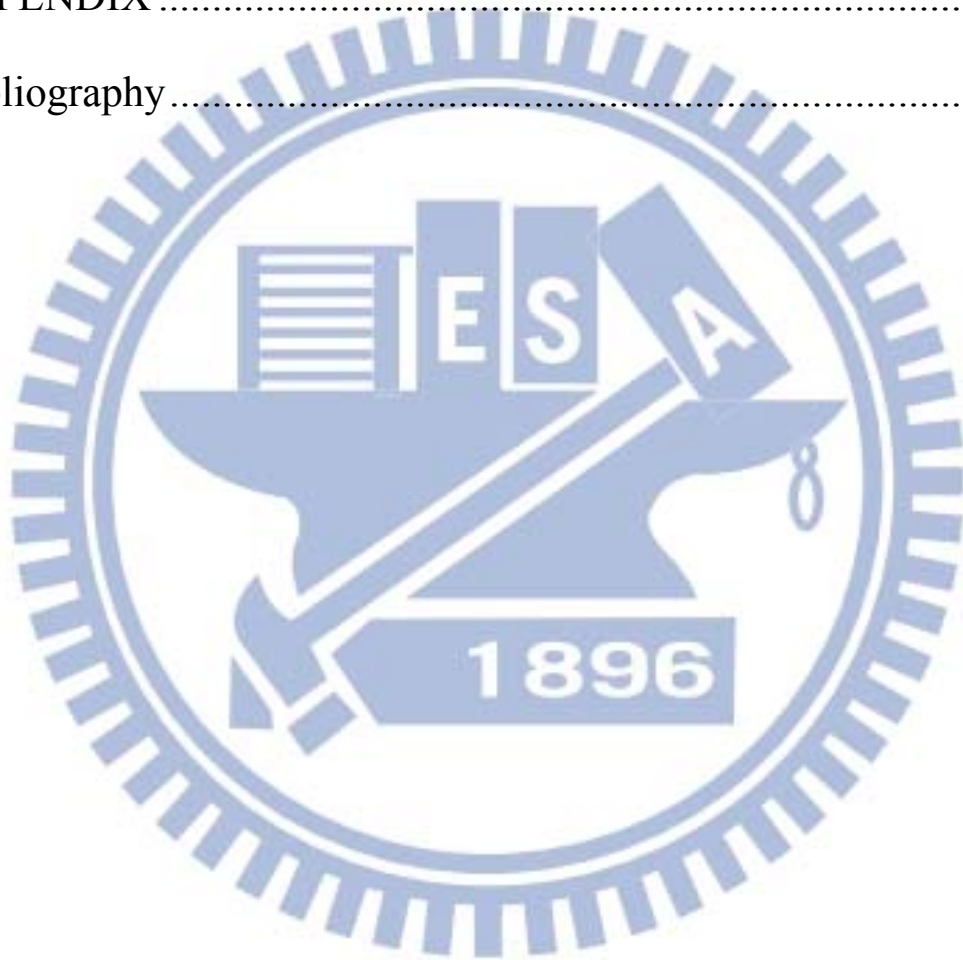


Table of Contents

Chinese Abstract.....	i
English Abstract	ii
Table of Contents.....	v
List of Figures	viii
List of Tables	xi
Acronym Glossary.....	xii
Notations	xv
Chapter 1 Introduction.....	1
1.1 Basics of Multi-Antenna Systems.....	1
1.2 Basics of MIMO Decoder.....	2
1.3 Related Literature Review	4
1.4 Main Contributions.....	9
1.5 Organization of Dissertation.....	10
Chapter 2 Efficient Search Algorithm for Over- determined	
MIMO systems	12
2.1 Overview.....	12
2.2 Signal Model.....	13
2.3 Proposed Sorting Algorithm and Hardware Architecture	18
2.3.1 Candidate Sequence Generator in Complex Plane	18
2.3.2 Architecture of Highly-Parallel Comparison Circuit (HPCC).....	25

2.3.3 Complexity Advantages	28
2.4 Proposed Search Strategy for Near-ML Performance	29
2.4.1 Preprocessing with Column Permutation	29
2.4.2 Proposed Search Strategy	30
2.4.3 Joint 2-Layer ML Search Algorithm.....	34
2.5 Computer Simulation and Discussions	38
2.6 Summary	48
Chapter 3 Geometry Based SDA for Under- determined MIMO	
systems	50
3.1 Overview.....	50
3.2 Signal Model for Underdetermined SDA.....	51
3.3 Proposed Decoding Algorithms for Underdetermined Systems.....	54
3.3.1 An Efficient Slab Search (ESS) Algorithm.....	55
3.3.2 A Multi-slab Sphere Decoding (MSSD) Algorithm.....	57
3.4 Proposed Preprocessing Technique for Complexity Reduction.....	60
3.4.1 A Preprocessing with Column Permutation.....	60
3.4.2 Complexity Analysis.....	64
3.5 Computer Simulation and Discussions	69
3.6 Summary.....	76
Chapter 4 Efficient Search Algorithm for Codebook Search in	
Uplink CoMP Systems	77
4.1 Overview.....	77
4.2 Signal Model.....	78
4.3 Propsoed Codebook Serach Algorithm.....	81

4.4 Simulation Results	85
4.5 Summary	88
Chapter 5 Conclusions and Future Works	91
5.1 Summary of Dissertation	91
5.2 Future Works.....	92
APPENDIX	94
Bibliography.....	101

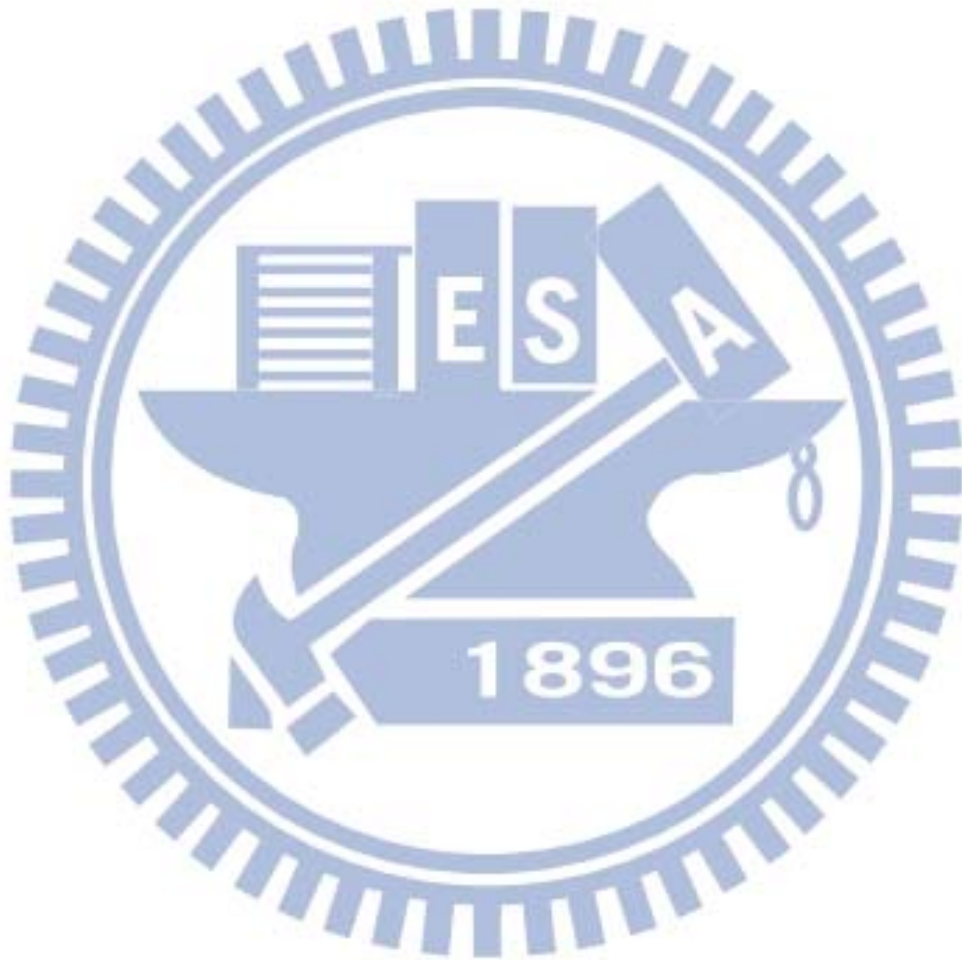


List of Figures

Figure 2-1: Illustration of the multi-index operation.	17
Figure 2-2: Modulo operation of the search center.	20
Figure 2-3: Partition of the search segments.	20
Figure 2-4: (a) Modulo unit of $\text{Re}(y_i)$. (b) Transformation unit of $y_{i,M}$	23
Figure 2-5: Hardware architecture of the candidate generator.	25
Figure 2-6: Illustration of the HPPC operations.	26
Figure 2-7: HPCC architecture.	27
Figure 2-8: Search constraints of the N th layer with $d' = 1.1$	32
Figure 2-9: Cdf curves of $r_{o,i,i}^2$. (a) 4x4 MIMO channel. (b) 8x8 MIMO channel.	32
Figure 2-10: Geometrical relationship illustrating the adopted property.	35
Figure 2-11: Performance of complex K -Best SDA for 4x4 MIMO systems. (a) 16-QAM modulation. $K = 4$ and 8 for complex K -Best SDA incorporating proposed CML strategy; $K = 4, 8,$ and 12 for regular complex K -Best SDAs. (b) 64-QAM modulation. $K = 4$ and 12 for complex K -Best SDA incorporating proposed CML strategy; $K = 4, 12,$ and 24 for regular complex K -Best SDAs.	41
Figure 2-12: Performance and complexity of SDA for 4x4 MIMO systems with 16-QAM modulation. (a) SER. (b) Complexity. $K = 8$ for K -Best SDAs.	42
Figure 2-13: Performance and complexity of SDA for 4x4 MIMO systems with 64-QAM modulation. (a) SER. (b) Complexity. $K = 8$ for K -Best SDAs.	43

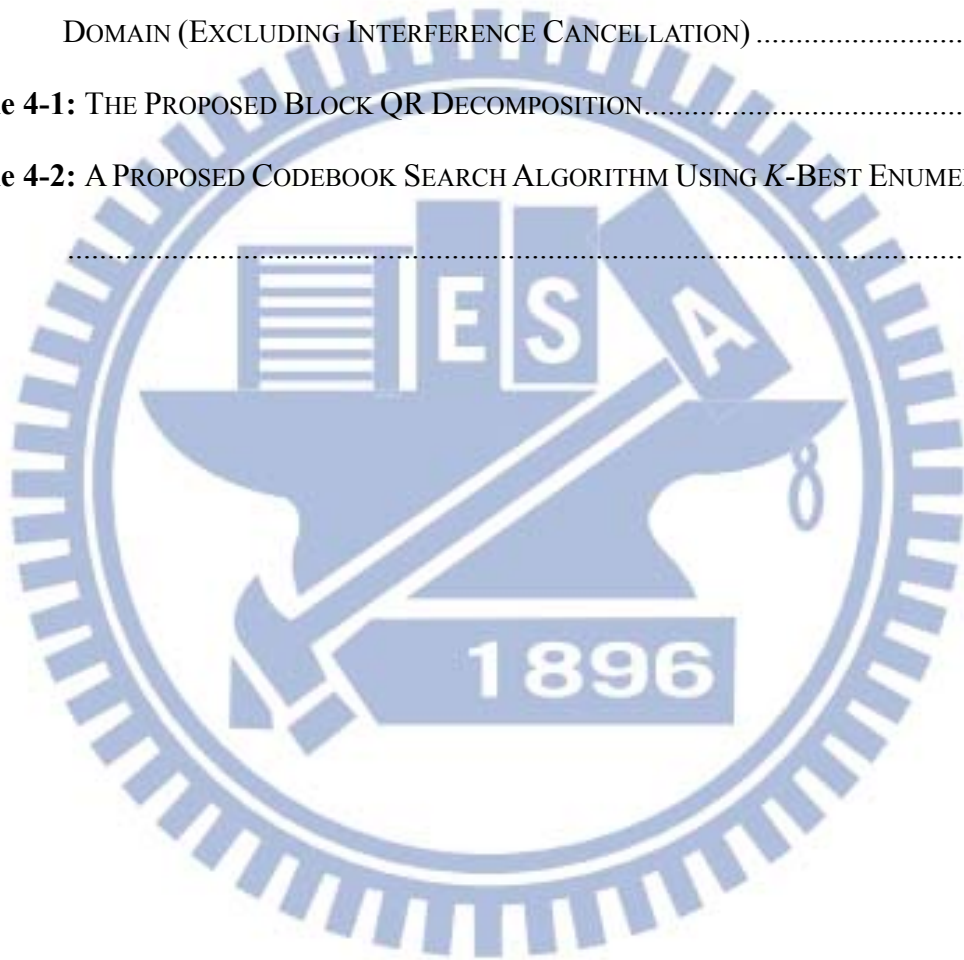
Figure 2-14: Performance and complexity of SDA for 8x8 MIMO systems with 16-QAM modulation. (a) SER. (b) Complexity. $K = 14$ for K -Best SDAs.	45
Figure 2-15: Performance and complexity of SDA for 8x8 MIMO systems with 16-QAM modulation. (a) SER. (b) Complexity. $K = 32$ for proposed K -Best SDA; $K = 32$ and 52 for conventional K -Best SDAs.	47
Figure 3-1: Geometrical diagram of slabs with different y	61
Figure 3-2: SER performance comparisons of SSD, ML and proposed decoder with 16-QAM modulation for various MIMO configurations.	71
Figure 3-3: SER performance and complexity comparisons of SSD, ML and proposed decoder with 64-QAM modulation for various MIMO configurations. (a) SER; (b) Complexity.	72
Figure 3-4: Probability density function of $ y'_M $ with various ordering rules with 16-QAM (4,2) MIMO configuration at SNR=15dB.	73
Figure 3-5: The comparison of the averaged complexity reduction ratio for various ordering rules.	73
Figure 3-6: Performance and complexity comparisons of the proposed decoder incorporated with and without greedy reordering scheme with 64 QAM modulation.	75
Figure 4-1: Illustration of centralized UL CoMP system model.	79
Figure 4-2: Illustration of centralized UL CoMP system model.	80
Figure 4-3: Sum-rate performance and complexity of the proposed and exhaustive search methods with $N_t=4$, $N_r=4$, $M=3$, $P=1$, $d_1=2$, $d_2=3$, and $d_3=4$	87
Figure 4-4: Sum-rate performance and complexity of the proposed and exhaustive	

search methods with $N_t=4$, $N_r=8$, $M=3$, $P=2$, and $d_1=d_2=d_3=4$ 87

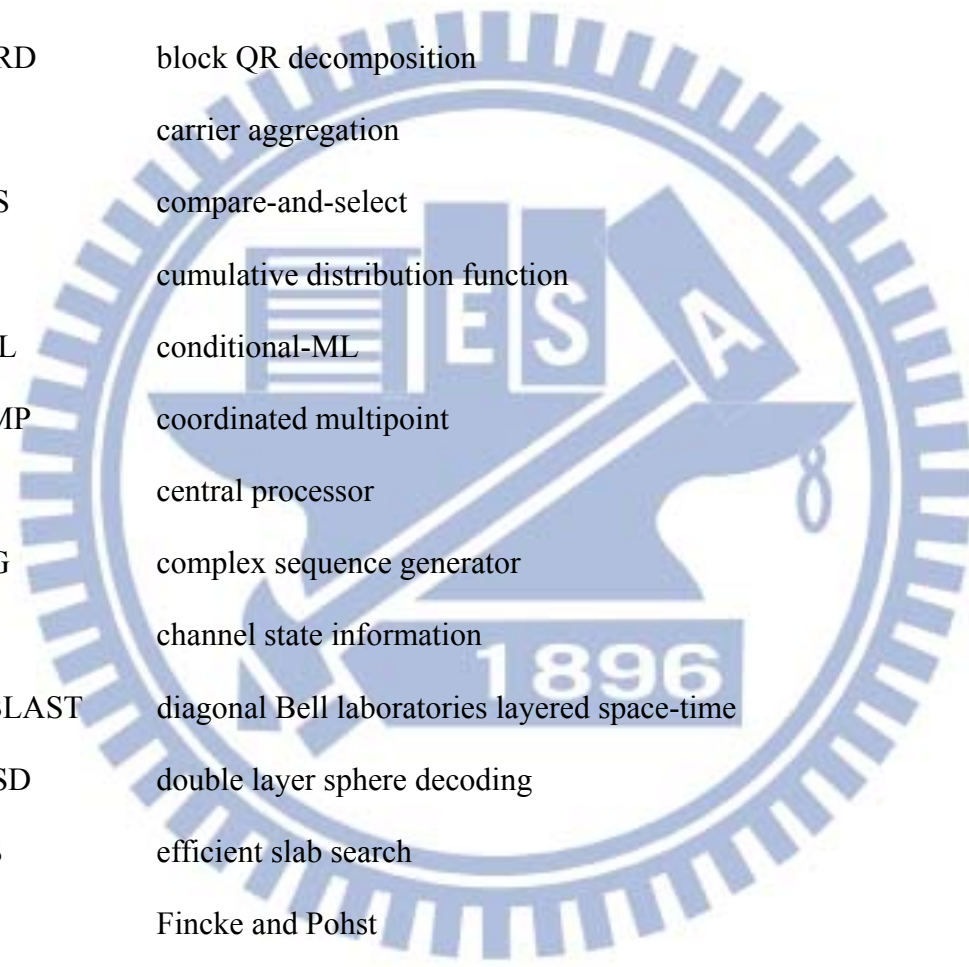


List of Tables

Table 2-1: LIST OF CANDIDATE SEQUENCES	22
Table 2-2: COMPUTATIONAL COMPLEXITY OF PROPOSED <i>K</i> -BEST SDA (EXCLUDING INTERFERENCE CANCELLATION).....	37
Table 2-3: COMPUTATIONAL COMPLEXITY OF CONVENTIONAL <i>K</i> -BEST SDA IN REAL DOMAIN (EXCLUDING INTERFERENCE CANCELLATION)	38
Table 4-1: THE PROPOSED BLOCK QR DECOMPOSITION.....	88
Table 4-2: A PROPOSED CODEBOOK SEARCH ALGORITHM USING <i>K</i> -BEST ENUMERATION	90



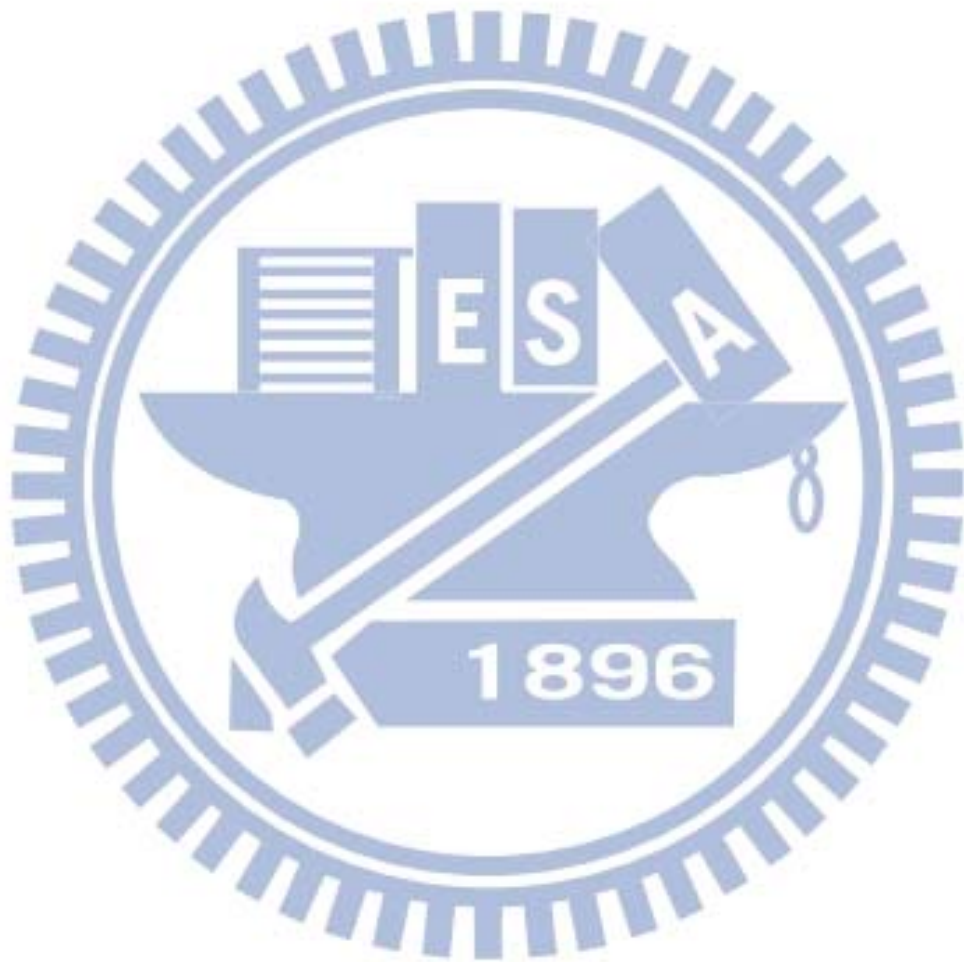
Acronym Glossary



3GPP	third generation partnership project
AWGN	additive white Gaussian noise
BS	base station
BQRD	block QR decomposition
CA	carrier aggregation
CAS	compare-and-select
cdf	cumulative distribution function
CML	conditional-ML
CoMP	coordinated multipoint
CP	central processor
CSG	complex sequence generator
CSI	channel state information
D-BLAST	diagonal Bell laboratories layered space-time
DLSD	double layer sphere decoding
ESS	efficient slab search
FP	Fincke and Pohst
GS	Gram-Schmidt
GSD	generalized sphere decoder
HPCC	highly-parallel comparison circuit
ICI	inter-cell interference
LTE	long term evolution
LTE-A	long term evolution-advanced

MIMO	multiple-input multiple-output
MISO	multiple-input-single-output
ML	maximum-likelihood
MMSE	minimum mean-square error
MSSD	multi slab sphere decoding
MU	multi-user
PDA	plane decoding algorithm
pdf	probability density function
PED	partial Euclid distance
PSASR	partial sum of achievable sum-rate
RVD	real-value decomposition
RRH	remote radio head
SDA	sphere decoding algorithm
SE	Schnorr and Euchner
SER	symbol error rate
SIC	successive interference cancellation
SINR	signal to interference and noise ratio
SLA	slab decoding algorithm
SNR	signal to noise ratio
SSD	slab sphere decoder
SVD	singular value decomposition
UE	user equipment
UL	uplink
V-BLAST	vertical Bell laboratories layered space-time
VLSI	very-large-scale integration

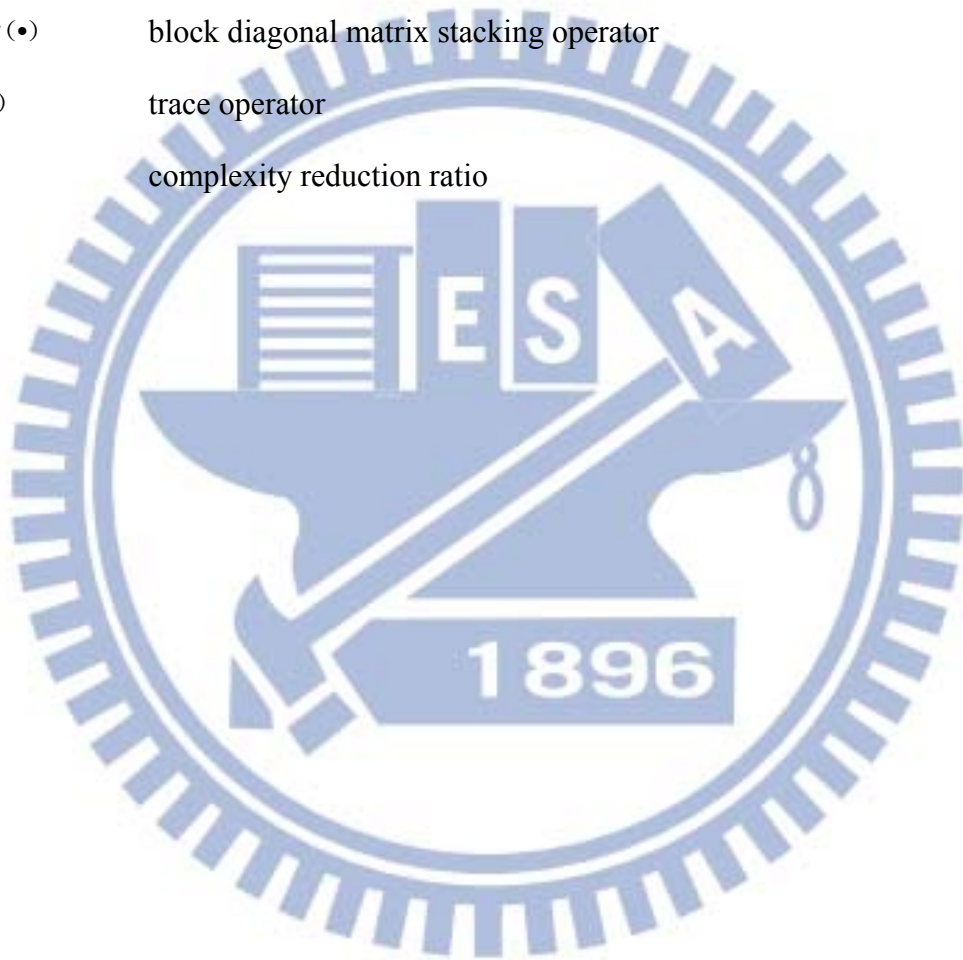
WiMAX Worldwide Interoperability for Microwave Access
ZF zero-forcing



Notations

$\lceil \cdot \rceil$	ceiling operator
$(\cdot)^*$	conjugate operator
$E \{ \cdot \}$	expectation operator
$\lfloor \cdot \rfloor$	floor operator
$(\cdot)^\dagger$	Moore-Penrose pseudo-inverse operator
$\lceil \cdot \rceil$	rounding operator
$(\cdot)^{-1}$	inverse operator
$Q(\cdot)$	quantization operator
$(\cdot)^T$	transpose operator
C	search radius
\mathbf{H}	channel matrix
N_r	number of receive antennas
M_c	constellation size
N_t	number of transmit antennas
P	transmit power
\mathbf{n}	noise vector
γ	average SNR at the receiver
\mathbf{x}	transmit signal vector
\mathbf{y}	received signal vector
\mathbf{H}_{qk}^m	channel between the q th receiver and the k th UE in cell m
$\mathbf{V}_{(m-1)P+k}$	precoder matrix for the k th UE in cell m

$\mathbf{x}_{(m-1)P+k}$	transmitted signal vector for the k th UE in cell m
d_T	number of total transmit data streams
R_{sum}	achievable sum-rate
$\mathbf{X}^{(i)}$	the i th column of matrix \mathbf{X}
$\{\mathbf{X}\}_i^j$	matrix consists of the i th column to of j th column of matrix \mathbf{X}
$diag(\bullet)$	block diagonal matrix stacking operator
$tr(\bullet)$	trace operator
η	complexity reduction ratio



Chapter 1

Introduction

In this introductory chapter, background materials about multi-antenna systems and well-known decoding algorithms are presented. The following sections include the literature survey, dissertation contribution and overview of this dissertation.

1.1 Basics of Multi-Antenna Systems

Next generation wireless communication systems are expected to provide users with higher data rate services for video, audio, data, and voice signals. Many innovative techniques have recently been proposed to improve the spectral efficiency and reliability of wireless communication links. Examples include coded multicarrier modulation, smart antennas, multiple-input multiple-output (MIMO) technology and adaptive modulation.

Among these technologies, MIMO technology has attracted substantial research and industrial interests. The MIMO technology involves the use of multiple antennas at both sides to provide more reliable communication link and/or higher spectral efficiency [1-3]. The theoretical analyses show that the MIMO system capacity linearly increases with the minimum value of the number of transmitting and receiving antennas [2]. As a result, the MIMO technology has been recognized as one of the most promising solutions for future wireless communication systems. There are two underlying techniques in MIMO system: spatial multiplexing [6] and diversity techniques [3]. Spatial multiplexing offers a linear increase of data rate by transmitting multiple independent data streams at the same time.

Spatial diversity provides diversity gain to mitigate fading effects by using the multiple (ideally independent) copies of the transmitted signal. They are usually trade-offs in the two techniques which provide an effective and promising solution while achieving high-data rate and reliable transmission.

The MIMO technology has been widely adopted in the next-generation wireless communications such as IEEE 802.16 and Third Generation Partnership Project (3GPP), Long Term Evolution (LTE), and LTE-advanced (LTE-A) systems.

1.2 Basics of MIMO Decoder

Multiple-antenna systems employing spatial multiplexing increase the spectral efficiency. However, this improvement comes at the cost of an increased receiver complexity. Finding the well balanced trade-off between communications performance and implementation complexity in MIMO detection is one of the key challenges in the receiver design.

The optimal detector for MIMO systems is the maximum likelihood (ML) detector, which search all possible combinations of transmitted symbols. The number of possible combinations increases exponentially with the number of antennas and the size of the legal modulation symbol set. Therefore, it is difficult to be implemented at the receiver in practice. As a remedy, many suboptimal detection algorithms have been developed with desired trade-off between performance and complexity. They can be divided into the following classes.

- **Linear MIMO Detection**

Zero-Forcing (ZF) and minimum mean square error (MMSE) filters apply linear operations to the received signal in order to restore the transmitted signal. These linear filters can be implemented at a low complexity; however, their communications

performance is poor. The MMSE filter considers the noise power in the interference cancellation and therefore shows a slightly better performance.

- **Successive Interference Cancellation**

The successive interference cancellation (SIC) technique was initially adopted by the vertical Bell Laboratories layered space-time (V-BLAST) system [4] - [7-8]. In contrast to the basic ZF and MMSE filters, SIC detects the transmitted streams sequentially and then removes the interference of each detected stream from the received data before continuing the detection process. The performance of the SIC algorithm is generally better than ZF and MMSE filters.

- **Breadth-First Tree Search Algorithms**

For further improvement of the communications performance, the MIMO detection problem can be mapped on a tree search. Tree search algorithms can be divided into breadth-first and depth-first search algorithms. Breadth-first algorithms can potentially provide a constant throughput with slight performance loss compared to an optimal detection. Among these techniques, the K -Best enumeration strategy is the most popular approach. While traversing the tree, the K -Best detector always retains the K best nodes in each search level. This additional sorting operation causes extra computational complexity. In general, the decoding performance of breadth-first algorithms depends on the number of survival nodes chosen in each search layer.

- **Depth-First Tree Search Algorithms**

The main idea of depth-first search is to apply pruning criteria to remove parts of the tree in the search to reduce the computational complexity. The typical sphere detectors can achieve the same decoding performance of ML detector with significant complexity reduction. Due to the nature of the depth-first search, their throughput is usually variable.

The sequential tree search order makes it difficult to parallelize the detection. There exist many sub-optimal variants regarding enumeration technique, pruning criterion, or simplified metric calculations to obtain desired trade-off between performance and complexity.

1.3 Related Literature Review

As the aforementioned, linear detection and SIC scheme are simple to implement, but their detection performance is far from optimal. ML detection is the optimal detection scheme, but its complexity grows exponentially with the size of the transmitted symbol alphabet and number of transmit antennas. To reduce the complexity of ML detection, the sphere decoding algorithm (SDA) has been introduced to achieve the same performance as ML detection with reduced complexity [9]-[12]. The SDA has received considerable attention as an effective detection scheme for MIMO systems.

The basic idea of the SDA is to locate the lattice point nearest to the received signal vector within a given sphere radius. In doing so, the SDA transforms the original problem into a tree search problem. Some candidate enumeration strategies have been proposed [9]-[12]. In the work by Fincke and Pohst SDA (FP-SDA) [9], [10], the radius is set as a scaled variance of the noise. If no lattice points satisfy the radius constraint, the algorithm increases the search radius and restarts the search. The Schnorr and Euchner SDA (SE-SDA) [12] is a variant of the FP-SDA. It shows that enumerating candidate symbols in ascending order based on their distance from the Babai estimate [13] (nulling-canceling solution) speeds up the tree search. This approach is likely to find the optimal solution faster than the FP-SDA and hence can reduce the computational complexity. With these efforts, the conventional SDA is still too

complex in the low SNR regime and its decoding throughput is not stable in general. Hence, it is not desirable for real time detection and hardware implementation. Previous works [14]-[16] proposed some architectures to explore the parallelism property of VLSI to improve the decoding throughput. These designs exhibit excellent performance in the higher SNR regime.

To overcome the drawbacks of the conventional SDA, the K -Best SDA has been introduced in [17]-[19]. The K -Best SDA uses a breadth-first search and keeps the K -Best candidates of each layer for the search of the next layer. Briefly, the main idea of the K -Best SDA is to keep only K candidates which have the smallest path weights as the most promising solutions. Hence, the decoding throughput of the K -Best SDA is stable. Unfortunately, applying a sorting algorithm to find the K -Best candidates in each layer requires many computational operations and a long decoding latency. Moreover, the value of K must be large enough to achieve near-ML performance, and this would increase the computational complexity, decoding latency, and implementation cost.

Sorting is a critical factor in reducing the complexity of a K -Best SDA. In [17] the bubble sort algorithm is applied to conduct sorting. More efficient sorting algorithms [18], [19] have also been adopted to reduce computational complexity. Recently, a high efficiency sorting architecture has been proposed, which can sort K values of partial Euclidean distances in $K/2$ clock cycles [20]. It is found that the quick sort algorithm [18] is not always more suitable than the bubble sort algorithm for a small value of K . Some efficient early-pruning schemes have been proposed in [18], [21] which eliminate the survival candidates that are unlikely to become ML solutions in the early search layers. The approach in [22] reduces the number of candidate nodes by adopting dynamic K values according to the index of search layers. The above approaches can effectively reduce decoding complexity, but also introduce performance degradation

due to that the ML solution can possibly be dropped.

To solve the above performance problem, the method presented in [23] always conducts the ML search in several preceding search layers, where ML search refers to an exhaustive search in a certain layer. In this case, the operation in the remaining layers is the same as the conventional K -Best SDA. This approach is a special case of the dynamic- K method, and increases complexity and power consumption significantly. In general, it is not necessary to perform the ML search especially when the channel condition is good. The method proposed in [24] chooses the optimal K dynamically according to the channel condition. An approximated algorithm [25] has been proposed to estimate channel conditions in an efficient way. Nevertheless, these methods require complicated procedures and some extra circuits. To the best of our knowledge, there are no efficient mechanisms for deciding the number of layers in which the ML search is conducted, or whether to perform the ML search under different K values and antenna numbers.

Most of the SDAs developed so far work in the real domain using the real-valued decomposition (RVD) [17], [26]-[27]. Although the real domain approaches lead to better performance and lower complexity, they require more search layers than the complex domain approaches [28], [29]. To reduce the number of search layers, some novel search methods which operate in the complex plane have been proposed [30], [31]. These methods introduce errors when evaluating path weights, which achieves the goal of reducing complexity but sacrificing performance significantly. On the other hand, some communication systems require rotating the constellation by a pre-defined angle before transmitting symbols to achieve a higher diversity gain. In this case, conventional real domain SDAs cannot be adopted directly, and some extra and complicated techniques are needed. To tackle these issues, a new SDA directly performing in the complex domain is desired.

Afterwards, we will consider an underdetermined MIMO system commonly existing in multi-user (MU) uplink transmission of 3GPP LTE/LTE-A or Mobile WiMAX where the number of users exceeds that of receiving antennas at the base station and decoupling the spatial signals from these users encounters difficulties due to insufficient number of receive antennas. In this circumstance, conventional SDAs are unable to identify a unique solution for the underdetermined MIMO systems. To overcome the aforementioned drawback of SDA, certain novel decoders have been proposed. First, the generalized sphere decoder (GSD) [42] performs an exhaustive search on specified dimensions to find the ML solution. Its decoding complexity increases with the constellation size and the difference between transmit-receive antenna numbers. Based on GSD, other efficient decoders have been proposed, such as the regularized sphere decoder [43]-[45], tree-search approach [46], [47], double-layer sphere decoder (DLSD) [48], [49], and slab sphere decoder (SSD) [50], [51]. In [43], the authors convert the original problem into an overdetermined form by the regularization technique with a constant modulus constellation constraint, and then apply the conventional SDA to obtain a near ML solution. Later, the works in [44] reformulate this approach to remove the constant modulus constraint for generalized M-QAM systems. In [46], authors propose an efficient tree-search decoding algorithm for binary constellation systems and extend this algorithm to M-PSK systems in [47]. This modified algorithm needs to decompose the constellation into a weighted sum of QPSK constellations for M-QAM systems. As a result, the decoding complexity increases rapidly with the size of transmit-receive antenna number difference and/or constellation. The DLSD utilizes an outer sphere decoder to find a valid candidate set, and an inner sphere decoder to find the ML solution. The SSD adopts a geometrical approach for finding the valid candidate set to reduce the search complexity of DLSD. Both DLSD and SSD need to perform the conventional SDA sequentially, so their

complexity remains an issue. Besides, algorithms for coded MIMO systems [52], hybrid approach [53] or heuristic search method [54] tackle the MIMO system from different perspectives. Comparing the results in [42]-[51], it is evident that the SSD exhibits the lowest complexity for the large constellation and is thus chosen as a benchmark. Unfortunately, as shown in [51], the decoding complexity increases rapidly with the size of transmit-receive antenna number difference and/or constellation; therefore, developing efficient decoding algorithm is still an active research field for practical applications.

Finally, we intended to consider a codebook search problem in Uplink Coordinated multipoint (CoMP) systems. CoMP has been adopted in LTE-A to improve the cell average and cell edge throughputs [61]. It uses the cooperation between points in several cooperation groups to coordinate the transmission for inter-cell interference (ICI) alleviation and link quality enhancement. An attractive CoMP scheme referred to as centralized CoMP, is a full cooperation approach that involves full channel state information (CSI) and full data information for providing improved performances. The full cooperation scheme between base stations (BS) and remote radio heads (RRH) is applicable in LTE-A because of the dedicated fiber links. In uplink (UL) centralized CoMP systems, cooperating BSs forward received signals and CSI to a central processor (CP), which computes the corresponding precoder matrix for each user equipment (UE). Therefore, the CP needs to feed back the exact precoder matrix to each UE, which is inefficient and impractical. A codebook-based scheme that feeds back only the precoder matrix index (rather than the matrix itself) is adopted as a remedy in real applications. Centralized CoMP with MIMO has attracted significant attention, and there are numerous studies that focus on the optimal precoder design [62-63]. However, efficient codebook search algorithms for the aforementioned scenario are uncommon. It is noted that, to the best of our knowledge, the issue remains

scarce in the literature.

1.4 Main Contributions

The contributions of this dissertation are summarized as follows:

1. A simple and efficient complex domain candidate sequence generator (CSG) is proposed. By combining the proposed CSG with an efficient sorting architecture, the proposed decoder can significantly reduce path weight calculations and comparison operations without sacrificing detection performance. Moreover, to address the performance issue, a new search strategy that incorporates the ML search in the preceding layers under poor channel conditions improves the performance of the proposed K -Best SDA even when the value of K is small. A judicious criterion is proposed that helps determine fewer ML search layers. Furthermore, an efficient search procedure is also proposed that fully utilizes existing hardware elements. Combining the above features, the proposed K -Best SDA exhibits lower complexity, excellent performance, and is well-suited to real-time applications.

2. We further develop an efficient decoder from the geometrical perspective for the underdetermined MIMO systems. The proposed decoder consists of two stages. First, an improved slab decoding algorithm is adopted to efficiently obtain valid candidate points within a given slab. Next, a multi-slab based decoding algorithm finds the optimal solution by conducting intersections on the obtained candidate set with dynamic radius adaptation. Furthermore, an optimal preprocessing technique is proposed from the geometrical perspective and the comprehensive analysis on the complexity reduction is also provided. The developed procedure can be applied to any static ordering rule even in non-linear ordering rule for QR based MIMO decoder.

3. By exploiting the developed efficient search techniques, we proposed an efficient

codebook search algorithm for UL CoMP systems. To break the interdependency among user equipments (UEs), a generalized blockwise QR decomposition procedure is proposed. By the proposed generalized block GS decomposition, the original codebook search problem can be reformulated as a problem of finding the longest path and be solved efficiently by conducting a tree search. To efficiently obtain this solution, a modified K -Best algorithm is also proposed. The proposed algorithm provides a significant improvement by one order of computational efficiency and provides a near ML performance compared to the exhaustive approach.

1.5 Organization of Dissertation

The remaining of this dissertation is organized as follows.

In Chapter 2, we will propose a low complexity near-ML K -Best sphere decoder. The proposed K -Best sphere decoding algorithm involves two stages. First, a new candidate sequence generator (CSG), which operates in the complex plane and efficiently generates sorted candidate sequences with precise path weights, is proposed. Using the CSG and an associated parallel comparator, the proposed K -Best SDA can avoid performing a large amount of operations. Next, a new search strategy based on a derived cumulative distribution function (cdf) and an associated efficient procedure is proposed. By incorporating detection ordering into the proposed SDA, it can provide near ML decoding performance with a lower complexity requirement than conventional K -Best SDAs.

In Chapter3, We further consider an underdetermined MIMO system and propose an efficient decoder from geometry perspective. The underdetermined MIMO systems can be found in the multi-user (MU) uplink transmission of 3GPP LTE/LTE-Advanced or Mobile WiMAX where the number of users exceeds that of receiving antennas at the

base station and decouples the spatial signals from these users encounter difficulties due to insufficient number of receive antennas. To tackle the problem, we will propose a geometry-based efficient decoder for underdetermined MIMO systems. The proposed decoder involves two stages. First, an improved slab search algorithm efficiently obtains valid candidate points within a given slab. Next, a multi-slab based decoding algorithm finds the optimal solution by taking intersections of the obtained candidate set with dynamic radius adaptation. By doing so, there is no need to perform SDA sequentially. The proposed decoder can thus provide near ML performance with much lower (non-exponential) complexity compared to the state-of-art methods. Furthermore, we propose an optimal preprocessing technique from the geometrical perspective and conduct comprehensive analysis on the complexity reduction. By introducing the proposed preprocessing scheme, the incorporated decoder can significantly reduce the decoding complexity in the low SNR regime without sacrificing performance. The advantage is useful and suitable for practical MU-MIMO operations.

In Chapter 4, we try to apply tree search techniques to solve codebook search problem in Uplink CoMP systems. CoMP techniques has been adopted in LTE-A to improve the cell average and cell edge throughputs. It uses the cooperation between points in several cooperation groups to coordinate the transmission for inter-cell interference (ICI) alleviation and link quality enhancement. We will propose an efficient codebook search algorithm to locate the optimal codebook set in centralized UL CoMP systems. The codebook search issue can be reformulated as a tree search form and the solution can be obtained efficiently using a modified K -Best enumeration strategy. The proposed algorithm can effectively perform precoder selection and maintain a significantly lower complexity compared to the exhaustive search method.

Finally, Chapter 5 concludes this dissertation and discusses future extensions of this research.

Chapter 2

Efficient Search Algorithm for Over-determined MIMO systems

2.1 Overview

As the mentioned in Chapter 1, the K -Best SDA uses a breadth-first search and keeps the K -Best candidates of each layer for the search of the next layer. Briefly, the main idea of the K -Best SDA is to keep only K candidates which have the smallest path weights as the most promising solutions. Hence, the decoding throughput of the K -Best SDA is stable. Unfortunately, applying a sorting algorithm to find the K -Best candidates in each layer requires many computational operations and a long decoding latency. Moreover, the value of K must be large enough to achieve near-ML performance, and this would increase the computational complexity, decoding latency, and implementation cost. For reducing the decoding complexity and obtaining reasonable performance for practical applications, the selected value of K is usually same as the constellation size. Therefore, how to trade off between performance and complexity is still an active research issue.

In this chapter, we will propose a simple and efficient complex domain candidate sequence generator (CSG) first. The CSG is developed based on the fact that neighboring points share the same candidate sequence in the complex plane, rendering the relevant rule invariant to constellation rotation. With a minor modification, the proposed decoder can be easily applied to wireless communication systems with constellation pre-rotation to obtain a larger diversity gain. By combining the proposed CSG with an efficient sorting architecture, the proposed decoder can significantly

reduce path weight calculations and comparison operations without sacrificing detection performance. Moreover, to address the performance issue, a new search strategy that incorporates the ML search in the preceding layers under poor channel conditions (i.e., channel matrix is ill-conditioned) improves the performance of the proposed K -Best SDA even when the value of K is small. A judicious criterion is proposed that helps determine fewer ML search layers than previous works [23], [27]. An efficient search procedure is also proposed that fully utilizes existing hardware elements. The procedure increases hardware utilization and significantly reduces implementation cost. Combining the above features, the proposed K -Best SDA exhibits lower complexity, excellent performance, and is well-suited to real-time applications.

2.2 Signal Model

Consider an MIMO system with N transmit antennas and M receive antennas. The received signal vector is denoted as $\mathbf{y} = [y_1 \ y_2 \ \cdots \ y_M]^T \in \mathbb{C}^{M \times 1}$, where y_m is the received signal at the m th receive antenna. Similarly, the transmitted signal vector is denoted as $\mathbf{x} = [x_1 \ x_2 \ \cdots \ x_N]^T \in \mathbb{Z}^N[j]$, where $\mathbb{Z}[j] := \{a + jb | a, b \in \mathbb{Z}\}$ is the set of Gaussian integers and x_n is the transmitted signal at the n th transmit antenna. The transmitted signal constellation is assumed to be either 16-QAM or 64-QAM. Assume $M \geq N$ and that the channel responses are frequency-flat fading and remain constant during a frame transmission. The channel matrix can be expressed as

$$\mathbf{H} = \begin{bmatrix} h_{1,1} & h_{1,2} & \cdots & h_{1,N} \\ h_{2,1} & h_{2,2} & \cdots & h_{2,N} \\ \vdots & \vdots & \ddots & \vdots \\ h_{M,1} & h_{M,2} & \cdots & h_{M,N} \end{bmatrix}, \quad (2.1)$$

where $h_{i,j}$ is the channel gain from the j th transmit antenna to the i th receive antenna.

Assuming that there is sufficient antenna separation at the transmit and receive sites, the entries of the channel matrix \mathbf{H} can be regarded as i.i.d. complex Gaussian random variables with zero-mean and unit variance. The relationship between the received signal vector and the transmitted signal vector can be expressed as

$$\mathbf{y} = \mathbf{H}\mathbf{x} + \mathbf{n}, \quad (2.2)$$

where $\mathbf{n} = [n_1 \ n_2 \ \dots \ n_M]^T \in \mathbb{C}^{M \times 1}$ is the i.i.d. complex additive white Gaussian noise (AWGN) vector with zero-mean and covariance matrix $\sigma^2 \mathbf{I}_M$.

The optimal detector for MIMO systems is the ML detector, which searches all possible combinations of transmitted symbols via the following criterion [10]

$$\hat{\mathbf{x}} = \arg \min_{\mathbf{x} \in S} \|\mathbf{y} - \mathbf{H}\mathbf{x}\|^2, \quad (2.3)$$

where $S = O^N$ denotes the set of all possible transmitted symbol vectors and O is the modulation symbol alphabet set with a size of M_c . The computational complexity of ML detection grows exponentially with N . Therefore, it is difficult to be implemented at the receiver in practice.

The basic idea of the SDA is to restrict the search region of the optimal solution to a smaller subset. Typically, the search region is constrained to the interior of a hyper-sphere of radius d centered around the received signal \mathbf{y} as described by [10]

$$d^2 \geq \|\mathbf{y} - \mathbf{H}\mathbf{x}\|^2. \quad (2.4)$$

First, performing complex QR-decomposition to the channel matrix produces

$$\mathbf{H} = \begin{bmatrix} \mathbf{Q}_1 & \mathbf{Q}_2 \end{bmatrix} \begin{bmatrix} \mathbf{R} \\ \mathbf{0} \end{bmatrix}, \quad (2.5)$$

where $\mathbf{Q}_1 \in \mathbb{C}^{M \times N}$ and $\mathbf{Q}_2 \in \mathbb{C}^{M \times (M-N)}$ are unitary matrices, \mathbf{R} is an $N \times N$ upper triangular matrix, and $\mathbf{0}$ is an $(M-N) \times N$ zero matrix. Substituting (2.5)

into (2.4), we have

$$(d')^2 \geq \|\mathbf{y}' - \mathbf{R}\mathbf{x}\|^2, \quad (2.6)$$

where $\mathbf{y}' = \mathbf{Q}_1^H \mathbf{y}$ and $(d')^2 = d^2 - \|\mathbf{Q}_2^H \mathbf{y}\|^2$. The right-hand-side of (2.6) can be expanded as

$$\begin{aligned} (d')^2 &\geq \|\mathbf{y}' - \mathbf{R}\mathbf{x}\|^2 = \sum_{i=1}^N \left\| y'_i - \sum_{j=i}^N r_{i,j} x_j \right\|^2 \\ &= \left\| y'_N - r_{N,N} x_N \right\|^2 + \left\| y'_{N-1} - r_{N-1,N} x_N - r_{N-1,N-1} x_{N-1} \right\|^2 + \dots \\ &= r_{N,N}^2 \left\| y''_N - x_N \right\|^2 + r_{N-1,N-1}^2 \left\| y''_{N-1} - x_{N-1} \right\|^2 + \dots, \end{aligned} \quad (2.7)$$

where $y''_i = \left(y'_i - \sum_{j=i+1}^N r_{i,j} x_j \right) / r_{i,i}$. Define the path weight P_k and branch weight B_k of the k th layer as

$$\begin{cases} P_k = 0, & \text{for } k = N + 1 \\ P_k = P_{k+1} + B_k, & \text{for } 1 \leq k \leq N \end{cases} \quad (2.8)$$

$$B_k = r_{k,k}^2 \left\| y''_k - x_k \right\|^2. \quad (2.9)$$

The path weight P_k is the partial Euclidean distance (PED) which is a positive and non-decreasing function of k . The iterative search for the candidates $x_N, x_{N-1}, \dots, x_2, x_1$ can be easily transformed into a tree search problem [10]. The decoding process of the K -Best SDA can then be regarded as descending a tree in which each parent node has M_c branches.

The main idea of the K -Best SDA is to keep only the K candidates with the smallest path weights as the most promising solutions. The procedure of the complex K -Best SDA is summarized as follows:

Step1:

(a). Set $k = N$. For each symbol in the complex-plane constellation,

calculate $P_N = B_N$.

(b). Choose those symbols having the K smallest paths.

Step2:

(a). $k \leftarrow k - 1$.

(b). **Path Evaluation:** For each partial symbol vector that survives the previous layer; for each symbol in the complex-plane constellation,

calculate: $P_k = P_{k+1} + B_k$.

(c). **Sorting and candidate selection:** Sort the KM_c PEDs, and select K partial nodes having the smallest PEDs among the entire candidate set.

Step3:

If $k = 1$

Output the vector with the smallest path weight as the estimated solution.

Else

Go back to Step 2.

In (2.8)-(2.9), path weights are defined for a given candidate symbol x . When performing the decoding procedure of Step 2, multiple candidate symbols need to be evaluated concurrently for finding the optimal solution. Therefore, a multi-index notation is needed and Step 2 can be further elaborated as follows:

Let $P_i^1, P_i^2, \dots, P_i^K$ denote the K smallest PEDs in the i th layer, where $P_i^1 \leq P_i^2 \leq \dots \leq P_i^K$. In performing search in the $(i-1)$ th layer, first conduct full path expansion from the K parent nodes to obtain KM_c branch weights $B_{i-1}^{1,1}, B_{i-2}^{1,2}, \dots, B_{i-1}^{1,M_c}, \dots, B_{i-1}^{K,1}, B_{i-2}^{K,2}, \dots, B_{i-1}^{K,M_c}$ and PEDs $P_{i-1}^{1,1}, P_{i-2}^{1,2}, \dots, P_{i-1}^{1,M_c}, \dots, P_{i-1}^{K,1}, P_{i-2}^{K,2}, \dots, P_{i-1}^{K,M_c}$ respectively, where $B_i^{m,n}$ and $P_{i-1}^{m,n}$ are the branch weight and

PED of the n th path expanded from the m th parent node. The associated PED of each designated node can be evaluated according to $P_{i-1}^{m,n} = P_i^m + B_{i-1}^{m,n}$. Next, sort the KM_c PEDs, and select K partial nodes having the smallest PEDs among the whole candidate set. The above operations are illustrated in **Figure 2-1**

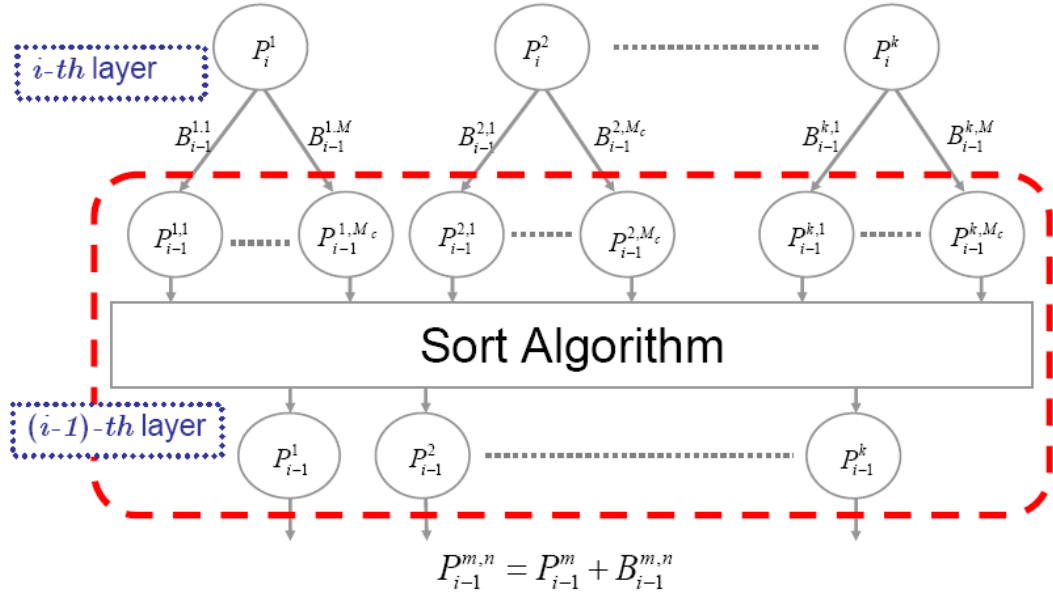


Figure 2-1: Illustration of the multi-index operation.

A popular alternative to the complex K -Best SDA works in the real domain by performing RVD on the complex signal model:

$$\tilde{\mathbf{y}} = \begin{bmatrix} \text{Re}(\mathbf{y}) \\ \text{Im}(\mathbf{y}) \end{bmatrix}, \quad \tilde{\mathbf{x}} = \begin{bmatrix} \text{Re}(\mathbf{x}) \\ \text{Im}(\mathbf{x}) \end{bmatrix}, \quad \tilde{\mathbf{n}} = \begin{bmatrix} \text{Re}(\mathbf{n}) \\ \text{Im}(\mathbf{n}) \end{bmatrix}, \quad \tilde{\mathbf{H}} = \begin{bmatrix} \text{Re}(\mathbf{H}) & -\text{Im}(\mathbf{H}) \\ \text{Im}(\mathbf{H}) & \text{Re}(\mathbf{H}) \end{bmatrix}, \quad (2.10)$$

which yield

$$\tilde{\mathbf{y}} = \tilde{\mathbf{H}}\tilde{\mathbf{x}} + \tilde{\mathbf{n}}, \quad (2.11)$$

where $\tilde{\mathbf{H}} \in \mathbb{R}^{2M \times 2N}$, $\tilde{\mathbf{y}} \in \mathbb{R}^{2M \times 1}$, $\tilde{\mathbf{n}} \in \mathbb{R}^{2M \times 1}$, and $\tilde{\mathbf{x}} \in \Lambda^{2N \times 1} \subset \mathbb{Z}^{2N \times 1}$. Note that $\Lambda = \{-3, -1, 1, 3\}$ for 16-QAM and $\Lambda = \{-7, -5, -3, -1, 1, 3, 5, 7\}$ for 64-QAM. After RVD, each component \tilde{x}_i of $\tilde{\mathbf{x}}$ is chosen from a set Λ of integer numbers with $\sqrt{M_c}$ elements. Since (2.11) has the same algebraic structure as (2.2), the complex

detection problem can be solved in the real domain using the same K -Best algorithm. This is denoted as the conventional K -Best SDA. In [28]-[29], it is shown that the conventional K -Best SDA slightly outperforms the complex K -Best SDA and requires lower complexity. However, the conventional K -Best SDA may not always be applicable in some communications systems with special diversity features. Modified K -Best SDA aim to reduce decoding complexity, but usually introduce performance degradation, which is more significant in the complex domain [30]-[31]. These prompt the development of a low-complexity and high-performance K -Best SDA directly operating in the complex domain.

2.3 Proposed Sorting Algorithm and Hardware Architecture

This subsection proposes a complex K -Best sphere decoder that achieves the same performance as the conventional K -Best SDA with lower complexity. As described in the previous procedural summary, the K -Best SDA involves three major operations: path evaluation, sorting, and candidate selection. In the following, new algorithms for sorting and candidate selection will be developed to achieve the reduction in computations. The path evaluation part remains unchanged so that the decoding performance of the K -Best SDA can be maintained.

2.3.1 Candidate Sequence Generator in Complex Plane

To search the symbols efficiently in the complex plane, it is useful to construct a table of candidate symbol sequences within a given region [14]. First, a primitive block is

defined to be a square block bounded by $\{1 + j, 1 - j, -1 + j, -1 - j\}$. The complex plane can be regarded as consisting of a lot of primitive blocks placed at equal distances. In **Figure 2-2**, a received symbol is located at y_i'' surrounded by four nearest candidate symbols 41, 42, 49 and 50 in the constellation diagram. A candidate symbol sequence, 49-50-41-42, can then be formed according to their distance from y_i'' in ascending order. Consider then the square area centered at the origin and surrounded by the candidate symbols 27, 28, 35 and 36. Shifting the symbols 41, 42, 49 and 50 to the symbols 27, 28, 35 and 36 respectively, a location $y_{i,M}''$ corresponding to y_i'' can be identified. A new candidate symbol sequence, 35-36-27-28, can be identified likewise according to their distance from $y_{i,M}''$ in ascending order. Apparently the relation in terms of the distance from y_i'' to nearby candidate symbols remains unchanged after the coordination transformation. On the other hand, since the symbols are placed symmetrically in the complex plane, once the relation between a received symbol and the associated candidate symbol sequence in one of the four quadrants is obtained, those in the other three quadrants can be readily derived. Next, **Figure 2-3** shows quadrant I of the solid-line square area in **Figure 2-2**. The area is divided into 30 segments (we will explain how to partition the specified square area later). It can be verified that all symbols inside any given segment share the same candidate symbol sequence of k symbols, where $k = 11$ in **Figure 2-3**.

QAM Constellation

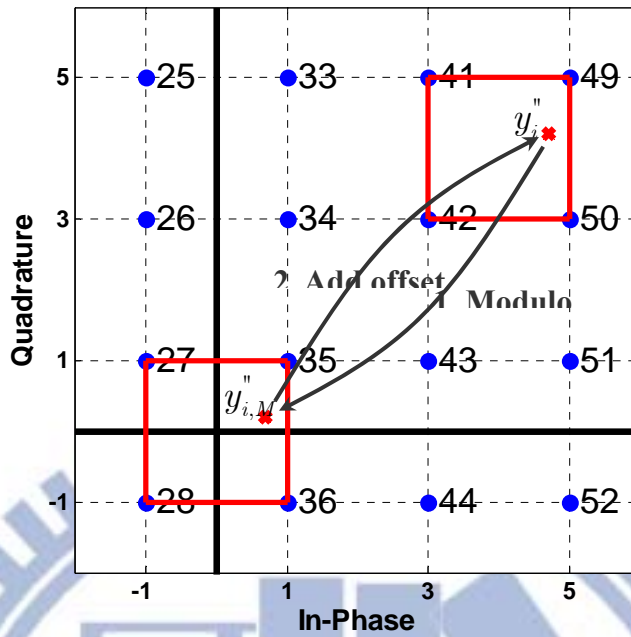


Figure 2-2: Modulo operation of the search center.

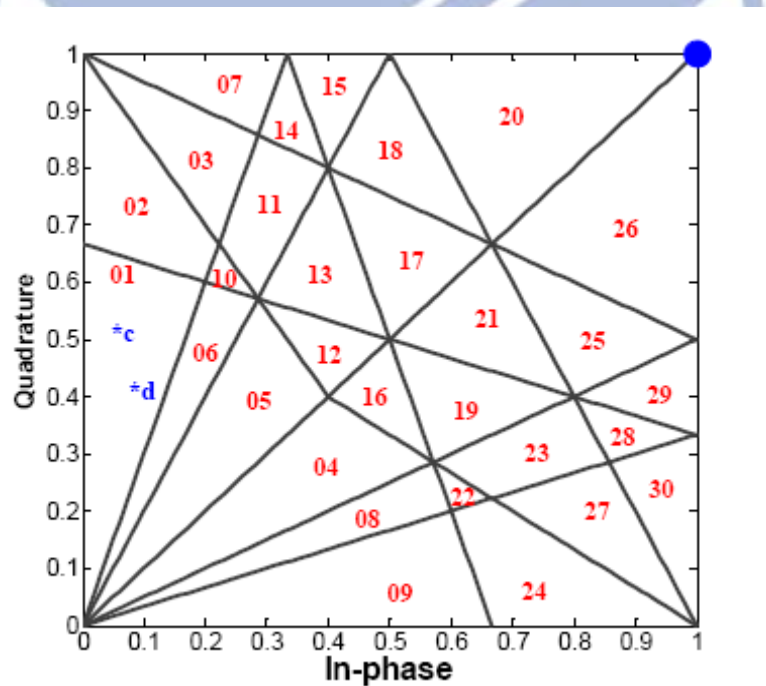


Figure 2-3: Partition of the search segments.

For example, consider two symbols “c” and “d” inside segment 01, and evaluate the distances between all valid candidate symbols and the two points. It is straightforward to

verify that the resulting two candidate sequences are identical, i.e. $\{1+j, -1+j, 1-j, -1-j, 1+j3, -1+j3, 3+j, -3+j, 3-j, -3-j, 1-j3\}$. For other segments, the same result applies.

Using the above properties, we can construct a table of candidate symbol sequences of the k nearest constellation symbols for all symbols bounded by $\{1+j, 1-j, -1+j, -1-j\}$ instead of generating approximated path weights [30]-[31]. Due to the symmetry of 16-QAM and 64-QAM, a simple transformation allows symbols in the region bounded by $\{1+j, 1-j, -1+j, -1-j\}$ in quadrants II, III, and IV to use the same table as quadrant I. Any symbol located within the bounded region is first mapped to quadrant I by a simple transformation. The transformed result acts as the search center for finding the k nearest candidate symbols by looking up the table of the symbol sequences, where k is a specified number. When the candidate symbol sequence $\{x_i\}$ is found, it can easily be transformed back to the original quadrant. **Figure 2-3** shows the partition of the search segments in quadrant I and the corresponding symbol sequences are listed in **Table 2-1**, where $k = 11$ is chosen as an example. This table can be constructed in advance by the following off-line procedure:

First, the bounded square area by $\{1+j, 1, j, 0\}$ is divided into u^2 grids, by $(u-1)$ equally-space horizontal and $(u-1)$ equally-space vertical lines, where u is chosen according to the required resolution. The corresponding distances between all valid candidate symbols and the center of each grid, which represents all possible received symbols within, are then evaluated. Next, by using some sorting procedure, the associated candidate sequence of any possible received symbol can be determined.

Finally, all these possible symbols are rearranged into several search segments such that each segment has the same candidate sequence. By this approach, it is easy to tackle any pre-defined constellation rotation during run-time processing. The following describes the run-time operation in detail:

Table 2-1: LIST OF CANDIDATE SEQUENCES

Segment ID	Candidate Sequence
01	$1+j, -1+j, 1-j, -1-j, 1+j3, -1+j3, 3+j, -3+j, 3-j, -3-j, 1-j3$
02	$1+j, -1+j, 1-j, -1-j, 1+j3, -1+j3, 3+j, -3+j, 3-j, -3-j, 3+j3$
:	:
29	$1+j, 1-j, -1+j, 3+j, -1-j, 3-j, 1+j3, -1+j3, 3+j3, 1-j3, -1-j3$
30	$1+j, 1-j, -1+j, 3+j, -1-j, 3-j, 1+j3, 1-j3, -1+j3, 3+j3, -1-j3$

For any given search center y_i'' in the complex plane, the CSG first rounds it to the relative position $y_{i,M}''$ which lies inside the region bounded by $\{1+j, 1-j, -1-j, -1+j\}$. This modulo operation is depicted in **Figure 2-2: Modulo operation of the search center**, and the associated relationship is described as follows:

For $\text{Re}(y_i'')$:

$$\begin{cases} X_offset = \lfloor \text{Re}(y_i'') \rfloor + \text{mod}(\lfloor \text{Re}(y_i'') \rfloor, 2) \\ \text{Re}(y_{i,M}'') = \text{Re}(y_i'') - X_offset \end{cases} \quad (2.12)$$

For $\text{Im}(y_i'')$:

$$\begin{cases} Y_offset = \lfloor \text{Im}(y_i^n) \rfloor + \text{mod}(\lfloor \text{Im}(y_i^n) \rfloor, 2) \\ \text{Im}(y_{i,M}^n) = \text{Im}(y_i^n) - Y_offset \end{cases} \quad (2.13)$$

Figure 2-4(a) shows the modulo unit of $\text{Re}(y_i^n)$ based on the 2's complement property, which is efficiently implemented by a single adder and a few bit manipulations. S is the sign bit (i.e. MSB) of $\text{Re}(y_i^n)$ and b_0 is the LSB of the integer part of $\text{Re}(y_i^n)$. Since the modulo operation of $\text{Im}(y_i^n)$ is the same as $\text{Re}(y_i^n)$, the modulo circuits of $\text{Im}(y_i^n)$ and $\text{Re}(y_i^n)$ are identical.

In the next step, if $y_{i,M}^n$ lies in quadrant II, III or IV, the CSG unit maps $y_{i,M}^n$ into quadrant I by rotating $\pi/2, \pi$ and $3\pi/2$ respectively. **Figure 2-4(b)** shows this transformation circuit. The multiplexers chooses a right data path based on the sign bits of $\text{Re}(y_{i,M}^n)$ and $\text{Im}(y_{i,M}^n)$. The coordinates dx_t and dy_t denote the transformed values of $\text{Re}(y_{i,M}^n)$ and $\text{Im}(y_{i,M}^n)$, respectively.

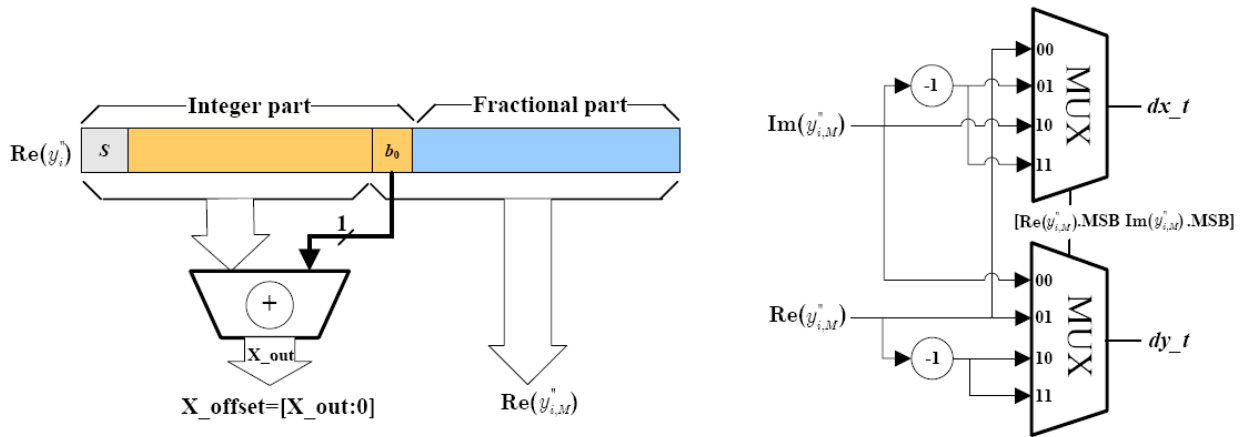


Figure 2-4: (a) Modulo unit of $\text{Re}(y_i^n)$. (b) Transformation unit of $y_{i,M}^n$.

The set (dx_t, dy_t) is sent to the candidate generator unit to generate the desired candidate sequence $\{x_i\}_{i=1}^k$ using a table look-up operation. The contents of the segment

identification (ID) and its corresponding candidate sequence are stored in ROM 1 and ROM 2, respectively, as shown in **Figure 2-5**, where the hardware architecture of the candidate generator is depicted. The found candidate symbol is first rotated into its original quadrant, and then the offset pair (X_offset, Y_offset) is added to the coordinates of the found candidate symbol. After the constellation restoration, the constellation boundary checker checks whether or not the found symbol lies inside the constellation boundary. If the found restored symbol is a legal one, the distance calculator calculates the value of $\|y_i'' - x_i\|^2$. Multiplying the value of $\|y_i'' - x_i\|^2$ by $r_{i,i}^2$ and adding the parent weight P_{i+1} to the multiplied result, we obtain the path weight P_i of the found symbol. The CSG can efficiently generate the coordination pairs of valid candidates and the associated path weights according to their path weights in an ascending order for each given received symbol. From **Figure 2-5**, the major hardware cost of the CSG involves 3 multipliers, 12 adders, and 2 ROMs. The ROM sizes (number of logic gates) are 2116 (ROM 1, with $u = 32$) and 731 (ROM 2), respectively, according the Synposys® synthesis tools.

For any given symbol and its neighbors, which share the same candidate sequence, the candidate sequence is generated from the k nearest constellation symbols by sorting their relative distance to the search center, though these distance values are different for each different search center. The proposed CSG utilizes this property to generate a candidate sequence in ascending order, and calculates the associated path weights so as to avoid a heavy load of path weight evaluations and sorting. Based on this concept, we can choose the appropriate k to fit the system requirement. The ROM size expands quickly when a large value of k is chosen. To remedy this, we can divide k into a set $\{k_i\}_{i=1}^p$ where $\sum_{i=1}^p k_i = k$ such that the ROM can be kept at a realizable size.

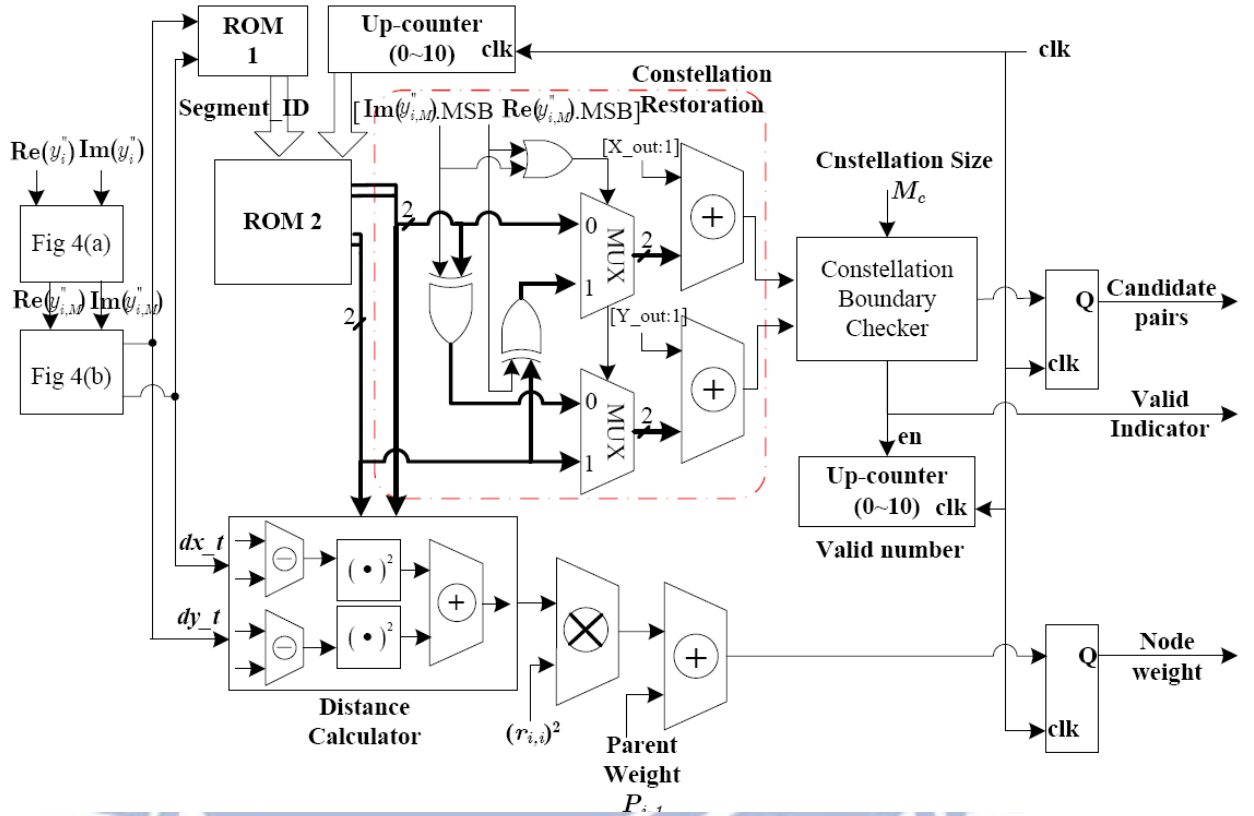


Figure 2-5: Hardware architecture of the candidate generator.

2.3.2 Architecture of Highly-Parallel Comparison Circuit (HPCC)

The sorting operations in the K -Best decoder dominate the major complexity at each search layer. Hence, sorting is a critical factor in reducing the complexity of the K -Best SDA. The previously proposed CSG module can be applied to the K -Best SDA by exploiting the inherent partial orders coming with the property of CSG. This can be efficiently accommodated by applying the K -merge algorithm [30], [33]. For a more practical implementation, an efficient architecture that can effectively reduce the sorting complexity is needed.

Recall the definitions of branch weights and PED in Section 2. Let $P_i^1, P_i^2, \dots, P_i^K$

denote the K smallest PEDs in the i th layer. After full path expansion, we have KM_c PEDs $P_{i-1}^{1,1}, P_{i-1}^{1,2}, \dots, P_{i-1}^{1,M_c}, \dots, P_{i-1}^{K,1}, P_{i-1}^{K,2}, \dots, P_{i-1}^{K,M_c}$ at layer i , where $P_{i-1}^{m,n}$ stands for the PED of the n th path expanded from the m th parent node at layer i . Moreover, based on the sorted results from the i th layer and the generated sequence from the proposed CSG module, we have $P_i^1 < P_i^2 < \dots < P_i^K$ and $P_{i-1}^{j,1} < P_{i-1}^{j,2} < \dots < P_{i-1}^{j,k}$ for each $1 \leq j \leq k$. Selecting the node with the smallest PED from the set $\{P_i^1, P_i^2, \dots, P_i^K\}$ is equivalent to finding the smallest PED from the full path expansion set containing KM_c nodes. These operations are illustrated in **Figure 2-6**. Exploiting these properties instead of using traditional sorting algorithms, we can realize an efficient comparison architecture for the K -Best sorting at each stage that avoids full path evaluation and significantly reduces the sorting complexity. **Figure 2-7** depicts this hardware architecture, and the following describes its operation.

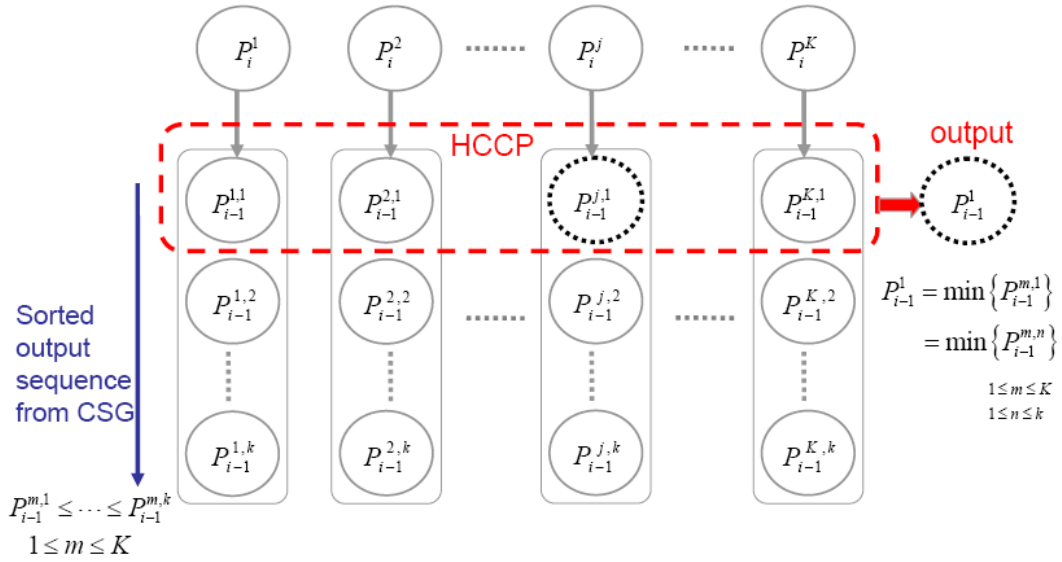


Figure 2-6: Illustration of the HPPC operations.

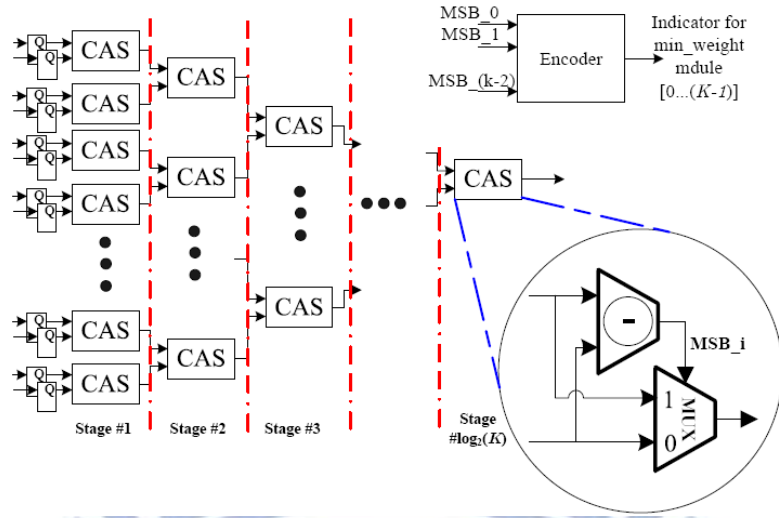


Figure 2-7: HPCC architecture.

The output sequence of the CSG module naturally forms a set in ascending order according to the evaluated PEDs while performing the N th layer search. We therefore only need to conduct a single coordination transformation and K path weight calculations. The generated results serve as the parent nodes of the next layer.

To search in the $(i - 1)$ th layer, we first calculate $\{P_{i-1}^{1,1}, P_{i-1}^{2,1}, \dots, P_{i-1}^{K,1}\}$ and feed them into the HPCC. The candidate node with the smallest PED among these candidates is obtained immediately after $(K - 1)$ compare-and-select (CAS) operations. If the chosen node comes from the p th parent node, then the $P_i^p + B_{i-1}^{p,2}$ PED is calculated, overwriting the previously-chosen node. The node with the 2nd smallest PED is obtained after $\log_2 K$ CAS operations (only $\log_2 K$ results need be re-computed). Repeating this procedure, we can successfully select K candidate nodes with the smallest PEDs from the entire valid candidate set. The survival set acts as the parent nodes of the $(i - 2)$ th layer. In searching the nodes in each layer, we use K coordination transformation, $(2K - 1)$ path weights evaluations, and $(K - 1)(1 + \log_2 K)$ CAS

operations. Note that the computational complexity of this approach is nearly fixed and independent of the constellation size M_c of the transmitted symbols. Furthermore, the nodes in the survival set still exhibit an ascending order according to their PEDs. In the final search layer, i.e., the 1st layer, we only need to choose the node with the smallest PED as the detection result. Hence, it takes only K coordination transformation, K PEDs evaluations, and $(K - 1)$ CAS operations.

Compared with the winner path expansion method [34]-[35], the proposed architecture, which is also frequently found in Viterbi decoder for choosing the minimal path metric, can avoid performing unnecessary operations thanks to the property of parallel computation. Moreover, it requires a smaller number of CAS $(K - 1)$ than that of the conventional bubble sort method (K) .

2.3.3 Complexity Advantages

Through the combination of the two proposed modules, we only need K coordination transformations, $(2K - 1)$ PED evaluations, and $(K - 1)(1 + \log_2 K)$ CAS operations in each layer to obtain K nodes with the smallest PEDs, regardless of the constellation size. These PEDs only need to be calculated when they are fed into the HPCC. Hence the proposed architecture avoids exhaustive path weight evaluations as required in the conventional bubble sort architecture.

Previous methods attempt to reduce computational complexity by eliminating the number of visited nodes based on the probability or statistical properties of the additive noise. These methods provide an approximate solution, and barter decoding performance for complexity reduction. As an alternative, this chapter presents another way to reduce complexity with the premise of carrying on high quality decoding results. The proposed approach utilizes operation decomposition, reconstruction, and associated efficient

hardware architecture to select and evaluate only the most promising candidate symbols. The proposed method also significantly reduces computational complexity and provides an efficient solution with a nearly fixed throughput. These advantages are further enhanced when a larger constellation size is adopted. Although the proposed method incurs the extra cost of coordination transformation and restoration, it eliminates many path calculations and sorting operations, and provides the same performance as the conventional K -Best SDA.

2.4 Proposed Search Strategy for Near-ML Performance

One way to reduce the complexity of the conventional K -Best SDA is to choose a smaller number of survival nodes in each layer. However, this can cause performance degradation in term of error rate. Instead of choosing a sufficiently large K to achieve the near-ML performance, a new search strategy is proposed. The proposed search strategy preserves all candidate symbols and performs the ML search in the preceding layers when dealing with poor channel conditions. Only K candidates are kept for the remaining lower layers. The following sections show how to determine the number of layers performing the ML search.

2.4.1 Preprocessing with Column Permutation

The channel matrix can be preprocessed with various techniques to reduce the complexity of candidate search and/or improve the performance of the K -Best SDA. Many preprocessing techniques can be used for this purpose, including column permutation [13], scaling [36] and lattice reduction [37]. In this chapter, column permutation is adopted, in which the permutation order is determined according to the

column norms of the channel matrix in ascending order. Given the QR decomposition of the ordered channel matrix $\mathbf{H}_o = \mathbf{Q}_o \mathbf{R}_o$, we characterize below the cumulative distribution function (cdf) of the square of the diagonal entries of \mathbf{R}_o denoted by $r_{o,i,i}^2$

(see the Appendix A):

for $i = 1$

$$F_{r_{o,i,i}^2}(r) = \int_0^r \frac{N!}{(N-1)!(M-1)!} \left[\sum_{k=0}^{M-1} \frac{x^k}{k!} e^{-x} \right]^{N-1} \cdot x^{M-1} e^{-x} dx \quad (2.14)$$

for $2 \leq i \leq N$

$$F_{r_{o,i,i}^2}(r) = C_{ii} \int_0^1 \int_0^{r/s} \left[1 - \sum_{k=0}^{M-1} \frac{x^k}{k!} e^{-x} \right]^{i-1} \left[\sum_{k=0}^{M-1} \frac{x^k}{k!} e^{-x} \right]^{N-i} \cdot x^{M-1} e^{-x} (s)^{M-i} (1-s)^{i-2} dx ds. \quad (2.15)$$

where

$$C_{ii} = \frac{N!}{(N-i)!(M-i)!(i-1)!(i-2)!}. \quad (2.16)$$

Comparing (2.14)-(2.16) with the results of [13], the ordering mechanism increases $E[r_{i,i}^2]$ in the preceding layers, producing two main benefits. First, for a fixed K in the K -Best SDA, increasing $E[r_{i,i}^2]$ in the preceding layers reduces the effective search range of the candidates. This in turn reduces the probability of the ML solution being dropped in the preceding layers. Another benefit is that it constrains the growth of the tree and hence reduces search complexity.

2.4.2 Proposed Search Strategy

For the N th layer, the candidate symbol should satisfy the following search

constraint according to (2.7):

$$\|y_N'' - x_N\|^2 \leq \left(\frac{d'}{r_{N,N}} \right)^2. \quad (2.17)$$

Clearly, $\frac{1}{r_{N,N}}$ will enlarge the constraint region when $r_{N,N}$ is smaller than 1. In this case, the probability of the ML solution being dropped will increase when only K nodes are kept in the N th layer. To avoid performance degradation, conducting the ML search in the preceding layers [27] is one of the approaches usually adopted. To further reduce the computational complexity, we propose to perform the ML search in the i th layer only when any $r_{i,i}$, where $N - L_{ML} + 1 \leq i \leq N$, is smaller than a given threshold T_r , with L_{ML} denoting the number of layers performing the ML search; the threshold T_r will be decided later. This proposed search strategy is named conditional-ML (CML) search. Hence, the number of layers performing the ML search depends on the distribution of $r_{i,i}^2$. Figs. **Figure 2-8(a)** and **Figure 2-8(b)** show the impact of $r_{N,N}$ on the constrained search region. Based on the derived results in (2.14)-(2.16), we can systematically determine the number of layers performing the ML search under different M and N .

Figure 2-9(a) shows the cdf curves of $r_{o,i,i}^2$ for the 4×4 MIMO channel. The probability of $r_{o,i,i}^2 < 1$ in the 4th layer is larger than that in the other layers. Hence, only the 4th layer needs to perform the ML search. **Figure 2-9(b)** shows the cdf curves of $r_{o,i,i}^2$ for the 8×8 MIMO channel. In this case, the probabilities of $r_{o,i,i}^2 < 1$ in the 8th and the 7th layers are larger than that in the other layers. However, the number of possible candidates in the 7th layer is $(M_c)^2$ in the worst case, which is too large to

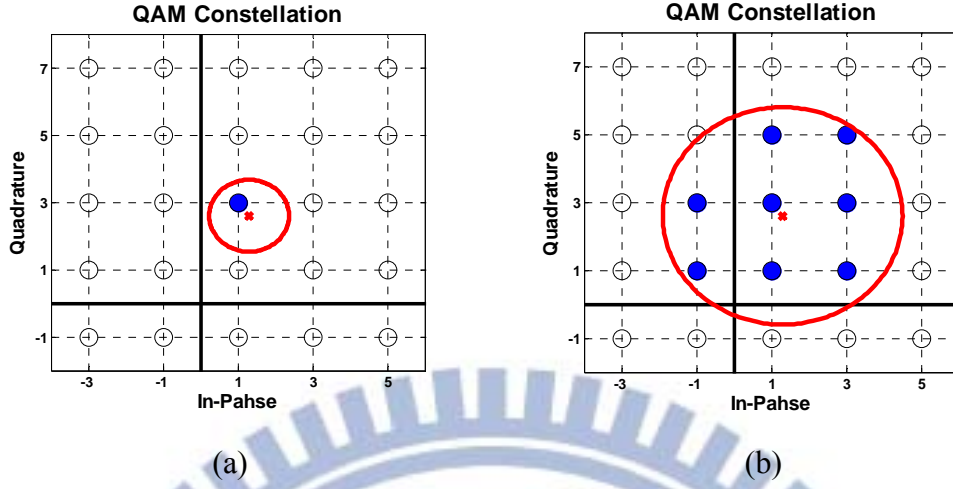


Figure 2-8: Search constraints of the N th layer with $d' = 1.1$.

(a) $r_{N,N} = 1$. (b) $r_{N,N} = 0.33$.

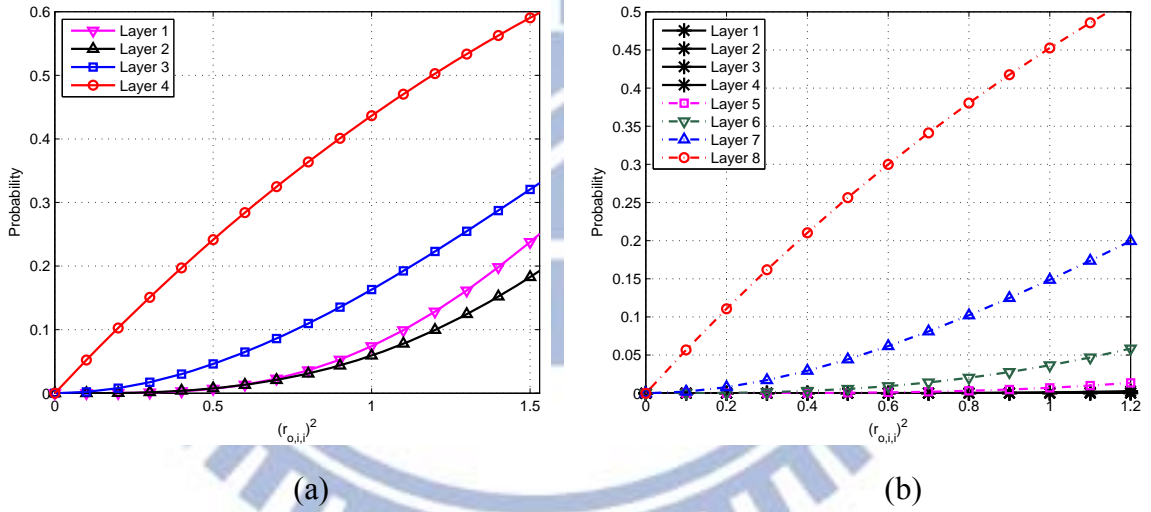


Figure 2-9: Cdf curves of $r_{o,i,i}^2$. (a) 4x4 MIMO channel. (b) 8x8 MIMO channel.

store in a hardware implementation when M_c is large. Hence, we keep all possible candidates in the 8th layer. For the 7th layer, we first find all possible candidates, and keep K survival nodes with the minimum path weights.

Next, we discuss how to decide the threshold T_r . Recall that for the N th layer, a search for the candidate symbols should satisfy the following constraint:

$$r_{N,N}^2 \|y_N'' - x_N\|^2 \leq (d')^2. \quad (2.18)$$

The proposed algorithm only keeps the k constellation symbols nearest to y_N'' where $k = \min(K, 11)$; hence, the value of $\|y_N'' - x_N\|^2$ has a limited range. The number 11 is chosen according to [38] which suggests that producing 11 candidate symbols yields quite good performance for practical applications. Therefore, we configure CSG to generate only 11 candidate symbols to reduce the implementation cost. From the previous argument and (2.18), it is straightforward to see that the threshold T_r can be chosen based on the following criterion:

$$T_r D \geq E\left[(d')^2\right], \quad (2.19)$$

$$D = \min(D_K, D_{11}), \quad (2.20)$$

where D_K and D_{11} denote the distances from the K th and 11th nearest constellation symbols to s_N respectively. $E\left[(d')^2\right]$ is the expected value taken with respect to the channel statistics; it is used in place of $(d')^2$ because d' is typically a random variable depending on the channel condition and SNR [10], [13].

By using (2.19), when the k nearest constellation symbols do not cover all the symbols inside the circle with a radius of $E\left[(d')^2\right]^{1/2}$, the ML search can be activated to retain all valid symbols. However, this will incur complexity increase because the probability of performing the ML search increases. The threshold T_r thus acts as a trade-off parameter between complexity and performance. Since $E\left[(d')^2\right]$ varies with SNR, we can choose $E\left[(d')^2\right]$ corresponding to the SNR at which the symbol error rate of the proposed K -Best SDA deviates from that of the ML detector by a certain normalized amount δ . This ensures that the performance of the proposed K -Best SDA

can be made close to ML detection. When applying the criterion in (2.19) to the $(N - 1)$ th layer and below, the obtained threshold is sure to be smaller than the threshold of the N th layer because the distance contributed by the N th layer is a positive value. Thus, we can use the threshold of the N th layer for other layers. In summary, the proposed CML search strategy only needs to check whether the values of $r_{o,i,i}$, that are already available from the QR decomposition, are smaller than T_r . It is not necessary to design any extra circuits to estimate the channel conditions for adjusting K as in [24].

By the proposed criterion in (2.19)-(2.20), the system performance is insensitive to the choice of K and the number of candidates generated by the CSG module. This is in contrast to the conventional K -Best SDA, in which the value of K must be large enough, usually close to the constellation size M_c , to archive near-ML performance. Using the proposed criterion with the self-adjustment mechanism, the proposed K -Best SDA can choose a smaller K , as small as a half of M_c , to archive near-ML performance. In fact, when a smaller value of K is chosen or the GSC module generates a shorter candidate sequence, the ML search will be activated more frequently trying to retain the possible ML solution.

The overall complexity of the proposed K -Best SDA can be predicted based on the complexity of the adopted sorting architecture, CML search procedure, choice of the value of K , the number of generated candidates of the CSG module, and the activation probability of the ML search. The decoder can thus achieve near-ML performance under a given complexity constraint without requiring a large value of K .

2.4.3 Joint 2-Layer ML Search Algorithm

According to the derived cdf of $r_{o,i,i}^2$ in (2.14)-(2.16) and observation in the previous sections, we only need to conduct a 2-layer full search in the worst case, which involve

choosing K survival nodes with the smallest path weights among $(M_c)^2$ nodes. In the original 2-layer ML search in the complex plane, for any received symbol, we need to evaluate all accumulated path weights between the search center and all valid candidate symbols while performing a full search of two layers. We then select K nodes with the smallest accumulated path weights.

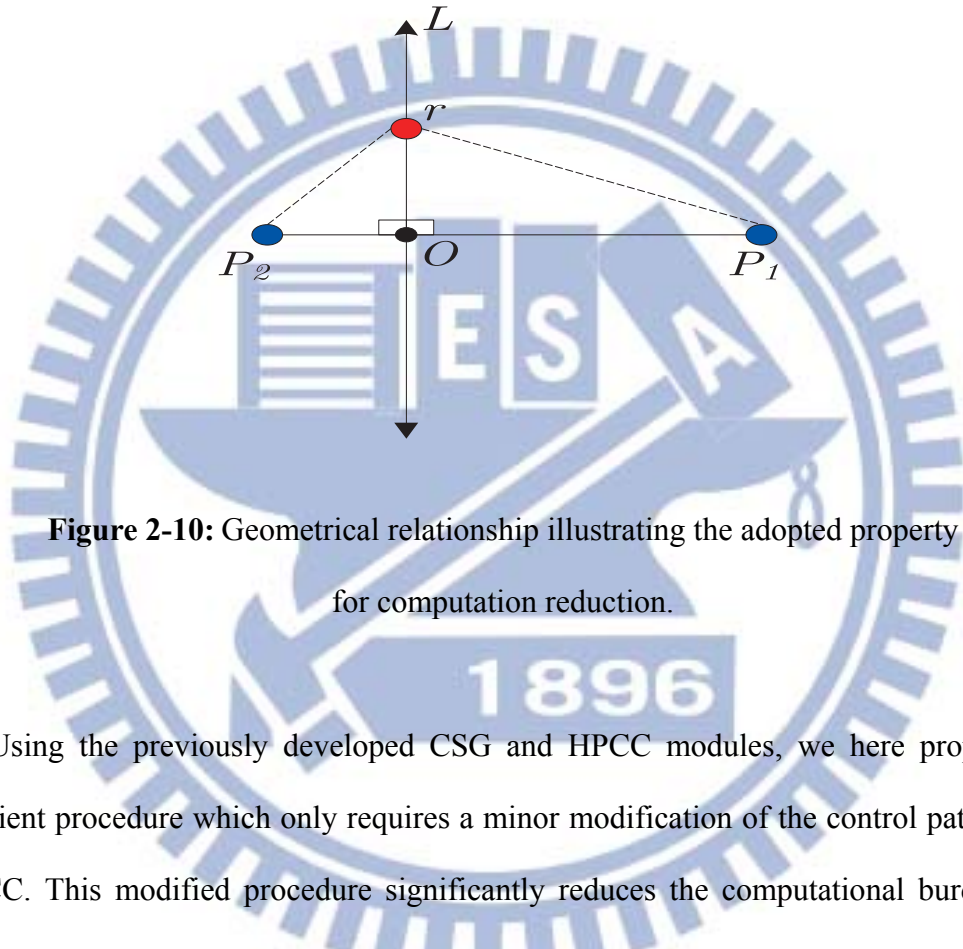


Figure 2-10: Geometrical relationship illustrating the adopted property for computation reduction.

Using the previously developed CSG and HPCC modules, we here propose an efficient procedure which only requires a minor modification of the control path of the HPCC. This modified procedure significantly reduces the computational burden and hardware implementation cost. The following describes the proposed procedure in detail:

First, for any received symbol in the complex plane, we evaluate the distances between the received symbol and all valid candidate symbols which lie on the same row of the square lattice before starting the sorting procedure. Consider the geometry shown in **Figure 2-10**. Let r lie on line L , which is perpendicular to $\overline{p_1p_2}$, and intersects with $\overline{p_1p_2}$ at o . It is easy to show that if $\overline{op_1} > \overline{op_2}$ then $\overline{rp_1} > \overline{rp_2}$. Using this property, these candidate symbols can be ordered by their coordinate values on the x-axis

following the SE enumeration rule [12]. Therefore, a table containing the row vectors of sorted candidate symbols for each x value would suffice and efficiently simplifies the sorting process [39].

Second, for any square lattice with M_c symbols, these candidate symbols can be divided into $\sqrt{M_c}$ groups. Each symbol in the same group has the same y-axis coordinate value. Based on the prepared table, the procedure can efficiently generate $\sqrt{M_c}$ groups. Each group contains $\sqrt{M_c}$ sorted candidate symbols for each received signal without any extra sorting operation. The structure of each sorted group is the same as the output sequence of the proposed CSG module in ascending order. Therefore, utilizing the HPCC, after $\sqrt{M_c} + K - 1$ path evaluations and $(\sqrt{M_c} - 1) + (K - 1)\log_2 \sqrt{M_c}$ CAS operations, the proposed procedure can generate K candidates with the smallest PEDs for each given received symbol. These selected K symbols are again arranged in ascending order according to their PEDs. Note that only these promising candidates are considered and completely evaluated.

Finally, when a full search of two layers is required, it is only necessary to repeat M_c times for M_c possible parent symbols to generate a total of KM_c promising symbols and divide them into M_c sorted groups. Each group is sorted in ascending order according to the evaluated PEDs. The HPCC is then utilized to choose the K survival symbols with the smallest PEDs. This can be done efficiently thanks to the naturally ascending order of each group.

The above procedure can achieve the same result as the ML exhaustive search, but its complexity is significantly reduced when K is small. The procedure fully re-utilizes the previously proposed hardware architecture as described in Section 3 except an extra memory is required for the intermediate storage. It also inherits the advantages of CSG

and HPCC which avoid the heavy load in path weight computation and sorting.

Tables 2.2 and **2.3** show the detailed computational complexity of the proposed K -Best SDA and the conventional K -Best SDA, respectively. Comparing the two tables, the required complexity of proposed K -Best SDA is approximately $\sqrt{M_c}$ times lower than the conventional one, and is insensitive to the constellation size M_c , as mentioned earlier in Section 3.2. Although extra computations are needed when the CML search is activated in the proposed SDA, the probability of activation is small, as long as the channel is not severely ill-conditioned. Therefore, the total required complexity of the proposed K -Best SDA can still be kept lower than that of the conventional SDA. As a final remark, since the proposed K -Best SDA can work with a smaller number of search layers and smaller value of K , compared to the conventional K -Best SDA, it has the potential of reducing the decoding latency of the latter because the decoding latency mainly depends on the number of search layers and required processing time per search layer, which in turn depends on K .

Table 2-2: COMPUTATIONAL COMPLEXITY OF PROPOSED K -BEST SDA
(EXCLUDING INTERFERENCE CANCELLATION)

	ML search deactivated		ML search activated		
	1st layer search	2nd layer search	Joint 2-layer ML search	3rd ~ (N - 1)th layer search	Nth layer search

CAS	0	$(K-1) \cdot (1 + \log_2 K)$	$M_c(K-1) \log_2(\sqrt{M_c}) + M_c(\sqrt{M_c} - 1) + m(2K-1) + (m-1)[\log_2(m) - 1]$	$(K-1) \cdot (1 + \log_2 K)$	$(K-1)$
Path Accumulation	0	$(2K-1)$	$M_c(\sqrt{M_c} + K - 1)$	$(2K-1)$	K
Path Calculation	K	$(2K-1)$	$M_c + M_c(\sqrt{M_c} + K - 1)$	$(2K-1)$	K

where $m = \begin{cases} \lceil M_c/K \rceil & \text{if } \text{mod}(M_c, K) == 0 \\ \lceil M_c/K \rceil + 1 & \text{otherwise} \end{cases}$

Table 2-3: COMPUTATIONAL COMPLEXITY OF CONVENTIONAL K -BEST SDA IN REAL DOMAIN (EXCLUDING INTERFERENCE CANCELLATION)

	1st layer search	2nd \sim $(2N-1)$ th layer search	2Nth layer search
CAS	$K\sqrt{M_c}$	$K^2\sqrt{M_c}$	$(K\sqrt{M_c} - 1)$
Path Accumulation	0	$K\sqrt{M_c}$	$K\sqrt{M_c}$
Path Calculation	$\sqrt{M_c}$	$K\sqrt{M_c}$	$K\sqrt{M_c}$

2.5 Computer Simulation and Discussions

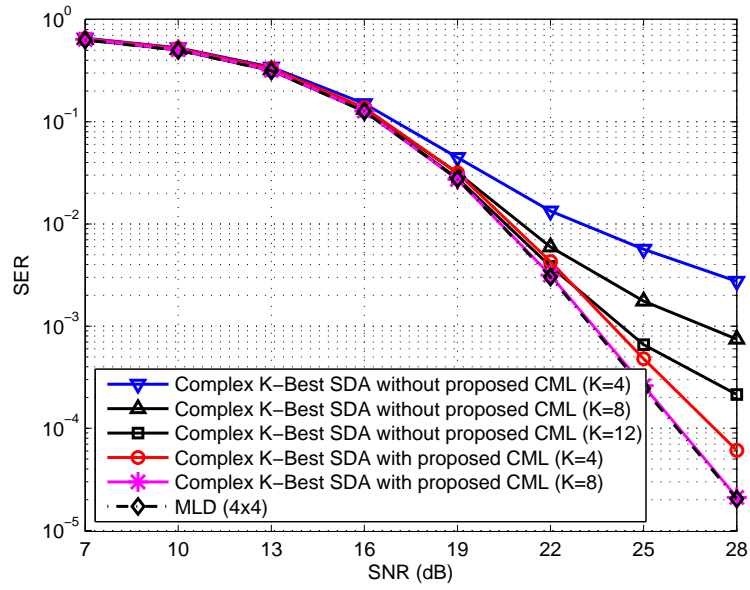
This section simulates the symbol error rate (SER) performance and complexity of the proposed K -Best SDA, and compares it with the SE SDA and conventional K -Best SDA [17]. Although many variants of the K -Best SDA have been proposed, the

conventional one has the best decoding performance and is chosen here as a benchmark. For a fair comparison in each simulation, the preprocessing technique mentioned in Section 4.1 is applied to all algorithms. Complexity is measured in terms of the average number of floating point operations (flops). All real additions, multiplications, memory read/write, and comparison are equally treated as flops. We set d' as the distance between the Babai estimate and the received signal [10], and $E[(d')^2]$ is then obtained in advance for each SNR as the average from 100000 independent trials. In each simulation, we generate 100 noise realizations per channel realization, and at least 5000 channel realization for each SNR value. The SER is obtained as the average from 500000 independent trials.

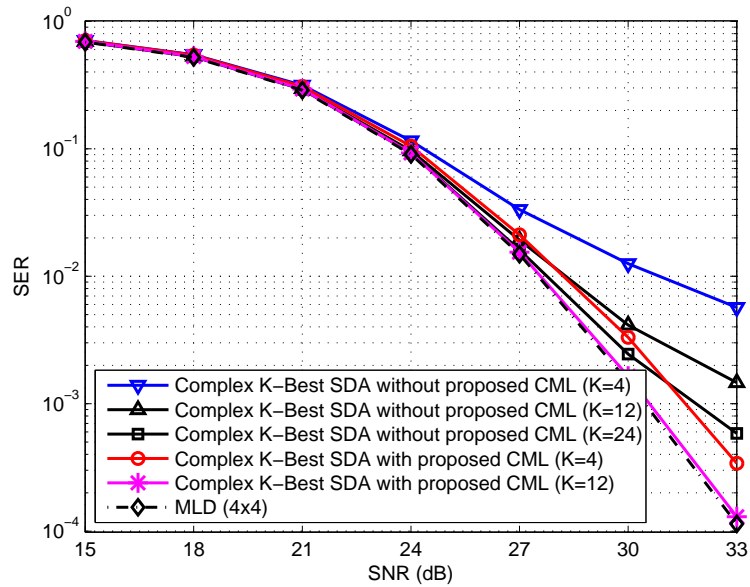
We first investigate the effectiveness of the proposed CML strategy by comparing the performance of the complex K -Best SDA, which is mentioned in Section 2, with various configurations. An extreme value of $K = 4$ is chosen for the complex K -Best SDA incorporating CML. Note that $K = 4$ is in general the maximal acceptable value for a MIMO-OFDM system, where the ML solution needs to be obtained for each sub-carrier. The normalized deviation of SER is set as $\delta = 15\%$, the threshold T_r is set as 0.42 according to (2.19), and the corresponding probability of performing the ML search is 9.08%, according to (2.14)-(2.16). On the other hand, the K values of the conventional complex K -Best SDA without CML are chosen as $K = 4, 8, 12$ for 4×4 16-QAM, and $K = 4, 12, 24$ for 64-QAM, respectively, to illustrate the performance difference. **Figure 2-11(a), (b)** show the 4×4 16-QAM and 64-QAM simulations of SER respectively. From the results, the complex K -Best SDA incorporating CML can significantly improve the decoding performance with a small K value. The reason is that the proposed CML strategy keeps all possible candidates in the first search layer when the channel is in a

poor condition, significantly reducing the probability of the ML solution being dropped. The conventional complex K -Best SDA needs to choose $K = 12$ and 24 respectively to achieve the similar performance. Such high K configurations would inevitably increase the computational complexity, decoding latency and infeasibility for practical MIMO-OFDM systems. For demonstration, we also include the cases of $K = 8$ and $K = 12$ for the complex K -Best SDA incorporating CML for 16-QAM and 64-QAM respectively. It is evident that both can achieve nearly the same performance as the ML detector.

Next, we evaluate the SER performance and complexity of the proposed complex K -Best SDA incorporating the CML strategy. **Figure 2-12(a)**, (b) and **Figure 2-13(a)**, (b), respectively, show the 4×4 16-QAM and 64-QAM simulations of SER and complexity with $K = 8$. The normalized deviation of SER is set as $\delta = 5\%$ and $\delta = 10\%$ respectively and the threshold T_r is set as 0.291 and 0.3532 respectively, according to (2.19), and the corresponding probability of performing the proposed ML search is 4.26% and 5.62% respectively, according to (2.14)-(2.16). Comparing **Figure 2-12(a)** with **Figure 2-13(a)**, the SER curves of the proposed K -Best SDA and the SE SDA are nearly the same. This shows that the threshold constraint significantly reduces the probability of performing the ML search and there is almost no performance degradation in the proposed K -Best SDA. In contrast, the SER of the conventional K -Best SDA tends to become saturated at high SNR. This is due to the fact that the conventional K -Best SDA with a smaller K drops the ML solution with a high probability when the channel is in poor conditions, which always occurs with a certain probability in practice. In the 64-QAM case, the proposed K -Best SDA achieves nearly a 3 dB gain over the conventional K -Best SDA at $\text{SER} = 10^{-3}$. Note that this performance gap between the proposed K -Best SDA and a conventional one is larger than that of the

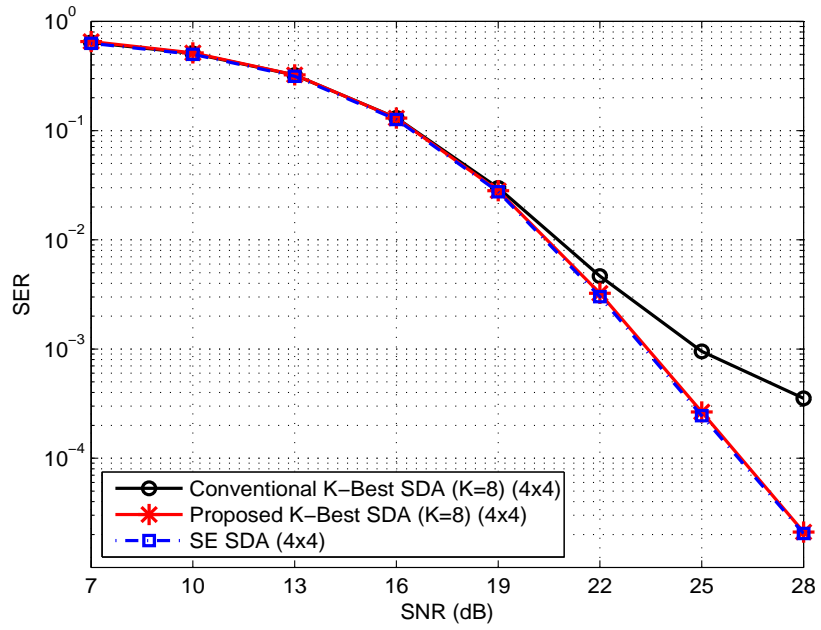


(a)

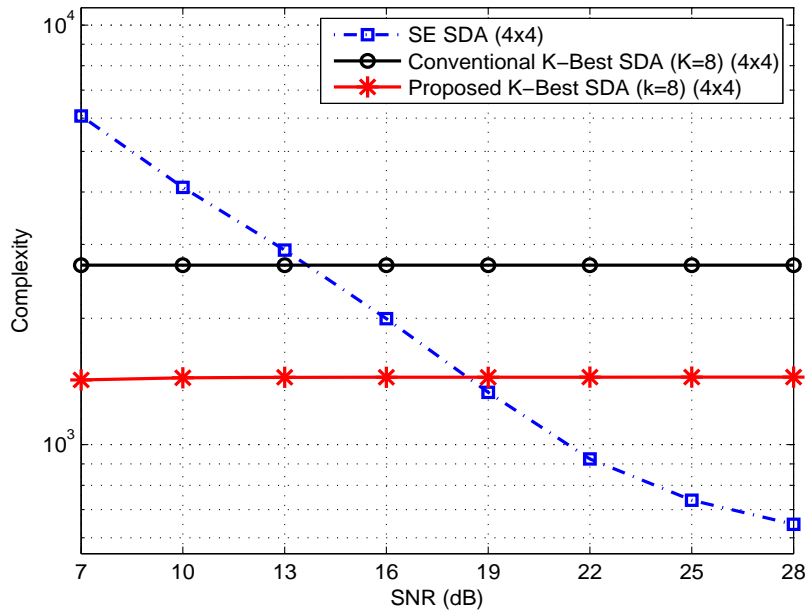


(b)

Figure 2-11: Performance of complex K -Best SDA for 4×4 MIMO systems. (a) 16-QAM modulation. $K = 4$ and 8 for complex K -Best SDA incorporating proposed CML strategy; $K = 4, 8$, and 12 for regular complex K -Best SDAs. (b) 64-QAM modulation. $K = 4$ and 12 for complex K -Best SDA incorporating proposed CML strategy; $K = 4, 12$, and 24 for regular complex K -Best SDAs.

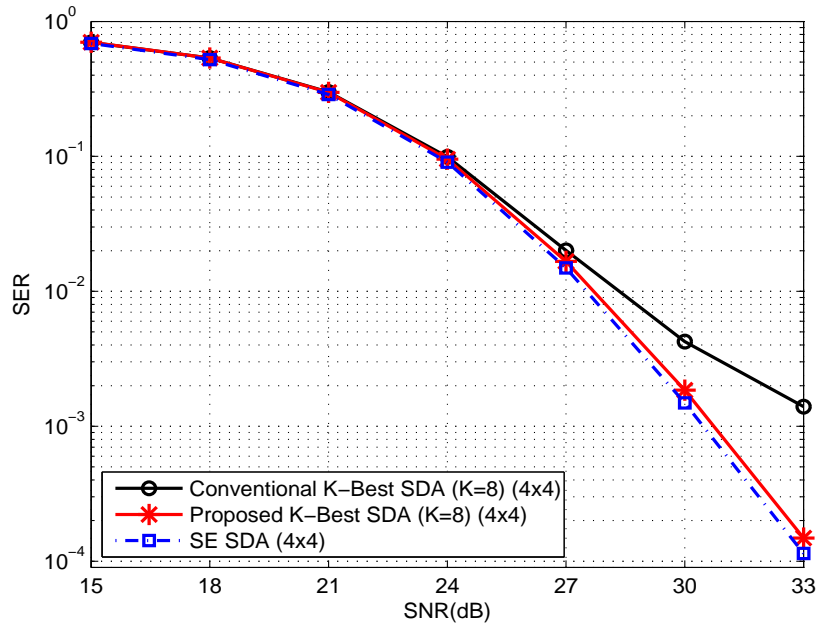


(a)

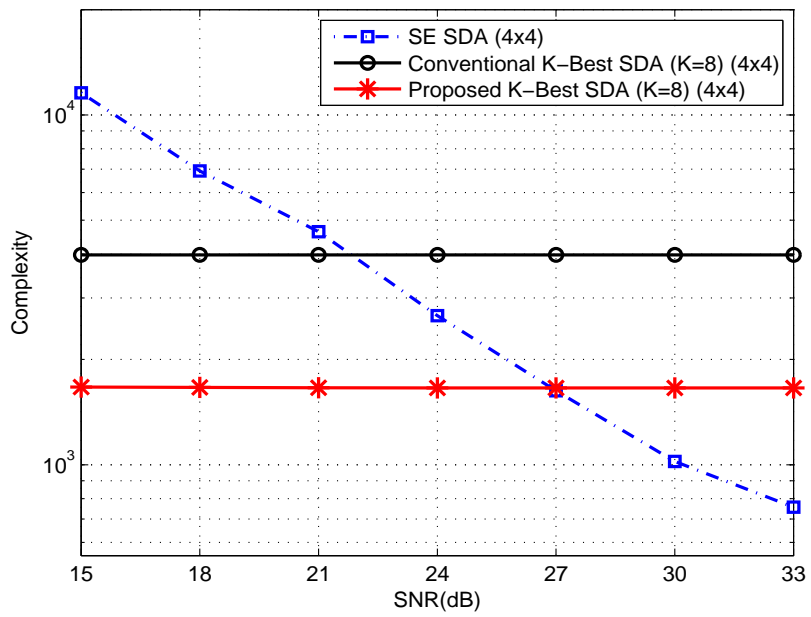


(b)

Figure 2-12: Performance and complexity of SDA for 4x4 MIMO systems with 16-QAM modulation. (a) SER. (b) Complexity. $K = 8$ for K -Best SDAs.



(a)

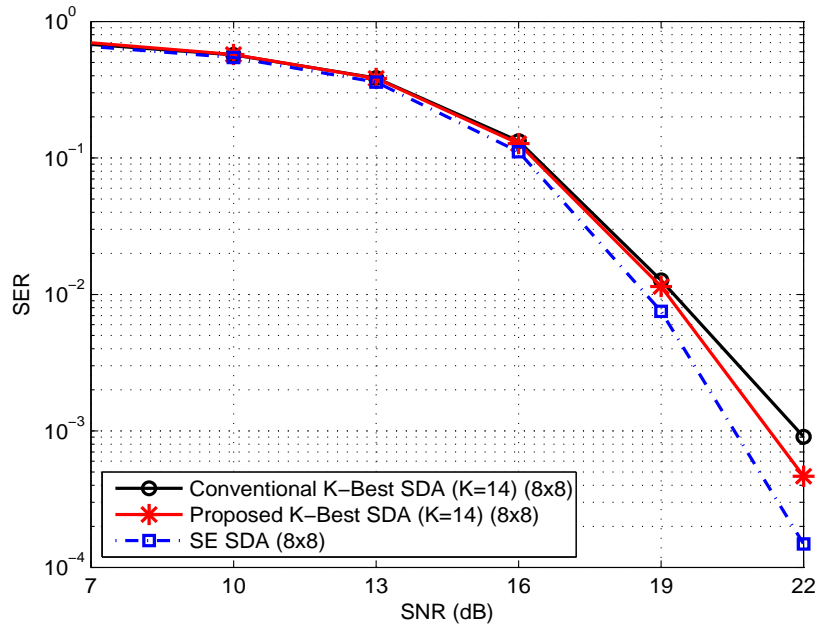


(b)

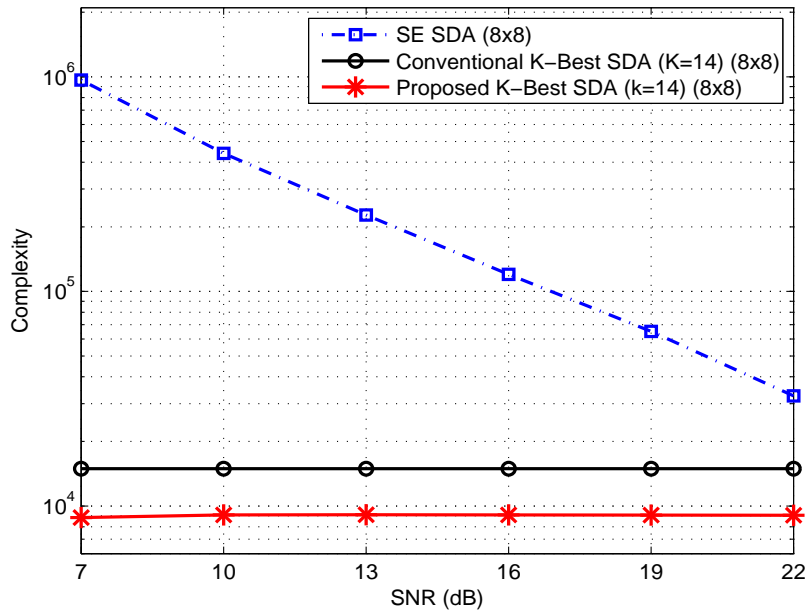
Figure 2-13: Performance and complexity of SDA for 4x4 MIMO systems with 64-QAM modulation. (a) SER. (b) Complexity. $K = 8$ for K -Best SDAs.

16-QAM case. This is because the probability of the ML solution being dropped increases as the modulation symbol alphabet becomes larger [17]. In contrast, the proposed CML search strategy keeps all possible candidates in the preceding layers, significantly reducing the probability of the ML solution being dropped. Comparing **Figure 2-12(b)** with **Figure 2-13(b)**, the proposed K -Best SDA has higher complexity than that of the SE SDA in the high SNR regime. This is due to the fact that the proposed K -Best SDA visits more candidate symbols than the SE SDA when the number of layers N is smaller. As shown in the simulation cases, the complexity of the SE SDA varies with SNR. This is not desirable in practice, because a steady SNR is not achievable in realistic wireless environments, such that the decoding throughput of the SE SDA cannot be stable. In contrast, the proposed K -Best SDA provides a nearly fixed throughput, with excellent performance and low complexity. The proposed efficient architecture reduces the number of path weight evaluations and sorting operations in each layer. As a result, the proposed K -Best SDA exhibits near-ML performance and reduces 46.62% and 58.14% complexity respectively over the conventional K -Best approach using the same K .

Figure 2-14(a) and **Figure 2-14(b)** show the 8×8 16-QAM simulations of SER and complexity with $K = 14$. The normalized deviation of SER is set as $\delta = 15\%$ and the threshold T_r is set as 0.833 and the corresponding probability of performing the proposed ML search is 43.9%. The probability of performing the ML search is higher than that of the 4×4 case because the probability of the ML solution being dropped in the K -Best SDA is higher in the 8×8 case. Again, the performance of the proposed K -Best SDA is better than the conventional K -Best SDA, and the complexity of the proposed K -Best SDA is lower than that of the SE SDA and the conventional K -Best SDA. Compared with the conventional K -Best SDA, the proposed method decreases complexity by more than 41.75%. Because the number of search layers is larger in this



(a)



(b)

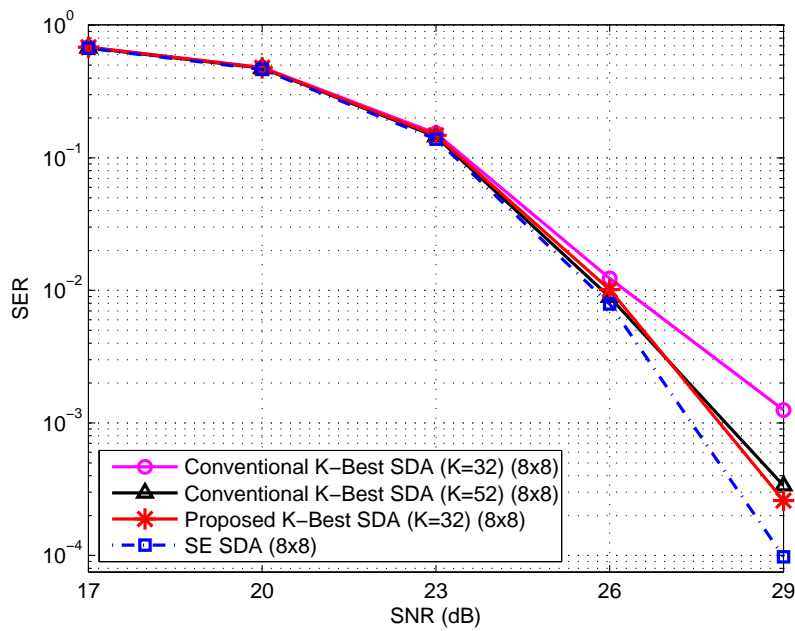
Figure 2-14: Performance and complexity of SDA for 8x8 MIMO systems with 16-QAM modulation. (a) SER. (b) Complexity. $K = 14$ for K -Best SDAs.

case, the proposed method reduces more complexity in path evaluations and sorting operations. In the 8×8 case, the value of K must be set larger to reduce the probability of the ML solution being dropped in the preceding layers. Hence, the gap in complexity between the proposed K -Best SDA and the conventional K -Best SDA is smaller than that in the 4×4 case. We can further improve the performance of the proposed K -Best SDA by choosing a higher threshold.

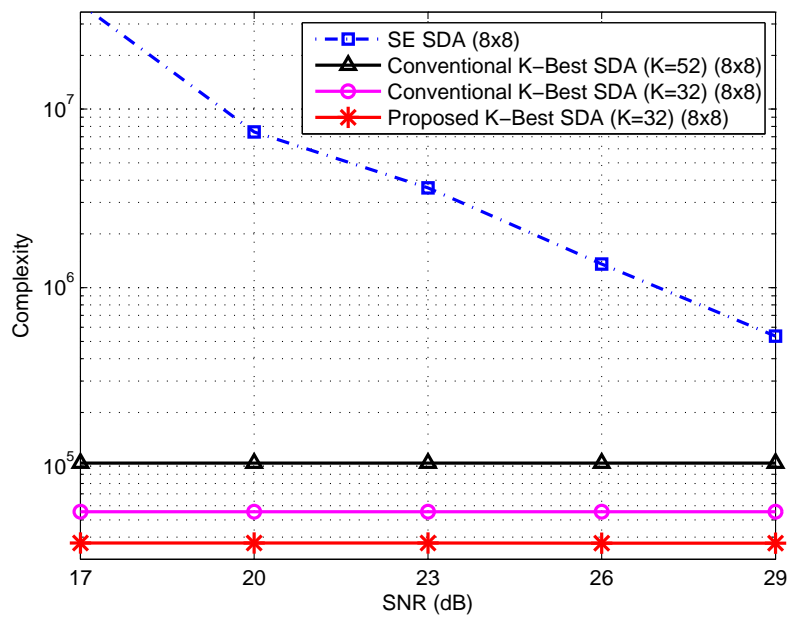
Figure 2-15(a) and **Figure 2-15(b)** show the 8×8 64-QAM simulations of SER and complexity with $K = 32$. The normalized deviation of SER is set as $\delta = 15\%$ and the threshold T_r is set as 1.143 and the corresponding probability of performing the ML search is 65.8%. In this case, the proposed K -Best SDA still works better than the conventional K -Best SDA. The gap in complexity between the proposed K -Best SDA and the conventional K -Best SDA is smaller than that in the 8×8 16-QAM case. This is because a higher threshold value causes the ML search operations to occur more frequently, though the proposed efficient sorting method reduces much more complexity for a larger modulation alphabet. The proposed CML search procedure significantly reduces the amount of path evaluations, but induces extra memory read/write and table access operations. Nevertheless, the proposed K -Best SDA still has lower average complexity than the conventional one. Finally, under the same channel conditions, the conventional K -Best SDA requires $K = 52$ to achieve near-ML performance.

The configuration increases the computational complexity and decoding latency. The proposed decoder with $K = 32$ can provide nearly the same performance, reducing 53.45% computational complexity over the conventional K -Best SDA with $K = 52$.

This section simulates the SER performance and complexity of the proposed SDA and compares it with the SE SDA and the conventional K -Best SDA. Although the value of $r_{o,i,i}$ does not directly reflect the channel condition in all cases, the proposed criterion



(a)



(b)

Figure 2-15: Performance and complexity of SDA for 8x8 MIMO systems with 16-QAM modulation. (a) SER. (b) Complexity. $K = 32$ for proposed K -Best SDA; $K = 32$ and 52 for conventional K -Best SDAs.

does help the decoder successfully produce a near ML solution over poor channels, without always performing the ML search in the preceding layers. This systematic approach thus requires fewer ML search layers than previous methods [23], [27]. The simulation results confirm that the proposed decoder exhibits excellent performance and requires lower complexity than the conventional K -Best SDA. It is also worth noting that the performance of the proposed decoder is close to that of the SE SDA (i.e., ML performance).

2.6 Summary

In this Chapter, we propose a modified K -Best SDA with a new sorting algorithm and search strategy to achieve near-ML performance with low complexity. In conventional K -Best SDA, path weight evaluation and sorting operations for all valid candidate symbols comprise the major computational cost in each search layer. The new CSG generates candidate sequences in the complex plane instead of producing actual path weights, thus making it possible for the child nodes of each parent node to be sorted without any extra effort. Combining the CSG with a highly-parallel comparison circuit, the proposed SDA can reduce computational complexity, while maintaining the same performance as the conventional K -Best SDA. To further improve decoding performance and efficiency, the new search strategy performs the ML search at a few preceding layers. A judicious criterion is proposed accordingly to determine when to activate the ML search. Simulation results show that the proposed SDA effectively reduces the complexity of the conventional K -Best SDA while offering superior SER performance at the high SNR regime. Its decoding performance is close to the ML performance even when the chosen value of K is small.

To facilitate practical applications of the proposed SDA, a corresponding hardware

architecture is also proposed. As such, the proposed SDA is suitable for real-time applications and provides a promising solution for next generation MIMO wireless communication systems such as IMT-Advanced.



Chapter 3

Geometry Based SDA for Under-determined MIMO systems

3.1 Overview

In [51], an underdetermined system incorporating conventional Turbo codes as adopted in IEEE 802.16 can achieve a very low bit error rate ($10^{-5} \sim 10^{-6}$) at an SNR of less than 10 dB for $(3, 2)^\dagger$ and $(4, 3)$ systems. The decoding complexity of well known existing decoders is still too high in low SNR regime especially when the antenna number is large. In practical systems, the decoding algorithm is often conducted in lower SNR regime and jointly operated with channel coding techniques. As a remedy, the conventional receiver usually introduces certain preprocessing techniques to reduce the complexity and/or improve the decoding performance. Unfortunately, these proposed methods cannot be directly applied into GSD-family decoders to significantly reduce the complexity due to the distinct search strategy in underdetermined problems.

In this chapter, we will propose a geometry-based efficient decoder for underdetermined MIMO systems. The proposed decoder involves two stages. First, an improved slab search algorithm [55] efficiently obtains valid candidate points within a given slab. Next, a multi-slab based decoding algorithm finds the optimal solution by taking intersections of the obtained candidate set with dynamic radius adaptation. By doing so, there is no need to perform SDA sequentially. The proposed decoder can thus

[†] The notation (N_t, N_r) is used to denote a MIMO system with N_t transmit antenna and N_r receive antennas.

provide near ML performance with much lower (non-exponential) complexity compared to SSD. Furthermore, we propose an optimal preprocessing technique from the geometrical perspective and conduct comprehensive analysis on the complexity reduction. By introducing the proposed preprocessing scheme, the incorporated decoder can significantly reduce the decoding complexity in the low SNR regime without sacrificing performance. The advantage is useful and suitable for practical MU-MIMO operations.

3.2 Signal Model for Underdetermined SDA

Consider an MIMO system with N_t transmit antennas and N_r receive antennas. The received signal vector is denoted as $\tilde{\mathbf{y}} = [\tilde{y}_1 \ \tilde{y}_2 \ \cdots \ \tilde{y}_{N_r}]^T \in \mathbb{C}^{N_r \times 1}$, where \tilde{y}_m is the received signal at the m th receive antenna. Similarly, the transmitted signal vector is denoted as $\tilde{\mathbf{x}} = [\tilde{x}_1 \ \tilde{x}_2 \ \cdots \ \tilde{x}_{N_t}]^T \in \mathbb{Z}^{N_t} [j]$, where $\mathbb{Z}[j] := \{a + jb | a, b \in \mathbb{Z}\}$ is the set of Gaussian integers [13] and \tilde{x}_n is the transmitted signal at the n th transmit antenna. The transmitted signal constellation is assumed to be an ordinary Q-QAM system, and the corresponding average transmit energy per antenna is $E_s = E[\tilde{x}_i^2] = 2, 10, \text{ and } 42$ for $Q = 4, 16, \text{ and } 64$, respectively. Let $\tilde{\mathbf{H}}$ denote the $N_r \times N_t$ channel matrix whose entry $\tilde{h}_{i,j}$ is the channel gain from the j th transmit antenna to the i th receive antenna. Assume that the channel is frequency-flat fading and remains constant over a frame duration, and that the entries of the channel matrix $\tilde{\mathbf{H}}$ can be regarded as i.i.d. complex Gaussian random variables with zero-mean and unit variance, i.e., $\tilde{h}_{i,j} \sim CN(0,1)$. The relationship between the received signal vector and the transmitted signal vector can be expressed as

$$\tilde{\mathbf{y}} = \tilde{\mathbf{H}}\tilde{\mathbf{x}} + \tilde{\mathbf{n}}, \quad (3.1)$$

where $\tilde{\mathbf{n}} = [\tilde{n}_1 \ \tilde{n}_2 \ \dots \ \tilde{n}_{N_r}]^T \in \mathbb{C}^{N_r \times 1}$ is the i.i.d. complex additive white Gaussian noise (AWGN) vector with zero-mean and covariance matrix $\sigma^2 \mathbf{I}_{N_r}$.

A commonly practiced alternative to the complex MIMO detections is to reformulate the model in the real domain by performing real-value decomposition (RVD) on the complex signal model:

$$\mathbf{y} = \begin{bmatrix} \text{Re}(\tilde{\mathbf{y}}) \\ \text{Im}(\tilde{\mathbf{y}}) \end{bmatrix}, \quad \mathbf{x} = \begin{bmatrix} \text{Re}(\tilde{\mathbf{x}}) \\ \text{Im}(\tilde{\mathbf{x}}) \end{bmatrix}, \quad \mathbf{n} = \begin{bmatrix} \text{Re}(\tilde{\mathbf{n}}) \\ \text{Im}(\tilde{\mathbf{n}}) \end{bmatrix}, \quad \mathbf{H} = \begin{bmatrix} \text{Re}(\tilde{\mathbf{H}}) & -\text{Im}(\tilde{\mathbf{H}}) \\ \text{Im}(\tilde{\mathbf{H}}) & \text{Re}(\tilde{\mathbf{H}}) \end{bmatrix}, \quad (3.2)$$

which yields

$$\mathbf{y} = \sum_{i=1}^N \mathbf{h}_i x_i + \mathbf{n} = \mathbf{H}\mathbf{x} + \mathbf{n}, \quad (3.3)$$

where \mathbf{h}_i is the i -th column vector of channel matrix \mathbf{H} , $\mathbf{x} \in \Lambda^{2N_t \times 1} \subset \mathbb{Z}^{N \times 1}$, $\mathbf{y} \in \mathbb{R}^{M \times 1}$, $\mathbf{n} \in \mathbb{R}^{M \times 1}$, $\mathbf{H} \in \mathbb{R}^{M \times N}$, $N = 2N_t$ and $M = 2N_r$. Note that $\Lambda = \{\pm 1, \dots, \pm(\sqrt{Q} - 1)\}$ for Q-QAM systems. After RVD, each component x_i of \mathbf{x} is chosen from a set Λ of integer numbers with \sqrt{Q} elements and Q is the constellation size.

Remarks:

(1). After RVD operation, the received signal \mathbf{y} at i th received antenna can be expressed as $y_i = h_{i1}x_1 + h_{i2}x_2 + \dots + h_{iN}x_N + n_i$. The corresponding probability density function (pdf) can be approximated as a Gaussian random variable with zero mean and the variance is equal to $\frac{NE_s}{4} + \sigma_n^2$.

(2). The $\{\mathbf{h}_1, \mathbf{h}_2, \dots, \mathbf{h}_N\}$ set is still an i.i.d Gaussian Random vector set, i.e., $\mathbf{h}_i \sim N\left(\mathbf{0}, \frac{1}{2}\mathbf{I}_M\right)$.

(3).The received signal vector \mathbf{y} , noise vector \mathbf{n} and $\{\mathbf{h}_1, \mathbf{h}_2, \dots, \mathbf{h}_N\}$ are mutually independent random vectors.

The ML detector searches all possible combinations of transmitted symbols via the following criterion [10]:

$$\hat{\mathbf{x}} = \arg \min_{\mathbf{x} \in S} \|\mathbf{y} - \mathbf{H}\mathbf{x}\|^2, \quad (3.4)$$

where S denotes the set of all possible transmitted symbol vectors whose size is $(\sqrt{Q})^N$. The computational complexity of ML detection grows exponentially with N . Therefore, it is difficult to be implemented at the receiver in practice.

For an overdetermined MIMO system with $M \geq N$, SDA has been proposed to achieve the ML performance with low complexity [10]. The basic idea of SDA is to restrict the search region within the interior of a hyper-sphere of radius C centered around the received signal vector \mathbf{y} :

$$\|\mathbf{y} - \mathbf{H}\mathbf{x}\|^2 \leq C^2. \quad (3.5)$$

By conducting QR-decomposition of \mathbf{H} , the decoding process of SDA, which iteratively search for the candidates $x_N, x_{N-1}, \dots, x_2, x_1$ can be regarded as a tree search problem. For an underdetermined MIMO system with $M < N$, SDA fails to identify a unique solution. The GSD was first proposed to cope with the issue of underdeterminedness, but its complexity is high [42]. The SSD algorithm has been proposed to achieve a more efficient search for (3.5) [50]. The SSD algorithm first performs QR-decomposition of \mathbf{H} , leading to

$$\|\mathbf{y}' - \mathbf{R}\mathbf{x}\|^2 \leq C^2, \quad (3.6)$$

where $\mathbf{y}' = \mathbf{Q}^T \mathbf{y}$. With $M < N$, we have

$$-C \leq y'_M - (r_{M,M}x_M + \dots + r_{M,N}x_N) \leq C \quad (3.7)$$

at the M th layer. Eq. (3.7) involves a detection in an $(N-M+1)$ -dimensional subspace, and is similar to a real-valued MISO problem [51], [56]. SSD then employs a 2-stage decoder, consisting of the plane decoding algorithm (PDA) and slab decoding algorithm (SLA), to obtain the constellation points (defined by $\mathbf{H}\mathbf{x}$) falling inside the slab described by (3.7) via $(N-M+1)$ 1-dimensional searches. These points form the candidate point set, and each point in the set can be substituted into (3.6) to obtain

$$\|\mathbf{y}_G - \mathbf{R}_1 \mathbf{x}_G\|^2 \leq C^2 - \left[y'_M - \sum_{j=M}^N r_{Mj} x_j \right]^2, \quad (3.8)$$

where $\mathbf{x}_G = [x_1, x_2, \dots, x_{M-1}] \in \mathbb{Z}^{M-1}$, $\mathbf{y}_G = [y_1, y_2, \dots, y_{M-1}] \in \mathbb{R}^{M-1}$ and $\mathbf{R}_1 \in \mathbb{R}^{M-1 \times M-1}$ consists of the first $M-1$ columns and rows of \mathbf{R} . Since \mathbf{R}_1 is a full rank upper triangular matrix, SDA can be adopted to find the ML solution for each given candidate point. Finally, the candidate point yielding the smallest Euclidean distance in (3.6) is chosen as the solution.

Although SSD achieves lower complexity than existing decoders, it has certain disadvantages. First, the PDA and SLA are independently and sequentially executed, leading to multiply evaluated 1-D searches when the transmit-receive antenna number difference is large. Second, the execution of SDA incurs a high computational load when the number of candidate points and/or M is large.

3.3 Proposed Decoding Algorithms for Underdetermined Systems

In this section, a new decoder is developed which further reduces the complexity of SSD. The decoder consists of two geometry based algorithms for finding the candidate points and performing decoding, respectively.

3.3.1 An Efficient Slab Search (ESS) Algorithm

The proposed search method is similar in principle to PDA and SLA, but requires the execution of only a single algorithm, such that multiple 1-D searches or candidate point searches can be avoided.

From (3.7), two boundary equations can be formulated. Along each 1-D search, two intersection points (one for the upper bound and the other for the lower bound) which satisfy the boundary equations can be obtained. The candidate points can then be determined to include those points falling inside the slab, i.e., points whose coordinates associated with the 1-D search lie between the two intersection points.

Consider a generalized slab described by the equation $\left| \sum_{i=1}^N w_i x_i - y \right| \leq C$. The proposed slab searching algorithm is summarized as follows:

Initialization

- For each candidate point, define a corresponding vector D_V , which acts as an indicator as to which dimensions have been visited. The “1” is for corresponding dimension having been searched, and “0” is for not having been searched. $D_V = [0, 0, \dots, 0] \in \mathbb{Z}^N$ indicates no dimensions have been visited in the beginning.
- For each candidate point, define a corresponding distance $dist = \left| \sum_{i=1}^N w_i x_i - y \right|$.
- Denote as X , X_V and X_{in} the sets that store, respectively, the candidate

points to be visited, the points having been visited, and the points falling inside the slab. Initialize with $X = X_V = X_m = \phi$, the empty set.

- Define a working variable $p = [p_1 \ p_2 \ \dots \ p_N]^T \in \mathbb{R}^N$, which represents the points involved in the current 1-D search. Initialize with $p = 0$.

Step1: Arbitrarily choose an initial point $x_{\text{int}} = [x_1^{\text{int}} \ x_2^{\text{int}} \ \dots \ x_N^{\text{int}}]^T$ and put it in X and X_V . Retrieve x_{int} from X and store it in p .

Step 2: If X is empty and p is 0, go to Step 5; otherwise, choose an arbitrary k such that the k th element of D_V is 0. Then calculate the upper and lower bounds:

$$x_{k,\text{up}} = p_k - \frac{\Delta y(p)}{w_k} + C, \quad x_{k,\text{low}} = p_k - \frac{\Delta y(p)}{w_k} - C,$$

$$\text{where } \Delta y(p) = \sum_{i=1}^N w_i p_i - y.$$

Step 3: In Step 2, candidate points lying between the two boundaries are obtained. If these points are not in X_V , add them to X , X_V and X_m . Set the k th entry of the corresponding D_V to be "1". Then calculate the corresponding *dist* using $\Delta y(\bullet)$. Next, construct two candidate points by replacing the k th entry of p by $(\lfloor x_{k,\text{up}} \rfloor + d)$ and $(\lfloor x_{k,\text{low}} \rfloor - d)$, respectively, where d is the minimum distance between constellation points. If these two points are not in X_V , add them to X and X_V . Set the k th entry of the corresponding D_V to be "1". So far, the k th 1-D search associated with point p has been evaluated; the k th entry of the corresponding D_V is set to be "1".

Step 4: If all entries of D_V corresponding to p are "1" or p does not satisfy the

search criterion $(x_{k,low} \leq p_k \leq x_{k,up})$, then retrieve an arbitrary point from X to replace the current p ; otherwise, p remains unchanged. Go to Step 2.

Step 5: Terminate the algorithm. Save the points in X_{in} and their corresponding distances $dist$.

Note: If X is an empty set and a point from X is to be selected, then set p to be 0.

3.3.2 A Multi-slab Sphere Decoding (MSSD)

Algorithm

With the candidate point set available, a decoding algorithm is next proposed. In SSD, only the last slab equation (Slab M) is used, as seen in (3.7). This may lead to an insufficient utilization of the available information and lower decoding efficiency. The proposed algorithm utilizes all available slab equations instead to find the optimal solution in an efficient way.

After performing ESS algorithm, a candidate set satisfying the (3.7) can be efficiently obtained. Hence, (3.5) can be rewritten as follows:

$$\sum_{i=1}^M \left[y_i' - \sum_{j=i}^N r_{ij} x_j \right]^2 \leq C^2. \quad (3.9)$$

The total number of slab equations included in (3.9) is M and each slab can be labeled with a corresponding ID:

$$\text{Slab } i : -C \leq y_i' - \left[r_{i,i} x_i + \dots + r_{M,N} x_N \right] \leq C. \quad (3.10)$$

The associated Euclidean distance of each candidate point obtained from Slab i equation is denoted as $dist_i$. Assume that radius C is large enough to include the ML

solution. Conducting the ESSD algorithm for both Slabs i and j , two candidate sets, i.e., $X_{in(i)}$ and $X_{in(j)}$ can be obtained and both contain the ML solution. The ML solution can be found inside the intersection of the two sets. However, it is inefficient to take the intersection of candidate sets sequentially because this would require a large memory size and many checking operations. As a remedy, the 2nd stage algorithm, i.e., the MSSD algorithm, utilizes all available slab equations in (3.5) instead of finding the optimal solution in an efficient way.

First, Slab M in (3.10) is chosen to obtain the candidate set using the proposed slab searching algorithm. Next, for each point $[x_M, x_{M+1}, \dots, x_N]$ in the obtained candidate set, the following augmented radius constraint

$$D_{M,M-1} = \left\| \begin{bmatrix} y'_{M-1} \\ y'_M \end{bmatrix} - \begin{bmatrix} r_{M-1,M-1} & r_{M-1,M} & \cdots & r_{M-1,N} \\ 0 & r_{M,M} & \cdots & r_{M,N} \end{bmatrix} \begin{bmatrix} x_{M-1} \\ x_M \\ \vdots \\ x_N \end{bmatrix} \right\|^2 \leq C^2 \quad (3.11)$$

is evaluated to determine x_{M-1} . The corresponding distance $dist_{M-1}$, upper bound $x_{M-1,up}$ and lower bound $x_{M-1,low}$ can be found by the following equations according to (3.11):

$$x_{M-1,up} = \frac{\sqrt{C^2 - (dist_M)^2} + \left(y'_{M-1} - \sum_{j=M}^N r_{M-1,j} x_j \right)}{r_{M-1,M-1}},$$

$$x_{M-1,low} = \frac{-\sqrt{C^2 - (dist_M)^2} + \left(y'_{M-1} - \sum_{j=M}^N r_{M-1,j} x_j \right)}{r_{M-1,M-1}},$$

$$dist_{M-1}^2 = \left(y'_{M-1} - \sum_{j=M-1}^N r_{M-1,j} x_j \right)^2 + (dist_M)^2.$$

Note that the two bounds define the region in which x_{M-1} lies. Those points which

do not satisfy (3.11) are discarded. By doing so, a new candidate set is obtained to include the intersection of candidate sets associated with Slabs M and $M-1$. To further reduce the decoding complexity, a radius shrinking strategy is also adopted after a new candidate set is updated. The minimal Euclidean distance associated with ZF-SIC solution among the updated candidate set will be used as the new radius. The procedure is executed successively until Slabs 2 and 1 to obtain the intersection of sets associated with all slabs. Finally, the point in the intersection with the smallest Euclidean distance $dist_1$ is the decoded solution. Hence the algorithm does not need to perform the demanding SDA on the candidate set in SSD. The detail procedure of MSSD algorithm is listed as follows:

Initialization

- Define a working variable *state* which records the internal state about radius shrinking. Initialize *state* with ‘RADIUS_INC’. Set $i = M$.

Step 1: Perform radius constraint evaluation in (11) for $D_{i,i-1}$. A $(N-i+2)$ -dimensional point is chosen from the updated candidate set with the minimum distance $dist_i$, to obtain the corresponding $(N-i+2)$ -dimensional zero-forcing SIC (ZF-SIC) solution. The Euclidean distance in (4) associated with the ZF-SIC solution is then calculated and denoted as C_{new} .

Step 2: Adjust the search radius using the internal variable *status* and obtain C_{new} from Step 1 according to the two rules: (1). **if** *state* = ‘RADIUS_DEC’ **then** { C_{new} replaces C if $C_{new} < C$; otherwise C remains unchanged.}

(2). **if** $state = \text{'RADIUS_INC'}$ **then** $\{C_{\text{new}}$ replaces C and change the state variable to 'RADIUS_DEC' if $C_{\text{new}} \leq C$; otherwise increase radius C such that the probability of ML solution falling inside the search region increases to γ according to Section IV.A in [10]. }

Step 3: When the point in the intersection with the smallest Euclidean distance $dist_1$ is obtained, or the candidate set becomes empty, terminate the procedure; otherwise set $i = i - 1$ and go to Step 1.

Note: If the candidate set at a certain stage becomes empty, then ZF-SIC is regarded as the decoding solution.

The proposed method also significantly reduces computational complexity and provides an efficient solution. These advantages are further enhanced when a larger constellation size is adopted.

3.4 Proposed Preprocessing Technique for Complexity Reduction

From the Section 3.3, the decoding complexity of the two-stage decoding algorithm depends on the number of candidate points (N_p) of the initial candidate set. In order to reduce the decoding complexity, N_p needs to be as small as possible. To ensure this, we propose an efficient preprocessing scheme to further reduce the decoding complexity and give a lower bound analysis of the proposed scheme.

3.4.1 A Preprocessing with Column Permutation

Performing QR decomposition, the rotated received signal vector \mathbf{y}' can be

represented as

$$\mathbf{y}' = [y'_1, y'_2, \dots, y'_M]^T = [\mathbf{q}_1^T \mathbf{y}, \mathbf{q}_2^T \mathbf{y}, \dots, \mathbf{q}_M^T \mathbf{y}]^T \in \mathbb{R}^M, \quad (3.12)$$

where $\mathbf{Q} = [\mathbf{q}_1 \ \mathbf{q}_2 \ \dots \ \mathbf{q}_M] \in \mathbb{R}^{M \times M}$. Generally, $|y'_M|$ represents the distance from the origin to the slab, as shown in **Figure 3-1**. In **Figure 3-1**, we assume that the selected slab equation is $h_1 x_1 + h_2 x_2 = y$, where h_i is a constant and y is a variable, and we define $|y'_M|$ as the location index of slab (ξ). It is obvious that N_p is small when ξ is larger. Therefore, we can properly choose the slab to maximize ξ for reducing the decoding complexity.

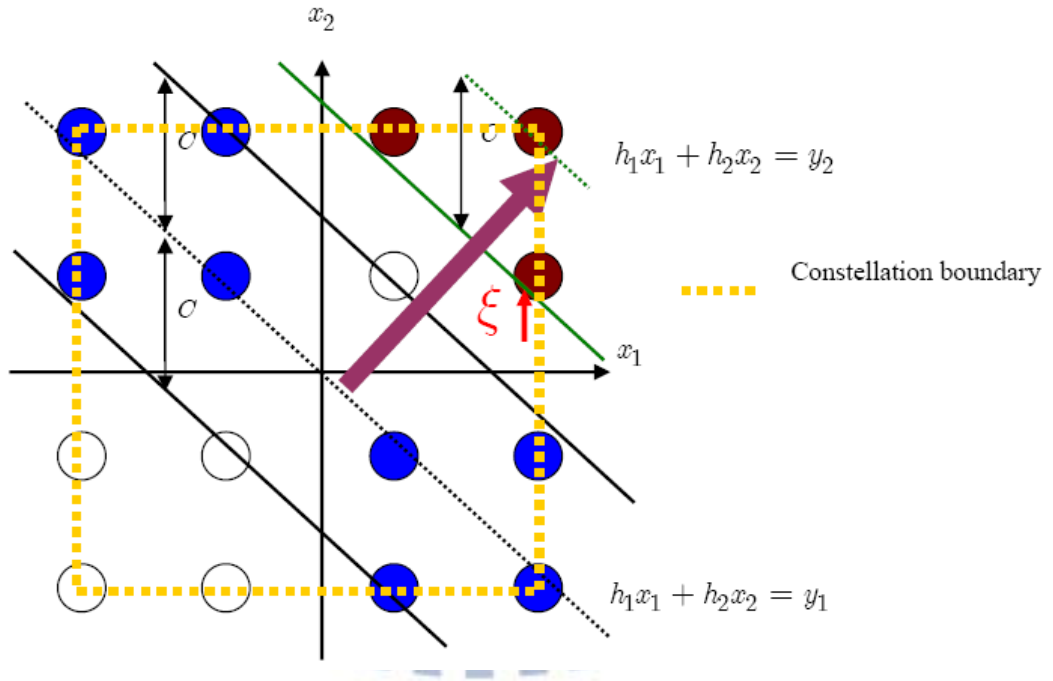


Figure 3-1: Geometrical diagram of slabs with different y .

Since different reordering rules of channel columns before QR decomposition will result in different \mathbf{q}_M . The optimization problem can be reformulated as finding the appropriate \mathbf{q}_M such that the value of $|y'_M|$ is maximal. The channel column reordering

is formulated as $\mathbf{H}\mathbf{P}$, where \mathbf{P} is a permutation matrix. It is well known that performing an exhaustive search for all permutation cases can obtain the optimal ordering, but the computational complexity (C_{N-M+1}^N) is large when the number of column vectors is large. In this subsection, an alternative approach of ordering scheme is proposed to avoid the exhaustive search and obtain good performance. The algorithm is developed according to the following two lemmas.

Lemma 1: Given the QR decomposition of the ordered channel matrix $\mathbf{H}_o = \mathbf{Q}_o \mathbf{R}_o$, the value of $|y'_M|$ only depends on the received signal vector \mathbf{y} and permutation of first $(M-1)$ column vectors of ordered channel matrix \mathbf{H}_o .

Proof: The channel matrix can be represented as $\mathbf{H} = [\mathbf{H}_1 \mathbf{H}_2]$, where $\mathbf{H}_1 \in \mathbb{R}^{M \times M}$ and $\mathbf{H}_2 \in \mathbb{R}^{M \times (N-M)}$. Performing the QR decomposition to matrix \mathbf{H}_1 yields $\mathbf{H}_1 = \mathbf{Q}_1 \mathbf{R}_1$. Furthermore, the channel matrix can be represented as $\mathbf{H} = \mathbf{Q}_1 [\mathbf{R}_1 \quad \mathbf{Q}_1^T \mathbf{H}_2]$. Therefore, the y'_M can be obtained by $\mathbf{q}_M^T \mathbf{y}$. Due to \mathbf{Q}_1 is a unitary matrix, \mathbf{q}_M can be uniquely decided when $\mathbf{q}_i, i=1, \dots, (M-1)$ are available and all diagonal elements of \mathbf{R}_1 are constrained to be positive values.

Lemma 2: The problem of maximizing $|y'_M|$ is equivalent to finding a unitary matrix \mathbf{Q}_1 such that the summation of the correlations of the first $(M-1)$ bases of \mathbf{Q}_1 with respect to the received vector \mathbf{y} is minimized.

Proof: Due to $\|\mathbf{y}'\|^2 = \|\mathbf{Q}_1^T \mathbf{y}\|^2 = \|\mathbf{y}\|^2$, the squared norm of \mathbf{y}' can be expressed as $\|\mathbf{y}'\|^2 = \sum_{i=1}^M (y'_i)^2 = \sum_{i=1}^{M-1} (y'_i)^2 + |y'_M|^2$; therefore, the problem of maximizing $|y'_M|$ is

equivalent to minimizing the term $\sum_{i=1}^{M-1} (y'_i)^2$ and then the original problem can be reformulated as minimizing $\sum_{i=1}^{M-1} (\mathbf{y}^T \mathbf{q}_i)^2$. In other words, the optimization problem is equivalent to finding an unitary matrix \mathbf{Q}_1 such that the summation of the correlations of the first $(M-1)$ bases of \mathbf{Q}_1 with respect to the received vector \mathbf{y} is minimized.

According to the aforementioned two derived lemmas, we propose two special ordering rules, namely, the projection ordering rule and greedy ordering rule. The QR decompositions with the two rules are referred to as Projection QR and Greedy QR decompositions, respectively.

Projection QR Decomposition: The procedure of the Projection QR decomposition is presented as follows.

Step1: Calculate the projected norm $\{\|\langle \mathbf{y}, \mathbf{h}_i \rangle\|\}_{i=1}^N$, where \mathbf{h}_i is the i th column of \mathbf{H} .

Step2: Find the permutation matrix \mathbf{P} such that the projected norm of the permuted matrix \mathbf{HP} from the left to right, are in ascending order.

Step3: Apply the standard QR decomposition to the permuted matrix \mathbf{HP} , yields $\mathbf{H}_o = \mathbf{Q}_o \mathbf{R}_o$.

Greedy QR Decomposition: The proposed Greedy QR decomposition consists of N recursive steps and can be described as follows:

Step1: Initialization of the vector set $\mathbf{V} = \{\mathbf{h}_i, i = 1, 2, \dots, N\}$ and the loop with index $k = 1$ is performed.

Step 2: If $k = M$, goes to Step 4; otherwise, the lowest correlation between \mathbf{y} and \mathbf{h}_i from \mathbf{V} is chosen according to the criterion $j = \arg \min_{1 \leq i \leq (N-k+1)} \{\|\langle \mathbf{y}, \mathbf{h}_i \rangle\|\}$. Afterwards,

the chosen vector should be normalized to be \mathbf{q}_k and discard the selected \mathbf{h}_j from \mathbf{V} .

Step 3: \mathbf{V} is then updated by $\mathbf{h}_i = \mathbf{h}_i - \langle \mathbf{h}_i, \mathbf{q}_k \rangle \mathbf{q}_k, \forall i$; then k is set to $k+1$, and go to Step 2.

Step 4: A column vector is randomly chosen from \mathbf{V} and is normalized to be \mathbf{q}_M . Finally, r_{jk} can be computed by $r_{jk} = \mathbf{q}_j \cdot \mathbf{h}_k$, where $j = 1, 2, \dots, k-1$ to obtain the QR decomposition of the reordering \mathbf{H} .

In summary, the projection norm ordering rule statically permutes the column vector of channel matrix according to absolute value of projected amount between received signal vector \mathbf{y} and each column vector of channel matrix \mathbf{h}_j in ascending order. The result suffers from the interference caused by other non-orthogonal column vectors. In contrast, the greedy ordering rule always attempts to eliminate these interferences at each search loop, so that the correlation between \mathbf{y} and k th column vector of \mathbf{Q} matrix can be as small as possible without performing exhaustive search.

3.4.2 Complexity Analysis

To our best knowledge, the distribution of y'_M with greedy ordering rule is difficult in obtaining an analytical form due to the dynamic column selection during iterative processing. Therefore, instead, a lower bound is analyzed here. Recalling the projection ordering rule, the channel matrix is re-ordered according to absolute value of each projection; therefore, we first define N random variables $z_i, 1 \leq i \leq N$:

$$z_i = |\mathbf{y}^T \mathbf{h}_i| = \left| \sum_{k=1}^M y_k h_{ki} \right|, \quad 1 \leq i \leq N, \quad (3.13)$$

and then derive the corresponding pdf as

$$f_{z_i}(z) = \begin{cases} \frac{2}{\sqrt{2\pi\sigma_z^2}} e^{-\frac{z^2}{2\sigma_z^2}} & z \geq 0 \\ 0 & z < 0 \end{cases}, \quad \text{where } \sigma_z^2 = M \sqrt{\frac{1}{2} \left(\frac{NE_s}{4} + \sigma_n^2 \right)}. \quad (3.14)$$

The distribution of y'_M depends on the distribution of diagonal elements of matrix \mathbf{R} , and also on the order of channel matrix. Therefore, we need to characterize the distribution of ordered channel vectors. For analyzing the distribution, the two random variables z_i defined in (3.13) and h_{1i} are paired and denoted as (z_i, h_{1i}) , where the h_{1i} is the first entry of the column vector \mathbf{h}_i . Based on remark (2) and (3) mentioned in Section II, it can be easily shown that these paired random variables $(z_i, h_{1i})_{i=1}^N$ are i.i.d. random variable pairs. Hence, the joint density functions of the paired random variables, denoted as $f_{z_i, h_{1i}}(z, h)$, can be obtained and expressed as follows:

$$f_{z_i, h_{1i}}(z, h) = \begin{cases} \frac{2}{\sqrt{2\pi\sigma_k^2}} e^{-\frac{z^2}{2\sigma_k^2}} \frac{2}{\sqrt{2\pi}} e^{-h^2} & z \geq 0 \\ 0 & z < 0 \end{cases}, \quad (3.15)$$

where $\sigma_k^2 = \frac{\sigma_z^2}{M} \left(h^2 \frac{2\sigma_z^2}{M} + (M-1) \right)$. Furthermore, we arrange these z_i ($1 \leq i \leq N$) in ascending order as $z_{1:N} \leq z_{2:N} \leq \dots \leq z_{N:N}$; then the h_{1i} ($1 \leq i \leq N$) paired with these order statistics are denoted by $h_{[1:N]}, h_{[2:N]}, \dots, h_{[N:N]}$. Since $(z_i, h_{1i})_{i=1}^N$ are i.i.d. random variables, the conditional pdf of $h_{[i:N]}$ given $z_{i:N} = z$ can be obtained by $f_{h_{[i:N]}}(h|z_{i:N} = z) = f(h|z)$. Hence, the statistical property of each ordered column vector $\mathbf{h}_{[i:N]}$ can be obtained by $f_{z_{i:N} h_{[i:N]}}(z, h) = f(h|z) f_{z_{i:N}}(z)$ and expressed as

$$\begin{aligned}
f_{h_{[i:N]}}(h) &= \int_{-\infty}^{\infty} f(h|z) f_{z_{i:N}}(z) dz = \int_{-\infty}^{\infty} \frac{f_{z_i h_i}(z, h)}{f_{z_i}(z)} f_{z_{i:N}}(z) dz \\
&= \frac{2I_{N,i}(h)N!}{\pi\sigma_k^2(i-1)!(N-i)!} e^{-\frac{h^2}{2}},
\end{aligned} \tag{3.16}$$

where $I_{N,i}(h) = \int_0^{\infty} e^{-\frac{z^2}{2\sigma_k^2}} \{F_{z_i}(z)\}^{i-1} \{1-F_{z_i}(z)\}^{N-i} dz$.

Furthermore, by performing the QR decomposition of the ordered channel matrix $\mathbf{H}_o = \mathbf{Q}_o \mathbf{R}_o$ according to the proposed projection ordering rule, we can characterize the cumulative distribution function (cdf) of the M th square of the diagonal entry of \mathbf{R}_o , denoted by $r_{o,M,M}^2$, as

$$\begin{aligned}
F_{r_{o,M,M}^2}(r) &= \int_0^1 \left\{ \int_0^{\frac{r}{s}} f_{w_{o,M},s_M}(w,s) dw \right\} ds = \int_0^1 \int_0^{\frac{r}{s}} f_{w_{o,M}}(w) f_{S_s}(s) dw ds \\
&= C \int_0^1 \int_0^{\frac{r}{s}} \int_{-\infty}^{\infty} \frac{1}{|w|} f_w(w) f_g\left(\frac{z}{w}\right) [F_z(z)]^{M-1} [1-F_z(z)]^{N-M} dz \left(s^{\frac{1}{2}} (1-s)^{\frac{(M-3)}{2}} \left(\frac{M-2}{2}\right)! \right) dw ds,
\end{aligned} \tag{3.17}$$

where $C = \frac{1}{\beta(M, N-M+1) \cdot \beta\left(\frac{M-1}{2}, \frac{1}{2}\right)}$. The detailed derivation of (3.17) is shown in Appendix B. Hence, according to (3.7), the random variable y'_M can be expressed as follows:

$$y'_M = r_{o,MM} x_{o,M} + \sum_{i=M+1}^N r_{o,M,i} x_{o,i} + \tilde{n}_M, \tag{3.18}$$

where $x_{o,i}$ is the corresponding transmitted symbol to the ordered channel vector $\mathbf{h}_{[i:N]}$.

In fact, the distribution function of $x_{o,i}$ is discrete uniform distribution and independent to channel ordering.

Lemma 3: The random variables $r_{M,i}$ and $h_{[i:N]}$ have the same pdfs

for $i = M + 1, \dots, N$.

Proof: The ordered channel matrix can be represented as $\mathbf{H}_o = [\mathbf{H}_{o,1} \mathbf{H}_{o,2}]$, Performing the QR decomposition to matrix $\mathbf{H}_{o,1}$ yields $\mathbf{H}_{o,1} = \mathbf{Q}_{o,1} \mathbf{R}_{o,1}$. Furthermore, the channel matrix can be represented as $\mathbf{H}_o = \mathbf{Q}_{o,1} [\mathbf{R}_{o,1} \quad \mathbf{Q}_{o,1}^T \mathbf{H}_{o,2}] = \mathbf{Q}_o \mathbf{R}_o$, where $\mathbf{H}_{o,2} = [\mathbf{h}_{[M+1:N]}, \dots, \mathbf{h}_{[N:N]}]$. The elements $r_{i,j}$ of the matrix \mathbf{R}_o can be obtained by $r_{i,j} = \mathbf{q}_i^T \mathbf{h}_{[M+1:N]}$ for $i = 1, \dots, M$, and $j = M + 1, \dots, N$. It is well known that the pdf of a Gaussian random vector is invariant under the orthogonal transformation by \mathbf{Q}_o . Therefore, The random variables $r_{M,i}$ and $h_{[i:N]}$ have the same pdfs for $i = M + 1, \dots, N$.

According to the Lemma 3 and substituting (3.16) and (3.17) into (3.18), the pdf of y'_M can be obtained by numerical approach.

Recalling the motivation of the proposed ordering scheme, we appropriately choose a specific slab for maximizing ξ for reducing the decoding complexity because the average decoding complexity can be expressed in terms of N_p , which is proportional to the intersectional volume of the constellation space and the specific (M th) slab for a given radius C . The N_p can be obtained by the approximated formulation proposed in [50] as follows:

$$N_p = \begin{cases} \left(2|Q|^{N-1} - 1\right) \left[1 - \left(\frac{y}{R}\right)^2\right]^{(N-1)/2} + 1 & \text{if } |y| \leq C, \\ 1 & \text{otherwise} \end{cases}, \quad (3.19)$$

where Q denotes the element number of QAM set. Hence, the expected value of N_p can be expressed as follows:

$$E[N_p(y)] = \int_C^\infty f_y(y)dy + \int_{-\infty}^{-C} f_y(y)dy + \int_{-C}^C \left\{ (2|Q|^{K-1} - 1) \left[1 - \left(\frac{y}{R} \right)^2 \right]^{\frac{(K-1)}{2}} + 1 \right\} f_y(y)dy, \quad (3.20)$$

where $f_y(y)$ denotes the associated pdf of the random variable y according to the given slab equation. Therefore, we can evaluate the expected value of N_p obtained by ESSD algorithm with and without projection ordering rule by substituting the pdf of y'_M and y_M into (3.20), respectively. Furthermore, the complexity reduction ratio, denoted by η , of the projection ordering rule is defined as

$$\eta = \frac{N_{p, \text{without_ordering}} - N_{p, \text{with_ordering}}}{N_{p, \text{without_ordering}}} = 1 - \frac{E[N_{o,p}(y'_M)]}{E[N_p(y_M)]}. \quad (3.21)$$

By the above procedure and the analytical results of (3.18), the average complexity reduction ratio can be also obtained by the numerical method instead of the time-consuming Monte-Carlo trials.

In this section, based on the searching philosophy of the efficient decoder proposed in Section III, we further propose a preprocessing scheme to reduce the decoding complexity from the geometrical perspective. The sub-optimal ordering rule is also analyzed; furthermore, the complexity reduction ratio can be obtained in an analytical form. The statistical properties of diagonal elements of \mathbf{R} matrix are crucial in the performance of the QR based detector. Appropriately ordered channel matrix can effectively generate the desired statistical properties of diagonal elements of \mathbf{R} matrix. An analytical framework to characterize statistical properties of diagonal elements of \mathbf{R} matrix under the general ordering rules is presented. The mathematical procedure can be applied to any static ordering rule even in non-linear ordering rule for QR based MIMO decoder.

3.5 Computer Simulation and Discussions

First, we evaluate the decoding performance and complexity of the proposed decoder presented in Section 3.3.1 and 3.3.2. The complexity is measured in terms of the average number of floating point operations (flops) and includes all involved operations (e.g. QR decomposition). All real additions, multiplications, and comparison are treated equally as flops. The radius C is chosen according to [10] with $\Phi = 0.99$, $\Delta = 0.01$ [50], and $\gamma = [0.9985 \ 0.9994 \ 0.9996 \ 0.99965 \ 0.9997 \ 0.99975]$. The SE-SDA [12] is adopted in SSD for finding the optimal solution. Note that the performance of SSD is the same as the ML detector.

We first investigate the SER performance of the proposed decoder with 16-QAM modulation, and compare the results with the (4, 4) ML detector. **Figure 3-2** shows that the performance of the proposed decoder is close to the ML performance with a slight loss in the high SNR regime. This is because the proposed decoder adopts the ZF-SIC solution when the updated candidate set becomes empty. The underdetermined system exhibits performance degradations compared to the (4, 4) system as expected. Note that for the underdetermined system, the total transmit power is normalized such that each stream is assigned less power than that of the (4, 4) system. This contributes to part of the performance loss of the (5, 4) and (4, 3) systems. As we can see in Figs. 8 and 9 of [50], an underdetermined system incorporating conventional Turbo codes as adopted in

IEEE 802.16 can achieve a very low bit error rate ($10^{-5} \sim 10^{-6}$) at an SNR of less than 10 dB for (3, 2) and (4, 3) systems. Such decoding performance is well acceptable for practical wireless communications, ascertaining the feasibility of underdetermined systems for MU-MIMO applications.

We next consider the 64-QAM modulation and evaluate the SER performance and complexity for the same set of MIMO systems. **Figure 3-3(a)** shows the same trend as in **Figure 3-2**, confirming that the proposed decoder is reliable for high order modulation. **Figure 3-3(b)** shows that the complexity of the proposed decoder is significantly lower than that of SSD. For instance, at SNR = 27dB, the complexity reduction ratio are 76.27% and 94.1%, respectively, for the (4,3) and (5,4) systems.

Afterwards, we investigate the probability density function of $|y'_M|$ under the aforementioned various ordering rules and show in **Figure 3-4** for a (4, 2) 16-QAM underdetermined MIMO system at SNR = 15dB. From **Figure 3-4**, the pdf of $|y'_M|$ using the proposed greedy ordering rule, with the advantage of lower complexity, shows that the probability density of $|y'_M|$ tends to be distributed away from the origin and is almost identical to the pdf of the exhaustive search approach. On the other hand, the results also show that the projection ordering rule is still an effective approach.

Furthermore, we choose 16-QAM underdetermined MIMO system with $N_r = 2$, $N_t = 3, 4$, and 5, respectively, and set SNR = 15 dB. The complexity reduction ratio of N_p is

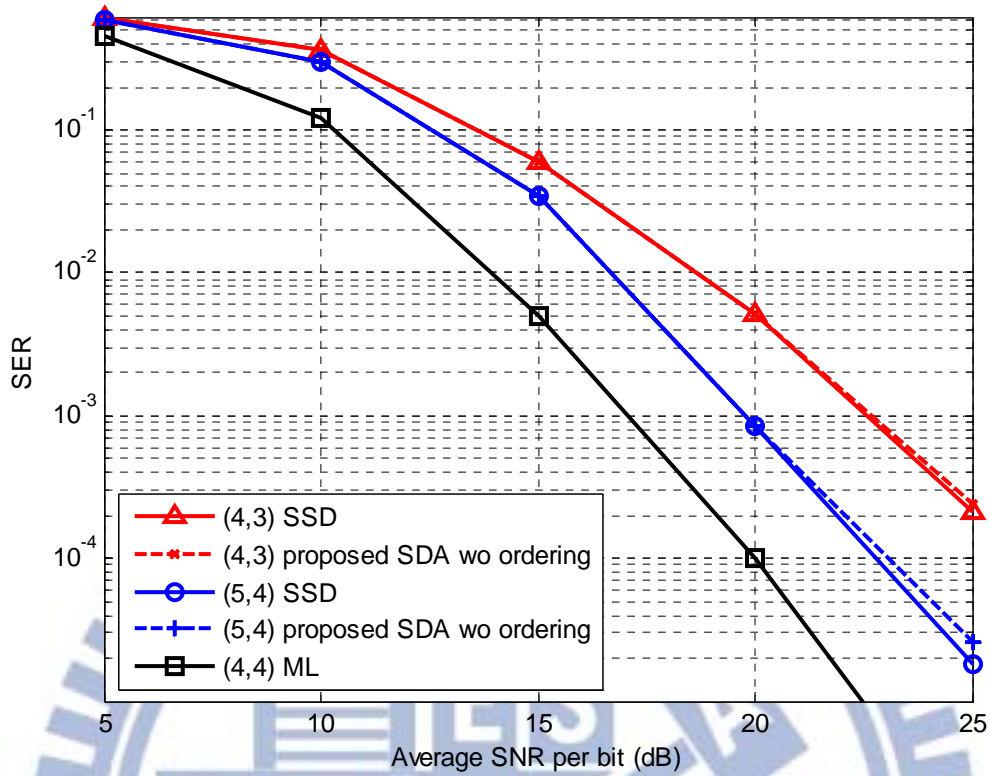


Figure 3-2: SER performance comparisons of SSD, ML and proposed decoder with 16-QAM modulation for various MIMO configurations.

shown in **Figure 3-5**. It is obvious that the reduction ratio will be saturated when the antenna number difference increases. The phenomenon is due to that the ratio of N_p increases faster rather than the value of $|y'_M|$ when the antenna number difference increases. However, the greedy ordering rule can still provide significant reductions even when the N_p increases exponentially. In **Figure 3-5**, it is observed that the numerical result of the developed framework closely follows the Monte-Carlo trials, which verifies the accuracy of the mathematical analysis.

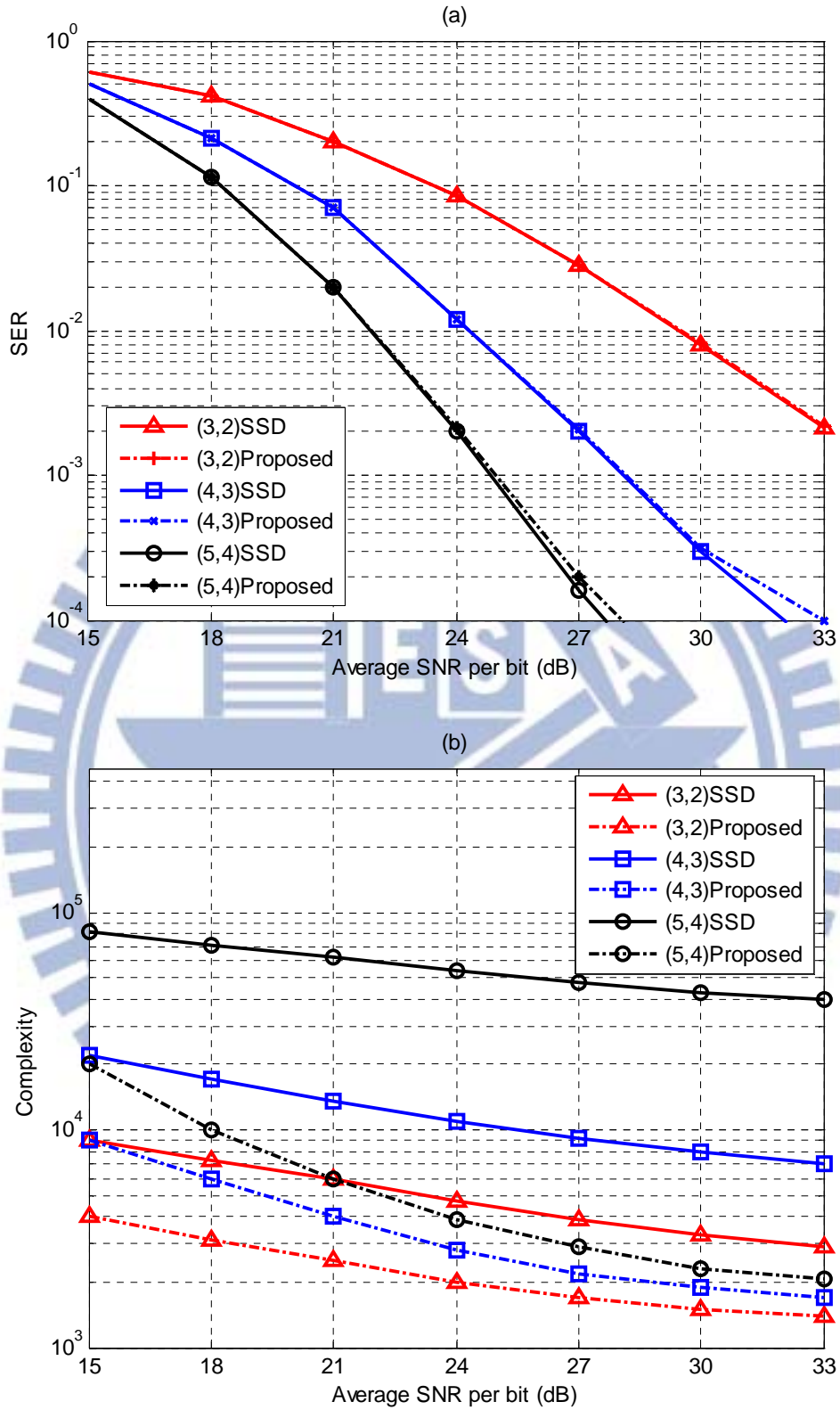


Figure 3-3: SER performance and complexity comparisons of SSD, ML and proposed decoder with 64-QAM modulation for various MIMO configurations. (a) SER; (b) Complexity.

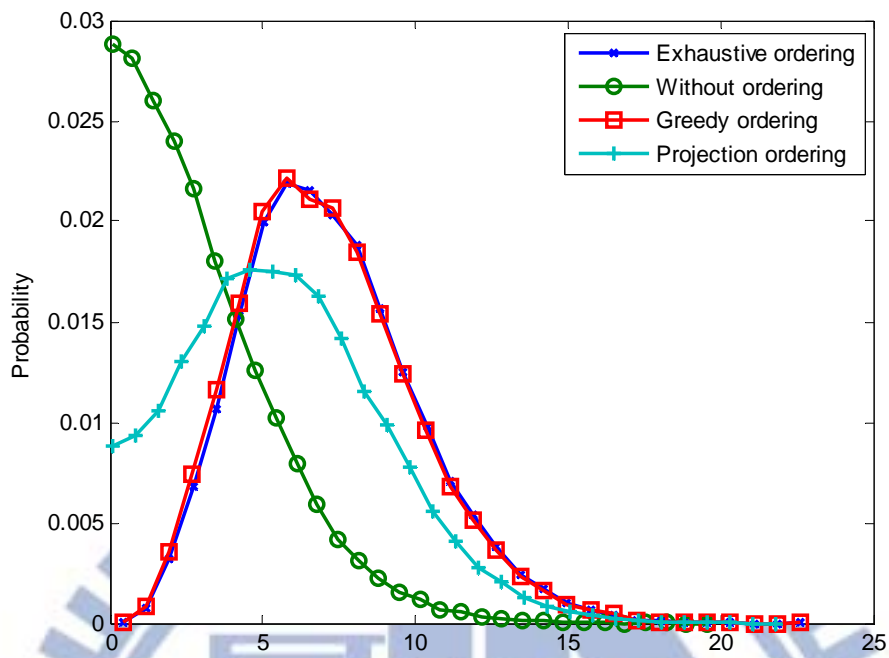


Figure 3-4: Probability density function of $|y'_M|$ with various ordering rules with 16-QAM (4,2) MIMO configuration at SNR=15dB.

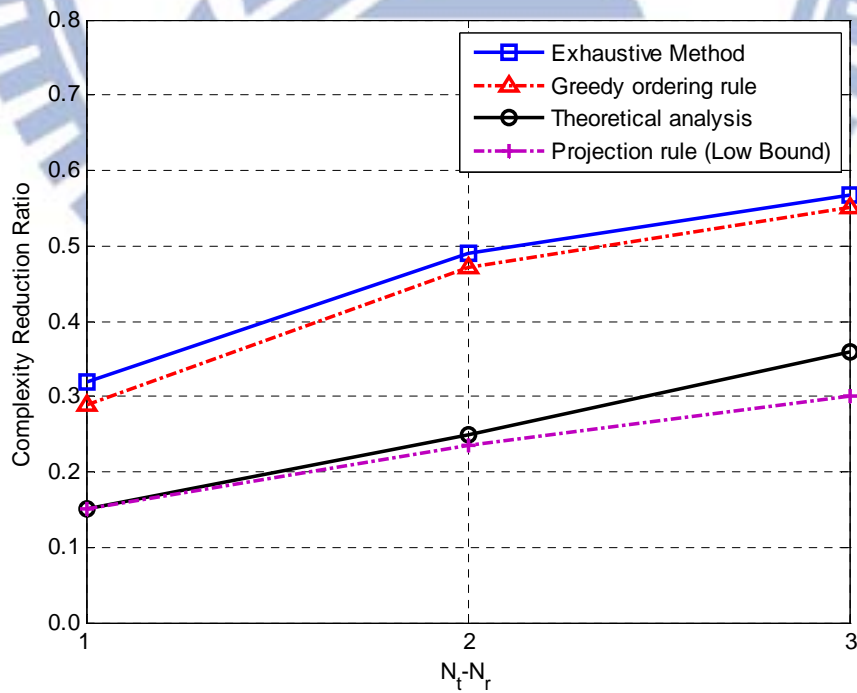


Figure 3-5: The comparison of the averaged complexity reduction ratio for various ordering rules.

Finally, we consider the 64-QAM modulation and evaluate the SER performance and complexity for the same set of MIMO systems, incorporated with and without the proposed greedy ordering rule. The average SER over various underdetermined MIMO systems is shown in **Figure 3-6(a)**. It is obvious that the decoding performance of the proposed decoders with and without greedy ordering rule are almost identical and close to that of the ML approach. The corresponding SERs are slightly different at high SNR, due to the use of greedy ordering rule. The performance difference between the decoders with and without preprocessing is due to different ZF-SIC solutions obtained by the different channel orderings. The incorporated decoder has little performance improvement due to larger $r_{o,M,M}^2$. **Figure 3-6(b)** shows that the greedy ordering rule can significantly reduce the decoding complexity especially in the low SNR regime due to the efficient reduction of the size of the obtained candidate set. The complexity decreases slowly with the increase of SNR due to the additional complexity of preprocessing scheme. The simulation result indicates that the complexity of the proposed decoder with greedy ordering scheme is in the polynomial order comparing to the SSD with exponential growth. The complexity is also less sensitive to the SNR variation; therefore, the proposed decoder is more suitable for real-time implementation than other existing decoders.

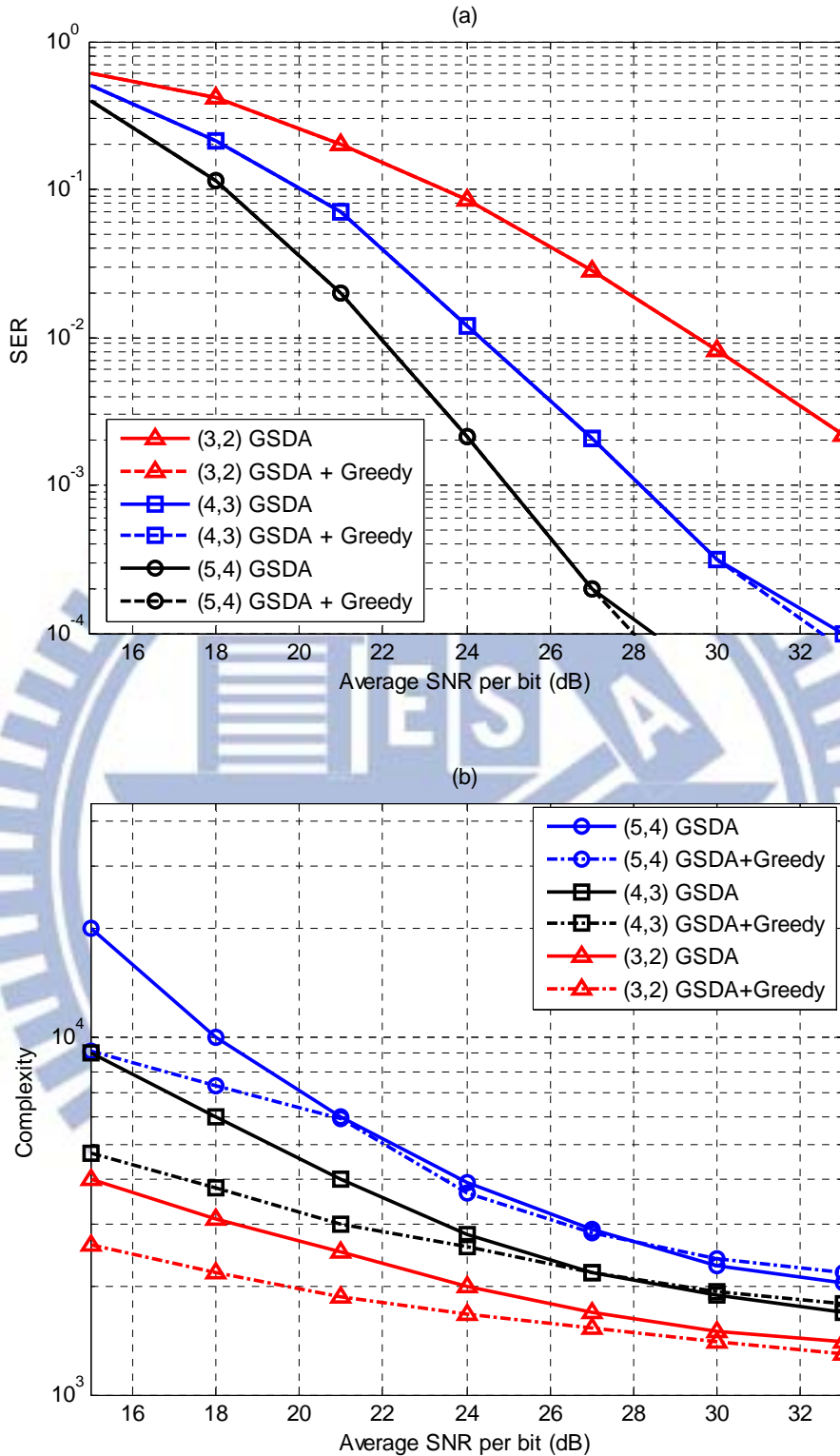


Figure 3-6: Performance and complexity comparisons of the proposed decoder incorporated with and without greedy reordering scheme with 64 QAM modulation for various MIMO configurations. (a) SER; (b) Complexity.

In this section, simulation results show that the complexity advantage of the proposed decoder becomes more significant when the number of antennas increases. Besides, the proposed preprocessing scheme can efficiently reduce the decoding complexity in the low SNR regime without degrading the decoding performance. The simulations also confirm that the theoretic analysis and mathematical derivation on the complexity closely align, and the analysis can be used for predicting the complexity reduction.

3.6 Summary

In this chapter, we propose a preprocessing scheme and prove that the search strategy can significantly reduce the computational complexity within lower SNR regime. A general analysis framework of the static ordering rule for QR based MIMO decoder is presented. Simulation results show that the decoder can achieve near-ML performance with low complexity and confirm the mathematical analysis. The result indicates that the optimal ordering rule depends on the column vectors of channel matrix and also on received signal vector. The proposed SDA provides near ML performance with lower than exponential complexity, is suitable for real-time applications, e.g., MU-MIMO, and provides a promising solution for next generation MIMO wireless communication systems such as IMT-Advanced.

Chapter 4

Efficient Search Algorithm for Codebook Search in Uplink CoMP Systems

4.1 Overview

(LTE is the next generation mobile communication standard developed by 3GPP, and will provide users with high-rate services including video, audio, and data communications [57]. Many innovative techniques were adopted in LTE for improving system capacity, link reliability, and spectral efficiency. Advanced techniques such as enhanced MIMO, carrier aggregation (CA), and CoMP were developed for further increasing the system performance and meeting the requirements for LTE-A standard [58-59].

The CoMP has been adopted in LTE-A to improve the cell average and cell edge throughputs [60]. The CoMP utilizes the cooperation groups to coordinate the transmissions for inter-cell interference (ICI) mitigation and link quality enhancement. The centralized CoMP is a full cooperation realization that involves full channel state information (CSI) and full data information for providing improved performances. The full cooperation scheme among base stations (BS) and remote radio heads (RRH) is applicable in LTE-A by using the dedicated backhaul fiber links. In uplink (UL) centralized CoMP systems, cooperating BSs forward received signals and CSI to a central processor (CP), which computes the precoder matrices for each user equipment

(UE). Therefore, the CP needs to feed back the exact precoder matrix to each UE, which is inefficient and impractical. A codebook-based scheme that feeds back only the precoder matrix index (rather than the matrix itself) is adopted as a practical remedy in real applications

In this chapter, we will propose an efficient codebook search algorithm for centralized UL CoMP systems. The codebook search issue can be reformulated as a tree search form and the solution can be obtained efficiently using a modified K -Best enumeration strategy. The approach originating from the sphere decoding algorithm (SDA) [9-12] is developed to reduce the computational load during the search for optimal precoder matrices. The proposed algorithm can effectively perform precoder selection and maintain a significantly lower complexity compared to the exhaustive search method. Therefore, the proposed approach is especially attractive and suitable for real applications.

4.2 Signal Model

The centralized UL CoMP system model is introduced in this section. Macro and micro cells operate at different transmission power levels and achieve fast transfers of signals and channel information over dedicated fiber links in heterogeneous networks (CoMP scenario 3 and 4) [61]. As in n **Figure 4-1**, the central BS collects information from each RRH and decodes the signal simultaneously.

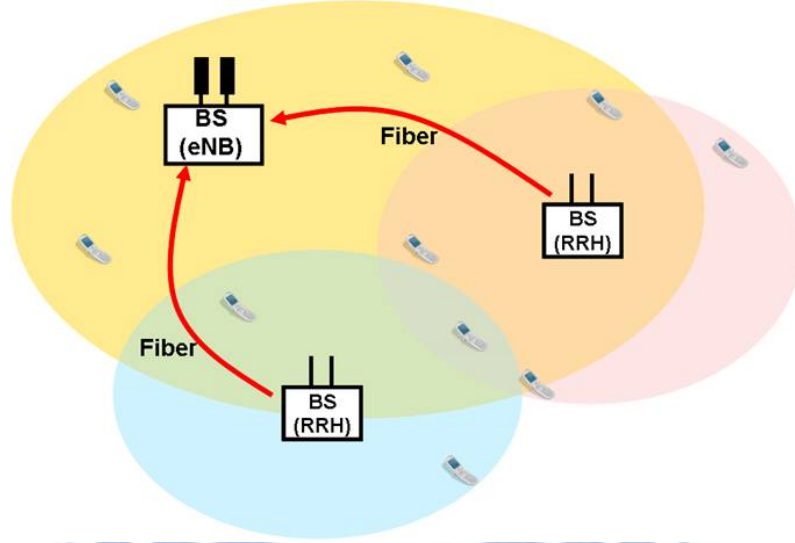


Figure 4-1: Illustration of centralized UL CoMP system model

The uplink CoMP systems involves M BSs (M cells) equipped with N_r antennas. Each BS connects up to P UEs equipped with N_t antennas as shown in **Figure 4-1**. To be applicable to block QR decomposition (BQRD) adopted in Section III., N_r is set to be the multiple of P . The transmitted signal vector $\mathbf{x}_l^q \in \mathbb{C}^{d_l \times 1}$ of the q th UE in the l th cell, which is processed by the precoder matrix $\mathbf{V}_l^q \in \mathbb{C}^{N_r \times d_l}$. For simplicity, we assume that all UE in the l th cell transmit the same number of layer d_l , and d_l is set to be equal or smaller than N_t . The channel matrix between the q th UE in the l th cell and the m th BS is denoted as $\mathbf{H}_{m,l}^q \in \mathbb{C}^{N_r \times N_t}$, whose elements are models as i.i.d. complex Gaussian random variables with distribution $CN(0,1)$ for serving links ($m=l$) and $CN(0,\epsilon)$ for coordinating links ($m \neq l$) [10]. The received signal at the m th BS is expressed as

$$\mathbf{y}_m = \sum_{l=1}^M \mathbf{H}_{m,l} \mathbf{V}_l \mathbf{x}_l + \mathbf{z}_m, \quad (4.1)$$

where the aggregated precoding matrix and transmitted signal at the l th cell are denoted as $\mathbf{V}_l = \text{diag}(\mathbf{V}_l^1, \dots, \mathbf{V}_l^P) \in \mathbb{C}^{N_r \times P \times d_l}$ and $\mathbf{x}_l = [(\mathbf{x}_l^1)^T, (\mathbf{x}_l^2)^T, \dots, (\mathbf{x}_l^P)^T]^T \in \mathbb{C}^{P d_l \times 1}$, respectively. The channel matrix between the m th BS and all UEs in the l th cell is denoted as

$\mathbf{H}_{m,l} \in \mathbb{C}^{N_r \times N_l P}$, and the noise vector at the m th BS is denoted as $\mathbf{z}_m \in \mathbb{C}^{N_r \times 1}$ with distribution $CN(\mathbf{0}_{N_r \times 1}, N_0 \mathbf{I}_{N_r})$. Therefore, the total dimension of the transmission system is $d_T = \sum_{l=1}^M P \times d_l$. Note that the transmit power for each UE is restricted to P_l , i.e., $\|\mathbf{V}_l^q \mathbf{x}_l^q\|_F^2 = P_l$.

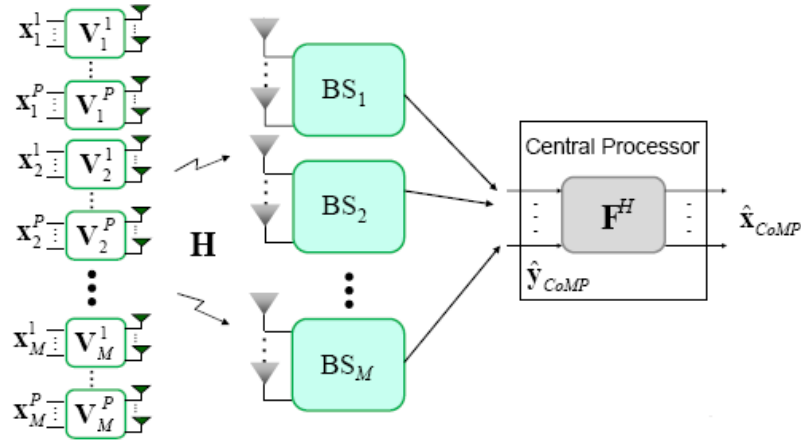


Figure 4-2: Illustration of centralized UL CoMP system model.

In the centralized CoMP, cooperation is available between BSs and RRHs. The received signal from all the BSs and RRHs collected by the CP (one of the BSs) is denoted as

$$\mathbf{y}_{\text{CoMP}} = \mathbf{H}\mathbf{V}\mathbf{x} + \mathbf{z}, \quad (4.2)$$

where $\mathbf{x} = [\mathbf{x}_1^T, \mathbf{x}_2^T, \dots, \mathbf{x}_M^T]^T \in \mathbb{C}^{d_T \times 1}$ is the stacked transmitted signal,

$\mathbf{z} = [\mathbf{z}_1^T, \mathbf{z}_2^T, \dots, \mathbf{z}_M^T]^T \in \mathbb{C}^{N_r \times M \times 1}$ is the stacked noise vector,

$\mathbf{V} = \text{diag}(\mathbf{V}_1, \dots, \mathbf{V}_M) \in \mathbb{C}^{N_l P M \times d_T}$ is the aggregated precoder matrix, and

$\mathbf{H} = \left[\left[\mathbf{H}_{1,1}, \dots, \mathbf{H}_{1,M} \right]^T, \dots, \left[\mathbf{H}_{M,1}, \dots, \mathbf{H}_{M,M} \right]^T \right]^T \in \mathbb{C}^{N_r \times M \times N_l P M}$ is the aggregated channel matrix. The CP processes the received signal by performing equalization for detecting transmitted signal as follows:

$$\hat{\mathbf{x}}_{\text{CoMP}} = \mathbf{F}^H \mathbf{H} \mathbf{V} \mathbf{x} + \mathbf{F}^H \mathbf{z}, \quad (4.3)$$

where $\hat{\mathbf{x}}_{\text{CoMP}}$ is the estimated signal, and $\mathbf{F} \in \mathbb{C}^{MN_r \times d_T}$ is the equalizing matrix.

Therefore, the equivalent channel matrix is $\mathbf{H}_{\text{eff}} = \mathbf{H} \mathbf{V} \in \mathbb{C}^{MN_r \times d_T}$, and the minimum mean square error (MMSE) equalizing matrix \mathbf{F}^H can be expressed as follows:

$$\mathbf{F}^H = \left(\mathbf{H}_{\text{eff}}^H \mathbf{H}_{\text{eff}} + N_0 \mathbf{I}_{d_T} \right)^{-1} \mathbf{H}_{\text{eff}}^H. \quad (4.4)$$

As a performance index, the achievable sum-rate of all layers in the aforementioned system is considered and defined as [64]:

$$R_{\text{sum}} = \sum_{k=1}^{MP} \sum_{j=1}^{d_k} \left[\log_2 \left(1 + \text{SINR}_{k,j} \right) \right], \quad (4.5)$$

where $\text{SINR}_{k,j}$ is a signal to interference-and-noise ratio (SINR) measured at the output of equalizer corresponding to the j th layer of k th UE.

In the aforementioned systems, the CP has to send the corresponding precoder matrix to each UE. However, the feedback information is limited by the capacity of the control channels, and the transmission of the exact precoder matrix to each UE is infeasible. A codebook-based scheme that adopts the existing codebook in LTE-A is proposed to reduce the amount of feedback information. By this system model, the diagonal precoding matrix composed by the codebook can be formulated as $\hat{\mathbf{V}} = \text{diag} \left\{ \left[\hat{\mathbf{V}}_1, \dots, \hat{\mathbf{V}}_{MP} \right] \right\}$, where $\hat{\mathbf{V}}_1, \dots, \hat{\mathbf{V}}_{MP}$ are chosen from a pre-defined codebook \mathbf{W} [58]. In summary, the objective of the precoder design problem is equivalently to locate a precoder index set which pursues sum-rate maximization from the given codebook, as opposed to the conventional precoder matrix design rationale [62-63].

4.3 Propsoed Codebook Serach Algorithm

The codebook search issue in UL CoMP systems is to efficiently locate a precoder

index set that corresponds to the maximal achievable sum-rate. The optimal solution can be obtained by the exhaustive search method, which searches all possible combinations of precoder matrices via the following criterion:

$$\hat{\mathbf{V}}_{op} = \arg \max_{\mathbf{V} \in S} \sum_{k=1}^{MP} \sum_{j=1}^{d_k} \left[\log_2 (1 + \text{SINR}_{k,j}) \right], \quad (4.6)$$

where $S = O^{MP}$ denotes the set of all possible combinations and O is the given precoder matrix set with size v . The computational complexity of the exhaustive search grows exponentially with MP .

As a remedy, an alternative approach is proposed here to efficiently tackle this problem. The main idea is to sequentially locate the precoder index, by which each UE can compute the interference term from others in advanced. Then the equalization operation is applied to eliminate inter-layer interference as to pursue the maximal total sum-rate. The whole procedure is described as follows.

First, performing the proposed BQRD (a generalized Gram-Schmidt (GS) based BQRD procedure is listed in **Table 4.1**) on channel matrix $\mathbf{H} \in \mathbb{C}^{MN_r \times MPN_t}$ produces

$$\mathbf{H} = \mathbf{Q}\mathbf{R}, \quad (4.7)$$

where $\mathbf{Q} \in \mathbb{C}^{MN_r \times MN_r}$ is an unitary matrix, $\mathbf{R} \in \mathbb{C}^{MN_r \times MPN_t}$ is a block upper triangular matrix partitioned into sub-matrices $\mathbf{R}_{i,j} \in \mathbb{C}^{(N_r/P) \times N_t}$, so that $\mathbf{R}_{i,j} = \mathbf{0}$ for $i > j$.

Substituting (4.8) into (4.2) yields

$$\mathbf{y}'_{\text{CoMP}} = \mathbf{R}\hat{\mathbf{V}}\mathbf{x} + \mathbf{z}', \quad (4.8)$$

where $\mathbf{y}'_{\text{CoMP}} = \mathbf{Q}^H \mathbf{y}_{\text{CoMP}}$ and $\mathbf{z}' = \mathbf{Q}^H \mathbf{z}$. Reformulation of (4.9) as an alternative form gives:

$$\mathbf{y}'_i = \sum_{k=i}^{MP} \mathbf{R}_{i,k} \hat{\mathbf{V}}_k \mathbf{x}_k + \mathbf{z}'_i, \quad i = 1, \dots, MP, \quad (4.9)$$

where $\mathbf{y}'_i \in \mathbb{C}^{(N_r/P) \times 1}$. Observing $i=MP$ to 1, we can see that the MP th equation is affected only by $\hat{\mathbf{V}}_{MP}$, and the $(MP-1)$ th equation depends on $\hat{\mathbf{V}}_{MP}$ and $\hat{\mathbf{V}}_{MP-1}$, etc. This recursive dependency is a direct consequence of the block-wise upper triangular structure \mathbf{R} . By this property, the interference caused by the UE with higher index can be pre-cancelled in advance through the same philosophy as in the successive interference cancellation (SIC) techniques. The interdependence relationship among UEs could be eliminated. Therefore, we can reformulate (4.7) by the tree search technique to locate the optimal precoder set $\hat{\mathbf{V}}$ as:

$$\hat{\mathbf{V}} = \arg \max_{\mathbf{V} \in \mathcal{S}} \sum_{k=1}^{MP} \log_2 \left(1 + \frac{\|\mathbf{R}_{k,k} \hat{\mathbf{V}}_k\|^2}{\sum_{i=k+1}^{MP} \|\mathbf{R}_{k,i} \hat{\mathbf{V}}_i\|^2 + \|\mathbf{z}'_k\|^2} \right). \quad (4.10)$$

By the appropriate path metric definition, the problem can be viewed equivalently as an issue for locating the longest path and can be efficiently solved by well established efficient algorithms [65]. In this work, the path weight P_m and branch weight metric $_m$ of the m th UE are defined as

$$\begin{aligned} P_m &= 0, \quad \text{for } m = MP + 1 \\ P_m &= P_{m+1} + \text{metric}_m, \quad \text{for } 1 \leq m \leq MP, \end{aligned} \quad (4.11)$$

where metric $_m$ is defined as follows:

$$\text{metric}_m = \log_2 \left(1 + \left(\frac{\|\mathbf{R}_{m,m} \hat{\mathbf{V}}_m\|^2}{\sum_{i=m+1}^{MP} \|\mathbf{R}_{m,i} \hat{\mathbf{V}}_i\|^2 + \|\mathbf{z}'_m\|^2} \right) \right), \quad (4.12)$$

and the path weight P_m is the partial sum of achievable sum-rate (PSASR), which is a positive and non-decreasing function of m . The iterative search for the candidates $\hat{\mathbf{V}}_{MP}, \dots, \hat{\mathbf{V}}_1$ can be regarded as a descending tree, where each parent node has branches, and the number of branches is equivalent to the codebook size. Finally, the MMSE equalizer can be applied to separate all data layers within the same UE for data decoding.

In tree search problems, there are mature searching strategies [65] pursuing the optimal solution with the trade-off between performance and complexity rather than exhaustive search. However, the complexity of the existing methods is still comparable to exhaustive search when the number of search layers is small. To obtain the solution efficiently, we perform a modified K -Best search strategy, with the detailed procedure listed in **Table 4.2**. Our approach uses a breadth-first search and always keeps only K candidates with the longest path weights for the next layer as the most promising solutions. This approach also maintains stable decoding throughput, which is very useful especially in practical implementations.

The computational complexity is also a critical factor for real-time applications. For complexity analysis, we here derived the required complexity of exhaustive search and modified K -Best strategy for comparison. The evaluations contain all operations including BQRD and equalization manipulations. For complexity analysis, the computational complexity is measured in terms of the number of floating point operations (flops). All additions, multiplications, divisions, and comparisons are equally treated as flops. We here derived the required complexity of exhaustive search and modified K -Best strategy for comparison.

The total flop requirement of the proposed algorithm incorporating with exhaustive search and modified K -Best search strategy could be expressed as

$$\left(\prod_{i=1}^{MP} n_i \right) \left(2N_r M N_t d_T + 5d_T^2 N_r M + d_T^3 + d_T^2 + 2d_T + \sum_{i=1}^{MP} \log(n_i) \right) \quad (4.13)$$

and

$$\begin{aligned}
& \frac{N_r^2 M^3 \left(3(MP-1)(2N_r + P) + 140N_r \right)}{6} + N_t^2 N_r \left(\frac{2}{P} + 4M \right) + \\
& \frac{MN_r^2 N_t (MP-1)(MP-2)}{P} + 2MN_r^2 N_t (MP+1) + \\
& n_{MP} \left(2 + \log(n_{MP}) + \frac{2N_r N_t d_{MP}}{P} + \frac{3N_r}{P} + \frac{4N_r^2}{P^2} + \frac{N_r^3}{P^3} \right) + \\
& K \sum_{k=1}^{MP-1} \left(\log(Kn_k) + n_k \left(2 + \frac{2N_r N_t}{P} \sum_{i=k}^{MP} d_i + \frac{3N_r}{P} + \frac{4N_r^2}{P^2} + \frac{N_r^3}{P^3} \right) \right), \tag{4.14}
\end{aligned}$$

respectively. Furthermore, to demonstrate the benefit of the proposed algorithm, the complexity reduction ratio (reduction amount normalized to exhaustive method) is defined and expressed as follows:

$$\eta = 1 - \frac{\text{Complexity}_{K_Best}}{\text{Complexity}_{exhaustive}} = O \left(1 - d_T^{-2} N_r^{-1} M^{-1} \left(\prod_{i=1}^{MP} n_i^{-1} \right) \sum_{k=1}^{MP-1} \log(Kn_k) \right), \tag{4.15}$$

where n_i is the codebook size belonging to i th UE. From (4.15), it is evident that the proposed algorithm can provide significant complexity reduction particularly in the larger CoMP size or/and a large number of data layers are transmitted.

By applying the proposed generalized BQRD procedure and incorporating the designed path weight, the criterion in (4.7) can be reformulated into an equivalent tree search form, in which a solution pursuing sum-rate maximization can be efficiently obtained. The complexity reduction ratio is also derived. Furthermore, the proposed approach removes the equalizer evaluation requirement when executing the tree search procedure.

4.4 Simulation Results

This section simulates the achievable sum-rate performance and complexity of the proposed algorithm, and compares the result with the exhaustive search using the maximal achievable sum-rate measured at the output of MMSE equalizer as the optimal solution among all possible precoder combinations. The channel matrices are set by

$\varepsilon=0.4$ in all cases [10].

A typical scenario in 3GPP recommendation is considered [5]: the scheme consists of three BSs in the cooperation group; each BS and UE is equipped with 4 antennas. One UE is in the coverage of each BS ($M = 3, P = 1$), and each UE transmits their respective 2, 3, and 4¹ signal layers. The average achievable sum-rate for the proposed search algorithm and exhaustive approach are shown in **Figure 4-3**. The result shows that the achievable sum-rate of the proposed algorithm is similar to the exhaustive approach with a slight performance decrease (2%). The reason for this is because the BRQD does not only fully eliminate the interference but also suppress the partial desired signal. Therefore, it cannot guarantee to obtain the exact solution as same as exhaustive search method. Compared to exhaustive search, the proposed algorithm can provide a 89% complexity reduction and a near constant average complexity regardless of the SNR variation. Furthermore, it confirms that the optimal precoder matrices are decided only by CSI without considering noise.

A larger CoMP size (than the former scheme) is considered: the scenario consists of three BSs and two UE in the coverage of each BS ($M = 3, P = 2$). Each BS is equipped with 8 antennas and each UE is equipped with 4 antennas. Each UE is presumed to transmit 4 signal layers to attain full use of the available spatial dimension. The average achievable sum-rate for the proposed search algorithm and exhaustive approach are also shown in **Figure 4-4**. The result shows that the proposed search algorithm can achieve a significant complexity reduction (98.6%) and maintain the excellent performance with only a slight decrease (1.2%) compared to exhaustive search.

¹ The LTE-A recommendation [10] provides precoder matrices (Identity matrix) in full spatial multiplexing cases (2X2, and 4X4). For 4X4 case, DL precoder codebook set is adopted instead of the UL precoder one. The corresponding codebook size for 2, 3, and 4 layers are 16, 12, and 16, respectively.

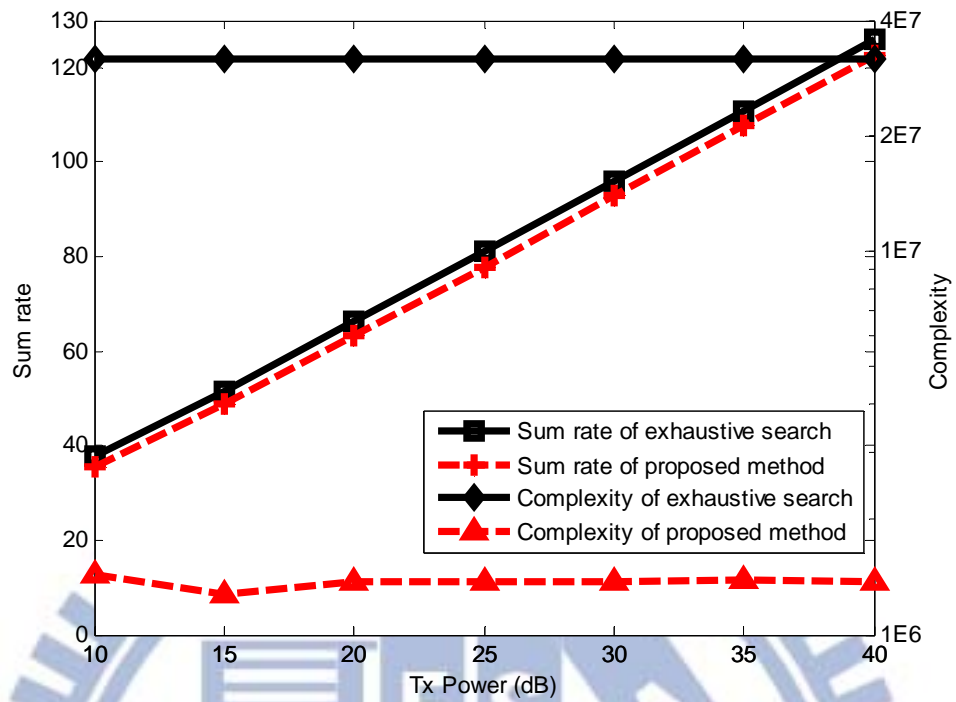


Figure 4-3: Sum-rate performance and complexity of the proposed and exhaustive search methods with $N_r=4$, $N_r=4$, $M=3$, $P=1$, $d_1=2$, $d_2=3$, and $d_3=4$.

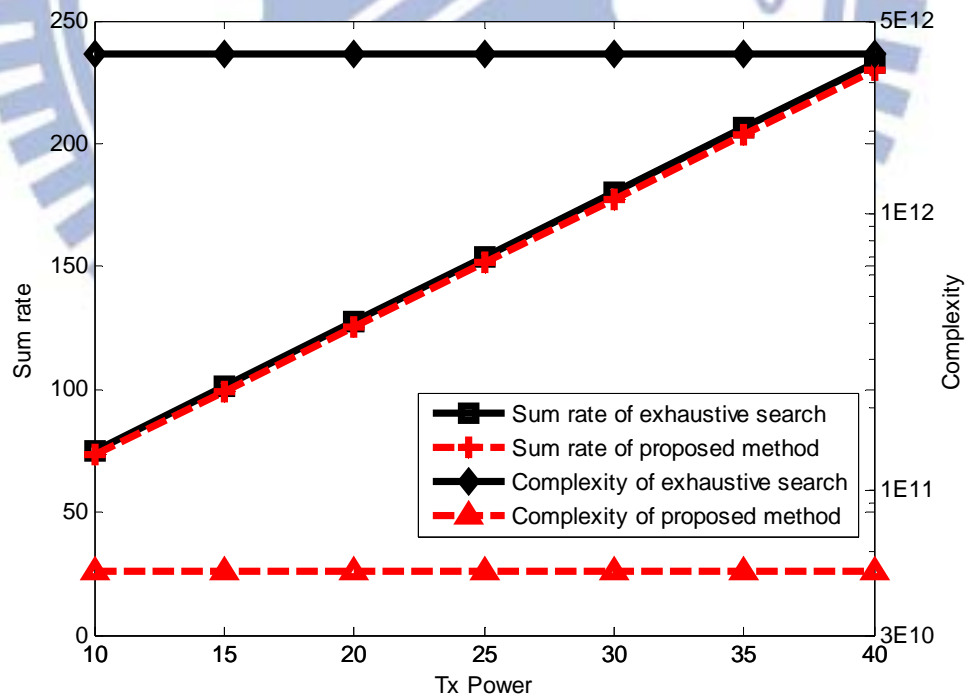


Figure 4-4: Sum-rate performance and complexity of the proposed and exhaustive search methods with $N_r=4$, $N_r=8$, $M=3$, $P=2$, and $d_1=d_2=d_3=4$.

Furthermore, this result confirms that the complexity advantage of the proposed approach becomes more significant when the CoMP size increases. The simulation results show that the proposed method significantly reduces nearly 90% complexity and still maintains the system performance.

4.5 Summary

An efficient codebook search algorithm is proposed for UL CoMP systems in this chapter. By the proposed generalized block GS decomposition, the search problem can be reformulated as a problem of finding the longest path which can be solved efficiently by conducting a tree search. Simulation results confirm that the proposed algorithm shows a significant improvement by one order in computational efficiency and provides the performance closely approaching that of the exhaustive search approach, particularly in the large-size CoMP system. Furthermore, these results show that the proposed algorithm is suitable in practical applications when each BS requires coordination with multiple CoMP groups simultaneously, and provides a promising solution for future wireless communication systems that incorporate CoMP techniques such as the LTE-A.

Table 4-1: THE PROPOSED BLOCK QR DECOMPOSITION

Set $a = M/P \in \mathbb{Z}^+$ and $b = N/P \in \mathbb{Z}^+$ to be the number of rows and columns of submatrices $\mathbf{R}_{i,j}$, respectively.

Step 1: Let $\tilde{\mathbf{H}}_1 = \mathbf{H}_1$ and conduct singular value decomposition (SVD) to $\tilde{\mathbf{H}}_1$, yields $\tilde{\mathbf{H}}_1 = \mathbf{U}_1 \Sigma_1 \tilde{\mathbf{V}}_1^H$. Set $\mathbf{Q} = \mathbf{Q}_1 = \tilde{\mathbf{V}}_1$.

Step 2: Calculate the corresponding effected terms $\mathbf{S}_{i,j}$ by projecting the remaining

$\{\mathbf{H}_1, \mathbf{H}_2, \dots, \mathbf{H}_P\}$ on the basis \mathbf{Q}_1 , according to $\mathbf{S}_{i,j} = \mathbf{Q}_1^H \mathbf{H}_j$, $1 = i < j \leq P$. Set $k = 2$.

Step 3: Perform the outer-loop generalize GS procedure: compute $\tilde{\mathbf{H}}_k$ as

$$\tilde{\mathbf{H}}_k = \mathbf{H}_k^H - \sum_{i=1}^{k-1} \mathbf{S}_{i,k}^H \mathbf{Q}_i^H.$$

Step 4: Conduct SVD to $\tilde{\mathbf{H}}_k$, yields $\tilde{\mathbf{H}}_k = \mathbf{U}_k \boldsymbol{\Sigma}_k \mathbf{V}_k^H$, where $\mathbf{U}_k \in \mathbb{C}^{b \times b}$, $\boldsymbol{\Sigma}_k \in \mathbb{C}^{b \times a}$, and $\mathbf{V}_k \in \mathbb{C}^{M \times a}$.

Step 5: Perform the inner-loop GS procedure to form an orthogonal set $\{\mathbf{b}^{(1)}, \mathbf{b}^{(2)}, \dots, \mathbf{b}^{(a)}\}$ using the current constructed \mathbf{Q} and obtained \mathbf{V}_k in **Step 4** according to $\mathbf{b}^{(i)} = \mathbf{V}_k^{(i)} - \sum_{j=1}^{a(k-1)+i-1} \mathbf{Q}^{(j)} \left(\mathbf{Q}^{(j)} \right)^H \mathbf{V}_k^{(i)}$, $1 \leq i \leq a$, where $\mathbf{Q}^{(i)}$ and $\mathbf{V}_k^{(i)}$ are the i th column of \mathbf{Q} and \mathbf{V}_k , respectively.

Step 6: Normalize the obtained $\mathbf{b}^{(i)}$ set as $\mathbf{Q}_k^{(i)} = \mathbf{b}^{(i)} / \|\mathbf{b}^{(i)}\|_F$, $1 \leq i \leq a$, for constructing $\mathbf{Q}_k^{(i)}$ and then stack $\{\mathbf{Q}_1, \mathbf{Q}_2, \dots, \mathbf{Q}_k\}$ to form an updated unitary matrix \mathbf{Q} as $\mathbf{Q} = [\mathbf{Q}_1, \mathbf{Q}_2, \dots, \mathbf{Q}_k]$.

Step 7: Calculate the corresponding compensated term $\mathbf{S}_{i,j}$ by projecting the remaining

$$\{\mathbf{H}_k, \mathbf{H}_2, \dots, \mathbf{H}_P\} \text{ on the basis } \mathbf{Q}_k \text{ according to } \mathbf{S}_{i,j} = \begin{cases} \mathbf{Q}_k^H \mathbf{H}_j, & k = i < j \leq P \\ \mathbf{Q}_k^H \tilde{\mathbf{H}}_k^H, & i = j = k \\ \mathbf{0} & , 1 \leq j < i = k \end{cases}.$$

Step 8: Set $k = k + 1$. If $k \leq P$, go to step 3; otherwise, calculate the corresponding upper triangular matrix \mathbf{R} , where $\mathbf{R}_{i,j}$ can be obtained according to

$$\mathbf{R}_{i,j} = \begin{cases} \mathbf{S}_{i,j} + \mathbf{Q}_i^H \tilde{\mathbf{H}}_j^H, & i < j \\ \mathbf{S}_{i,j}, & i \geq j \end{cases}, 1 \leq i, j \leq P. \text{ Finally, output the evaluated } \mathbf{Q} \text{ and } \mathbf{R}$$

matrices and terminate the procedure.

Table 4-2: A PROPOSED CODEBOOK SEARCH ALGORITHM USING K -BEST ENUMERATION

Step 1:

(a) Set $k = MP$.

(b) For each UE evaluate the corresponding metric using all possible precoder matrix index $P_{MP} = \text{metric}_{MP}$.

(c) Choose those precoder matrix having the K longest paths.

Step 2:

(a) $k \leftarrow k - 1$.

(b) For each partial UE combination, evaluate the corresponding PSASR: $P_k = P_{k+1} + \text{metric}_k$.

(c) Sort the K_V accumulated path metrics, and select K partial nodes having the longest PSASR among the entire candidate set.

Step 3:

If $k = 1$

output the vector with the longest path weight as the estimated solution.

Else

Go back to Step 2.

Chapter 5

Conclusions and Future Works

5.1 Summary of Dissertation

This dissertation mainly addresses the efficient decoding algorithms design for wireless MIMO systems. Furthermore, we apply tree search techniques to locate the optimal codebook set in centralized UL CoMP systems. The main contribution lies in that we propose efficient decoding algorithms for different MIMO configurations. Furthermore, a generalize analysis framework is developed to characterize the statistical properties of diagonal elements of \mathbf{R} matrix. The analytical result can provide more insight for QR based MIMO detectors. Finally, we apply the tree search techniques to solve the codebook search problem in widely investigated CoMP systems. By the proposed block decomposition procedure incorporating with appropriate path definition, the proposed algorithm can provide the advantages of low computational complexity and nearly the same performance of the exhaustive search. The benefit of the developed algorithm is attractive and suitable in practical applications.

The introductory chapter includes the background overview, literature review, and contribution of this dissertation. In Chapter 2, a low complexity near-ML K -Best sphere decoder is proposed and the corresponding hardware architecture is also presented. For obtaining excellent decoding performance with less computation burden, a new search strategy based on a derived CDF and an associated efficient procedure is proposed. The simulation results confirm that the proposed decoder can provide near ML performance with less complexity.

In Chapter 3, we extend the search strategies proposed in Chapter 2 to develop a two-stage generalized sphere decoder from geometry perspective. Furthermore, to reduce the complexity especially in low SNR regime, a preprocessing scheme is also proposed from geometrical perspective. Another important contribution is that we develop a generalized analysis framework to characterize statistical properties of diagonal element of \mathbf{R} matrix under the general ordering rule. The framework can be applied on any static ordering rule even in non-linear ordering rule for QR MIMO detector.

In Chapter 4, we further study the uplink CoMP system which has been adopted in LTE-A to improve the cell average and cell edge throughputs. An efficient codebook search algorithm with lower complexity is proposed. By the proposed generalized block QR decomposition, the codebook search problem can be reformulated as a problem of finding the longest path which can be solved efficiently by conducting a tree search. Moreover, the required computational complexity of exhaustive search and proposed algorithm are also derived. The result shows that the complexity advantage of the proposed algorithm tend to be more significant when the CoMP size increases.

5.2 Future Works

The sphere decoding algorithm is actually a powerful tool to efficiently decouple multiplexed data streams with excellent performance in MIMO systems. It also can be applied to tackle multi-dimensional search problem in discrete space. Based on the proposed block QR decomposition, the codebook search problem can be solved, but the optimal selection ordering rule is not investigated yet. As mentioned in Chapter 3, a spatial multiplexing MIMO system usually incorporates advanced channel coding techniques to pursue maximal channel capacity in practical communication systems. To obtain the optimal solution, the iterative approach originating from the turbo decoding

algorithm is a popular approach. In this dissertation, these proposed decoding algorithms can be easily extended to provide soft output and act as the inner decoder. Unfortunately, the complexity of the state-of-art decoding algorithms is still high; therefore, to develop efficient decoding algorithm with iterative approach, the associated hardware architecture, and framework for performance/ complexity evaluation are potential future research topics.



APPENDIX

A Derivation of Equation (2.14)-(2.16)

The expression in (2.14)-(2.16) shows that reordering the columns of \mathbf{H} according to their vector norms in ascending order leads to

$$\mathbf{H}_o = [\mathbf{h}_{o(1)}, \mathbf{h}_{o(2)}, \dots, \mathbf{h}_{o(N)}], \quad (\text{A.1})$$

where $\|\mathbf{h}_{o(1)}\| \leq \|\mathbf{h}_{o(2)}\| \leq \dots \leq \|\mathbf{h}_{o(N)}\|$. From [13], $\mathbf{h}_{o(i)}$ can be expressed as

$$\mathbf{h}_{o(i)} = \sqrt{X_i} \boldsymbol{\theta}_i, \quad (\text{A.2})$$

where X_i is the i th order statistic of N independent $\text{Gamma}(M, 1)$ distributed random variables with $X_1 \leq X_2 \leq \dots \leq X_N$ and $\{\boldsymbol{\theta}_i\}$ s are i.i.d. uniformly distributed on the unit sphere in \mathbb{C}^M . Note that X_i and $\boldsymbol{\theta}_i$ are independent. With the QR decomposition of $\mathbf{H}_o = \mathbf{Q}_o \mathbf{R}_o$, we are now going to characterize the distribution of the square of the diagonal entries of \mathbf{R}_o denoted by $r_{o,i,i}^2$.

Letting $\mathbf{Q}_o = [\mathbf{q}_{o(1)}, \mathbf{q}_{o(2)}, \dots, \mathbf{q}_{o(N)}]$ and performing the QR decomposition of \mathbf{H}_o ,

we obtain

$$r_{o,i,i}^2 = X_i \left[1 - \sum_{k=1}^{i-1} (\mathbf{q}_{o(k)}^H \boldsymbol{\theta}_i)^2 \right] = X_i \left[1 - \sum_{k=1}^{i-1} \boldsymbol{\theta}_i^2(k) \right] = \begin{cases} X_i, & \text{for } i = 1 \\ X_i S_i, & \text{for } 2 \leq i \leq N \end{cases}$$

(A.3)

where

$$S_i = \left[1 - \sum_{k=1}^{i-1} \boldsymbol{\theta}_i^2(k) \right], \quad (\text{A.4})$$

and $\boldsymbol{\theta}_i(k)$ denotes the k th element of $\boldsymbol{\theta}_i$. Note that the second equation holds due to the

fact that the distribution of $\boldsymbol{\theta}_i$ is invariant under the orthogonal transformation \mathbf{Q}_o . To derive the cdf of $r_{o,i,i}^2$, we should first obtain the probability density function (pdf) of X_i and S_i . The pdf of X_i is available in [40] as

$$f_{X_i}(x) = \frac{N![F(x)]^{i-1}[1-F(x)]^{N-i}f(x)}{(i-1)!(N-i)!}, \quad (\text{A.5})$$

where

$$f(x) = \frac{x^{M-1} \cdot e^{-x}}{\Gamma(M)} \quad \text{for } x > 0, \quad (\text{A.6})$$

$$F(x) = 1 - \sum_{i=0}^{M-1} \frac{x^i}{i!} e^{-x}. \quad (\text{A.7})$$

From [41], $\boldsymbol{\theta}_i$ can be modeled from a $2M$ -dimensional random vector $\mathbf{V} = [v_1 \ v_2 \ \cdots \ v_{2M}]^T$ with $v_i \sim \text{i.i.d. } N(0,1)$, where

$$\boldsymbol{\theta}_i(k) = \frac{v_{2k-1} + j \cdot v_{2k}}{\|\mathbf{V}\|} = \frac{v_{2k-1} + j \cdot v_{2k}}{\sqrt{v_1^2 + v_2^2 + \cdots + v_{2M}^2}}, \quad (\text{A.8})$$

Due to the fact that $\boldsymbol{\theta}_i^H \boldsymbol{\theta}_i = 1$, S_i can be rewritten as

$$S_i = \left[1 - \sum_{k=1}^{i-1} \boldsymbol{\theta}_i^2(k) \right] = \left[\sum_{k=1}^{M-i+1} \boldsymbol{\theta}_i^2(k) \right], \quad (\text{A.9})$$

Substituting (A.8) into (A.9), we have

$$S_i = \sum_{k=1}^{M-i+1} \boldsymbol{\theta}_i^2(k) = \frac{v_1^2 + v_2^2 + \cdots + v_{2(M-i+1)}^2}{v_1^2 + v_2^2 + \cdots + v_{2M}^2} = \frac{Q_i}{P_i}, \quad (\text{A.10})$$

where Q_i and P_i are chi-square random variables with $2 \cdot (M - i + 1)$ and $2M$ degrees of freedom, respectively.

The joint pdf of Q_i and P_i is

$$\begin{aligned} f_{Q_i, P_i}(q, p) &= f_{Q_i}(q) \cdot f_{P_i - Q_i}(p - q) = f_{\chi^2(2(M-i+1))}(q) \cdot f_{\chi^2(2i-2)}(p - q) \\ &= \frac{q^{(M-i)} \cdot (p - q)^{(i-2)} \cdot e^{-p/2}}{2^M \cdot \Gamma(M - i + 1) \cdot \Gamma(i - 1)}, \quad \text{for } p > 0 \text{ and } q > 0, \end{aligned} \quad (\text{A.11})$$

where $f_{\chi^{(k)}}(x)$ denotes the pdf of the chi-square random variable with k degrees of freedom. The pdf of S_i can be obtained by

$$\begin{aligned} f_{S_i}(s) &= \int_{-\infty}^{\infty} |p| f_{Q_i, P_i}(ps, p) dp = \int_0^{\infty} p \cdot \frac{(ps)^{(M-i)} \cdot (p-ps)^{(i-2)} \cdot e^{-p/2}}{2^M \cdot \Gamma(M-i+1) \cdot \Gamma(i-1)} dp \\ &= \frac{s^{(M-i)} \cdot (1-s)^{(i-2)}}{2^M \cdot \Gamma(M-i+1) \cdot \Gamma(i-1)} \int_0^{\infty} p^{(M-1)} \cdot e^{-p/2} dp = \frac{s^{(M-i)} \cdot (1-s)^{(i-2)} \cdot (M-1)!}{\Gamma(M-i+1) \cdot \Gamma(i-1)}. \end{aligned} \quad (\text{A.12})$$

Since X_i and S_i are independent, the joint pdf of X_i and S_i is

$$f_{X_i, S_i}(x, s) = f_{X_i}(x) \cdot f_{S_i}(s), \quad (\text{A.13})$$

the cdf of $r_{o,i,i}^2$ for $2 \leq i \leq N$ can be obtained by

$$F_{r_{o,i,i}^2}(r) = \int_0^1 \left\{ \int_0^{r/s} f_{X_i, S_i}(x, s) dx \right\} ds = \int_0^1 \int_0^{r/s} f_{X_i}(x) f_{S_i}(s) dx ds, \quad (\text{A.14})$$

finally, the cdf of $r_{o,i,i}^2$ is as follows:

For $i = 1$

$$F_{r_{o,i,i}^2}(r) = \int_0^r \frac{N!}{(N-1)!(M-1)!} \left[\sum_{k=0}^{M-1} \frac{x^k}{k!} e^{-x} \right]^{N-1} \cdot x^{M-1} e^{-x} dx \quad (\text{A.15})$$

For $2 \leq i \leq N$

$$F_{r_{o,i,i}^2}(r) = C_{ii} \int_0^1 \int_0^{r/s} \left[1 - \sum_{k=0}^{M-1} \frac{x^k}{k!} e^{-x} \right]^{i-1} \left[\sum_{k=0}^{M-1} \frac{x^k}{k!} e^{-x} \right]^{N-i} \cdot x^{M-1} e^{-x} (s)^{M-i} (1-s)^{i-2} dx ds \quad (\text{A.16})$$

where

$$C_{ii} = \frac{N!}{(N-i)!(M-i)!(i-1)!(i-2)!}. \quad (\text{A.17})$$

B Derivation of Equation (3.17)

We reorder the columns of \mathbf{H} to be $\mathbf{H}_o = [\mathbf{h}_{o,1}, \mathbf{h}_{o,2}, \dots, \mathbf{h}_{o,N}]$ according to the projection norm of received signal vector \mathbf{y} in ascending order $\|\mathbf{y}^T \mathbf{h}_{o,1}\| \leq \|\mathbf{y}^T \mathbf{h}_{o,2}\| \leq \dots \leq \|\mathbf{y}^T \mathbf{h}_{o,N}\|$. Here $\mathbf{h}_{o,i}$ can be expressed as $\mathbf{h}_{o,i} = \sqrt{w_{o,i}} \boldsymbol{\theta}_i$, where $w_{o,i}$ is the i th order statistic of N independent Gamma $(M,1)$ distributed random variables; the $\{\boldsymbol{\theta}_i\}$ are i.i.d. uniformly distributed on the unit sphere in \mathbb{R}^M [20]; $w_{o,i}$ and $\boldsymbol{\theta}_i$ are mutually independent. With QR decomposition of $\mathbf{H}_o = \mathbf{Q}_o \mathbf{R}_o$, we are to characterize the distribution of the M th square of the diagonal entry of \mathbf{R}_o , denoted by $r_{o,M,M}^2$.

First, letting $\mathbf{Q}_o = [\mathbf{q}_{o,1}, \mathbf{q}_{o,2}, \dots, \mathbf{q}_{o,M}]$ and performing the QR decomposition of \mathbf{H}_o ($\mathbf{H}_o = \mathbf{Q}_o \mathbf{R}_o$), we obtain

$$r_{o,i,i}^2 = w_{o,i} \left[1 - \sum_{k=1}^{i-1} (\mathbf{q}_{o,k}^T \boldsymbol{\theta}_i)^2 \right] = w_{o,M} \left[1 - \sum_{k=1}^{i-1} \boldsymbol{\theta}_i^2(k) \right] = w_{o,i} s_i, \quad (\text{B.1})$$

where

$$s_i = \left[1 - \sum_{k=1}^{i-1} \boldsymbol{\theta}_i^2(k) \right] \quad (\text{B.2})$$

and $\boldsymbol{\theta}_i(k)$ denotes the k th element of $\boldsymbol{\theta}_i$. Note that the second equation holds due to the fact that the distribution of $\boldsymbol{\theta}_i$ is invariant under the orthogonal transformation by \mathbf{Q}_o .

To drive the cdf of $r_{o,M,M}^2$, we should first obtain the pdf of $w_{o,M}$ and s_M . In order to obtain the characteristic of $w_{o,M}$, we first define a new random variable

$z_i = \|\mathbf{y}^T (\sqrt{2} \mathbf{h}_i)\|^4$ and the projection ordering rule can be formulated as sorting process dealing with z_i as follows:

$$\begin{aligned}
& \left\{ \|\mathbf{y}^T \mathbf{h}_{o(1)}\|, \|\mathbf{y}^T \mathbf{h}_{o(2)}\|, \dots, \|\mathbf{y}^T \mathbf{h}_{o(N)}\| \right\} \\
&= \text{sort} \left\{ \|\mathbf{y}^T \mathbf{h}_1\|, \|\mathbf{y}^T \mathbf{h}_2\|, \dots, \|\mathbf{y}^T \mathbf{h}_N\| \right\} \\
&= \text{sort} \left\{ \|\mathbf{y}^T (\sqrt{2}\mathbf{h}_1)\|^4, \|\mathbf{y}^T (\sqrt{2}\mathbf{h}_2)\|^4, \dots, \|\mathbf{y}^T (\sqrt{2}\mathbf{h}_N)\|^4 \right\} = \text{sort} \{z_1, z_2, \dots, z_N\}
\end{aligned} \tag{B.3}$$

From [22], $\boldsymbol{\theta}_i$ can be modeled from a M -dimensional random vector

$$\mathbf{V} = \begin{bmatrix} v_1 & v_2 & \dots & v_M \end{bmatrix}^T \quad \text{with} \quad v_i \sim \text{i.i.d.} \quad N(0,1), \quad \text{where}$$

$$\boldsymbol{\theta}_i(k) = \frac{v_k}{\|\mathbf{V}\|} = \frac{v_k}{\sqrt{v_1^2 + v_2^2 + \dots + v_M^2}}. \quad \text{Therefore, the random variable } z_i \text{ can be}$$

expressed as follows

$$z_i = \|\mathbf{y}^T (\sqrt{2}\mathbf{h}_i)\|^4 = w_i \frac{\left(\sum_{k=1}^M y_k \boldsymbol{\theta}_i(k) \right)^2}{v_1^2 + v_2^2 + \dots + v_M^2} = w_i \frac{m_i}{t_i} = w_i g_i, \tag{B.4}$$

where the random variables w_i and t_i have the Gamma distribution $(M,1)$ and chi-square distribution with M degrees of freedom, respectively. The pdf of the random variable m_i can be approximated as follows

$$f_m(m) = \begin{cases} \frac{1}{\sqrt{2\pi\sigma_m^2}} m^{-\frac{1}{2}} e^{-\frac{m}{2\sigma_m^2}} & m > 0 \\ 0 & m \leq 0 \end{cases}, \text{ where } \sigma_m^2 = M\sigma_y^2. \tag{B.5}$$

According to (3.25), we can derive the pdf of g_i as the form as follows:

$$f_{g_i}(g) = \int_{-\infty}^{\infty} |t| f_m(tg) f_t(t) dt = \frac{\sigma_v g^{-\frac{1}{2}} \left(1 + \frac{\sigma_v^2}{\sigma_m^2} g \right)^{-\frac{M+1}{2}}}{\sigma_m \beta \left(\frac{M}{2}, \frac{1}{2} \right)}. \tag{B.6}$$

With the characteristic of g_i , the cdf of z_i can be obtained and expressed as

$$F_{z_i}(z) = \int_0^{\infty} f_{g_i}(g) F_w \left(\frac{z}{g} \right) dg. \tag{B.7}$$

Since both w_i and g_i are non-negative random variables, according the order statistics

[23], we can obtain the characteristic of $f_{o,z_i}(z)$ as the form of

$$f_{o,z_i}(z) = \frac{N! [F_z(z)]^{i-1} [1 - F_z(z)]^{N-i} f_z(z)}{(i-1)!(N-i)!}. \text{ Combined with } f_{g_i}(g) \text{ and } F_{z_i}(w), \text{ the}$$

pdf of $w_{o,i}$ can be obtained as

$$\begin{aligned} f_{w_{o,i}}(w) &= \int_{-\infty}^{\infty} f(w|z) f_{o,z_i}(z) dz = \int_{-\infty}^{\infty} \frac{f_{z_i w_i}(z, w)}{f_{z_i}(z)} f_{z_{o,i}}(z) dz \\ &= \frac{1}{\beta(i, N-i+1)} \int_{-\infty}^{\infty} \frac{1}{|w|} f_w(w) f_{g_i}\left(\frac{z}{w}\right) [F_z(z)]^{i-1} [1 - F_z(z)]^{N-i} dz \end{aligned} \quad (\text{B.8})$$

Next, due to the fact that $\theta_i^H \theta_i = 1$, s_i can be rewritten as

$$s_i = \left[1 - \sum_{k=1}^{i-1} \theta_i^2(k) \right] = \sum_{k=i}^M \theta_i^2(k). \quad (\text{B.9})$$

Therefore, we have

$$s_i = \sum_{k=i}^M \theta_i^2(k) = \frac{v_i^2 + v_{i+1}^2 + \dots + v_M^2}{v_1^2 + v_2^2 + \dots + v_M^2} = \frac{q_i}{p_i}, \quad (\text{B.10})$$

where q_i and p_i are chi-square random variables with $(M-i+1)$ and M degrees of freedom, respectively. The joint pdf of q_M and p_M is

$$\begin{aligned} f_{q,p}(q, p) &= f_q(q) \cdot f_{p-q}(p-q) = f_{\chi(1)}(q) \cdot f_{\chi(M-1)}(p-q) \\ &= \frac{q^{\frac{1}{2}} \cdot (p-q)^{\frac{M-3}{2}} \cdot e^{-\frac{p}{2}}}{2^{\frac{M}{2}} \cdot \Gamma\left(\frac{1}{2}\right) \cdot \Gamma\left(\frac{M-1}{2}\right)}, \text{ for } p > 0 \text{ and } q > 0, \end{aligned} \quad (\text{B.11})$$

where $f_{\chi(k)}(x)$ denotes the pdf of the chi-square random variable with k degrees of

freedom. The pdf of s_M can be obtained by

$$\begin{aligned}
f_{s_M}(s) &= \int_0^\infty |p| f_{q,p}(ps, p) dp \\
&= \frac{s^{-\frac{1}{2}} (1-s)^{\frac{(M-3)}{2}} \left(\frac{M-2}{2}\right)!}{\Gamma\left(\frac{(M-1)}{2}\right) \Gamma\left(\frac{1}{2}\right)} \left(\because \int_0^\infty x^n e^{-\mu x} dx = n! \mu^{-n-1}\right). \quad (\text{B.12})
\end{aligned}$$

Since $w_{o,M}$ and s_M are independent, the joint pdf of $w_{o,M}$ and s_M is

$$f_{w_{o,M}, s_M}(w, s) = f_{w_{o,M}}(w) \cdot f_{s_M}(s). \quad (\text{B.13})$$

Finally, the cdf of $r_{o,M,M}^2$ can be obtained by

$$\begin{aligned}
F_{r_{o,M,M}^2}(r) &= \int_0^1 \left\{ \int_0^{r/s} f_{w_{o,M}, s_M}(w, s) dw \right\} ds = \int_0^1 \int_0^{r/s} f_{w_{o,M}}(w) f_{s_M}(s) dw ds \\
&= C \int_0^1 \int_0^{r/s} \int_{-\infty}^\infty \frac{1}{|w|} f_w(w) f_g\left(\frac{z}{w}\right) [F_z(z)]^{M-1} [1 - F_z(z)]^{N-M} dz \left(s^{-\frac{1}{2}} (1-s)^{\frac{(M-3)}{2}} \left(\frac{M-2}{2}\right)! \right) dw ds, \quad (\text{B.14})
\end{aligned}$$

where $C = \frac{1}{\beta(M, N - M + 1) \cdot \beta\left(\frac{M-1}{2}, \frac{1}{2}\right)}$.

Bibliography

- [1] E. Telatar, "Capacity of multi-antenna Gaussian channels," *AT&T Bell Labs Internal Tech. Memo.*, June 1995.
- [2] G. J. Foschini and M. J. Gans, "On limits of wireless communications in a fading environment when using multiple antennas," *Wireless Personal Commun.*, vol. 6, no.3, pp. 311-355, Mar. 1998.
- [3] S. M. Alamouti, "A simple transmitter diversity scheme for wireless communication," *IEEE J. Select. Areas Commun.*, vol. 16, pp. 1451-1458, Oct. 1998.
- [4] G. J. Foschini, "Layered space-time architecture for wireless communication in a fading environment when using multi-element antennas," *AT&T Bell Labs Tech. J.*, pp. 41-59, Aug. 1996.
- [5] A. J. Goldsmith and S. G. Chua, "Variable-rate variable-power MQAM for fading channels," *IEEE Trans. Commun.*, vol. 45, no. 10, pp. 1218-1230, Oct. 1997.
- [6] S. Catreux, V. Erceg, D. Gesbert, and R. W. Heath, "Adaptive modulation and MIMO coding for broadband wireless data networks," *IEEE Commun. Mag.*, vol. 40, no. 6, Junly 2002.
- [7] G. J. Foschini, G. D. Golden, R. A. Valenzuela, and P. W. Wolniansky, "Simplified processing for high spectral efficiency wireless communication employing multi-element arrays," *IEEE J. Select. Areas Commun.*, vol. 17, no. 11, pp. 1841-1852, Nov. 1999.
- [8] P. W. Wolniansky, G. J. Foschini, G. D. Golden, and R. A. Valenzuela, "Detection algorithm and initial laboratory results using V-BLAST

- space-time communication architecture,” *Electronic Letters*, vol. 35, no. 1, pp. 14-16, Jan. 1999.
- [9] U. Fincke and M. Pohst, “Improved methods for calculating vectors of short length in a lattice, including a complexity analysis,” *Math. Comput.*, vol. 44, pp. 463-471, Apr. 1985.
- [10] B. Hassibi and H. Vikalo, “On the sphere-decoding algorithm I. expected complexity,” *IEEE Trans. Signal Processing*, vol. 53, no. 8, pp. 2806-2818, Aug. 2005.
- [11] H. Vikalo and B. Hassibi, “On the sphere-decoding algorithm II. generalizations, second-order statistics, and applications to communications,” *IEEE Trans. Signal Processing*, vol. 53, no. 8, pp. 2819-2834, Aug. 2005.
- [12] C. P. Schnorr and M. Euchner, “Lattice basis reduction: improved practical algorithms and solving subset sum problems,” *Math. Programming*, vol. 66, pp. 181-191, 1994.
- [13] W. Zhao and G. B. Giannakis, “Reduced complexity closest point decoding algorithms for random lattices,” *IEEE Trans. Wireless Commun.*, vol. 5, no. 1, pp. 101-111, Jan. 2006.
- [14] Z. Guo and P. Nilsson, “Algorithm and implementation of the K-best sphere decoding for MIMO detection,” *IEEE J. Select. Areas Commun.*, vol. 24, no. 3, pp. 491-503, Mar. 2006.
- [15] A. Burg, M. Borgmann, M. Wenk, M. Zellweger, W. Fichtner, and H. Bölcskei, “VLSI implementation of MIMO detection using the sphere decoding algorithm,” *IEEE J. Solid-State Circuits*, Vol. 40, No.7, pp. 1566–1577, July 2005.

- [16] X. Huang, C. Liang, and J. Ma, "System architecture and implementation of MIMO sphere decoders on FPGA," *IEEE Tans. VLSI Systems*, vol. 16, no. 2, pp. 188-197, Feb. 2008.
- [17] K. Wong, C. Tsui, R. S. Cheng, and W. Mow, "A VLSI architecture of a K-best lattice decoding algorithm for mimo channels," in *Proc. IEEE ISCAS'02*, vol. 3, May 2002, pp. 273-276.
- [18] Y. H. Wu, Y. T. Liu, Y. C. Liao, and H. C. Chang, "Early-pruned K-best sphere decoding algorithm based on radius constraints," in *Proceedings of IEEE International Conference on Communications, ICC 2008*, May 2008, pp. 4496-4500.
- [19] Q. Li and Z. Wang, "Reduced complexity K-best sphere decoder design for MIMO systems," *Circuits, Systems, and Signal Processing*, Birkhäuser Boston, vol. 27, no.4, pp. 491-505, Aug. 2008.
- [20] M. Shabany and P. G. Gulak, "A 0.13um CMOS, 655Mbps, 4x4 64-QAM K-best MIMO detector," *International Solid-State Circuits Conference*, Feb. 2009, pp. 256-257.
- [21] B. Shim and I. Kang, "Sphere decoding with a probabilistic tree pruning," *IEEE Tans. Signal Processing*, vol. 56, no. 10, pp. 4867-4878, Oct. 2008.
- [22] Q. Li and Z. Wang, "Improved K-best sphere decoding algorithms for MIMO systems," in *Proc. IEEE ISCAS'06*, May 2006, pp. 4-7.
- [23] J. W. Choi, B. Shim, A. C. Singer, and N. I. Cho, "A low-complexity near-ML decoding technique via reduced dimension list stack algorithm," in *Proc. IEEE SAM 2008*, July 2008, pp. 41-44.

- [24] S. Roger, A. Gonzalez, V. Almenar, and A. M. Vidal, "Combined K-best sphere decoder based on the channel matrix condition number," in *Proc. ISCCSP'08*, May 2008, pp. 1058-1061.
- [25] S. Roger, A. Gonzalez, V. Almenar, and A. M. Vidal, "MIMO channel matrix condition number estimation and threshold selection for combined K-best sphere decoders," *IEICE Trans. Commun.*, no. 4, pp. 1380-1383, Apr. 2009.
- [26] L. Azzam and E. Ayanoglu, "Reduced complexity sphere decoding for square QAM via a new lattice representation," in *Proc. IEEE GLOBECOM*, Nov. 2007, pp. 4242-4246.
- [27] K. Amiri, C. Dick, R. Rao, and J. R. Cavallaro, "Novel sort-free detector with modified real-Vvalued decomposition (M-RVD) ordering in MIMO systems," in *Proc. IEEE GLOBECOM*, Nov. 2008, pp. 4217-4221.
- [28] M. Myllylä, M. Juntti, and J. R. Cavallaro, "Implementation aspects of list sphere detector algorithms," in *Proc. IEEE GLOBECOM*, 2007, pp. 2915-3920.
- [29] M. Myllylä, M. Juntti, and J. R. Cavallaro, "Implementation aspects of list sphere detector algorithms for MIMO-OFDM systems," *Signal Processing*, vol. 90, issue 10, pp. 2863-2876, 2010.
- [30] H. L. Lin, R. C. Chang, and H. L. Chen, "A high speed SDM-MIMO decoder using efficient candidate searching for wireless communication," *IEEE Trans. Circuits and Systems- II*, vol. 55, no. 3, pp. 289-293, Mar. 2008.
- [31] S. Mondal, K. N. Salama, and W. H. Ali, "A novel approach for K-best MIMO detection and its VLSI implementation," in *Proc. IEEE ISCAS'08*, May 2008, pp. 936-939.
- [32] E. Dekel and I. Ozsvath, "Parallel external sorting," *J. Parallel and Distributed Computing*, vol. 6, pp. 623-635, 1989.

- [33] Z. Wen, "Multi-way merging in parallel," *IEEE Trans. Parallel and Distributed Systems*, vol. 7, no. 1, pp. 11-17, Jan. 1996.
- [34] S. Mandal, A. Eltawil, and K.N. Salama, "Architectural optimizations for low-power K-best MIMO decoders," *IEEE Trans. Vehicular Technology*, vol. 58, no. 7, pp. 3145-3153, Sept. 2009.
- [35] S. Mondal, A. Eltawil, C. A. Shen, and K. N. Salama, "Design and Implementation of a sort-free K-best sphere decoder," *IEEE Trans. Very Large Scale Integr. (VLSI) Syst.*, vol. 18, no. 10, pp. 1497-1501, Oct. 2010.
- [36] K. Lee and J. Chun, "ML symbol detection based on the shortest path algorithm for MIMO systems," *IEEE Trans. Signal Processing*, vol. 55, no. 11, pp. 5477-5484, Nov. 2007.
- [37] A. K. Lenstra, H. W. Lenstra, and L. Lovasz, "Factoring polynomials with rational coefficients," *Math. Ann.*, vol. 261, no. 4, pp. 513-534, 1982.
- [38] H. C. Chang, Y. C. Liao, and H. C. Chang, "Low-complexity prediction techniques of K-best sphere decoding for MIMO systems" *Signal Processing Systems, 2007 IEEE Workshop*, Oct. 2007, pp. 45-49.
- [39] A. Wiesel, X. Mestre, A. Pages, and J. R. Fonollosa, "Efficient implementation of sphere demodulation," *IEEE Workshop on Signal Processing Advances in Wireless Communications (SPAWC)*, June, 2003, pp. 36-40.
- [40] N. Balakrishnan and A. C. Cohen, *Order Statistics and Inference Estimation Methods*, New York: Academic, 1991.
- [41] M. E. Muller, "A note on a method for generating points uniformly on n-dimensional spheres," *Comm. Assoc. Comp. Mach.*, vol. 2, pp. 19-20, Apr. 1959.

- [42] M. O. Damen, K. Abed-Meraim, and J.-C. Belfiore, "A generalised sphere decoder for asymmetrical space-time communication architecture," *Elect. Lett.*, vol. 36, no. 2, pp. 166–167, Jan. 2000.
- [43] T. Cui and C. Tellambura, "An efficient generalized sphere decoder for rank-deficient MIMO systems," *IEEE Commun. Lett.*, vol. 9, no. 5, pp. 423-425, May 2005.
- [44] P. Wang and T. L. Ngoc, "A low-complexity generalized sphere decoding approach for underdetermined MIMO systems," in *Proc. IEEE ICC*, 2006, pp. 4266-4271.
- [45] P. Wang and T. L. Ngoc, "A low-complexity generalized sphere decoding approach for underdetermined linear communication systems: performance and complexity evaluation," *IEEE Trans. Commun.*, vol. 57, no. 11, pp. 3376-3388, Nov., 2009.
- [46] G. Romano, F. Palmieri, P. S. Rossi, and D. Mattered, "A tree-search algorithm for ML decoding in underdetermined MIMO systems," in *Proc. ISWCS 2009*, pp. 662-665.
- [47] G. Romano, F. Palmieri, P. S. Rossi, and F. Palmieri, "Tree-search ML detection for underdetermined MIMO systems with M-PSK constellations," in *Proc. ISWCS 2010*, pp. 102-106.
- [48] Z. Yang, C. Liu, and J. He, "A new approach for fast generalized sphere decoding in MIMO systems," *IEEE Signal Processing Lett.*, vol. 12, no. 1, pp. 41-44, Jan. 2005.
- [49] X. W. Chang and X. Yang, "An efficient tree search decoder with column recording for underdetermined MIMO systems," in *Proc. IEEE GLOBECOM 2007*, pp. 4375-4379.

- [50] K. K. Wong and A. Paulraj, "Efficient near maximum-likelihood detection for underdetermined MIMO antenna systems using a geometrical approach," *EURASIP Journal on Wireless Commun. and Networking*, Oct. 2007.
- [51] K. K. Wong, A. Paulraj and R. D. Murch, "Efficient high-performance decoding for overloaded MIMO antenna systems," *IEEE Trans. Wireless Commun.*, vol. 6, no. 5, pp. 1833-1843, May 2007.
- [52] L. Bai, C. Chen, and J. Choi, "Prevoiting cancellation-based detection for underdetermined MIMO systems," *EURASIP Journal on Wireless Commun. and Networking*, vol. 2010, April 2010, article no. 96.
- [53] K. Liu, and S. S. Xing, "Combined multi-stage MMSE and ML multiuser detection for underdetermined MIMO systems," in *Proc. CCWMC 2011 IET*, 2011, pp. 10-14.
- [54] T. Datta, N. Srinidhi, A. Chockalingam, and B. S. Rajan, "Low-complexity near-optimal signal detection in underdetermined large-MIMO systems," in *Proc. NCC 2012*, 2012, pp. 1-5.
- [55] C. J. Huang, C. Y. Wu, and T. S. Lee, "Geometry based efficient decoding algorithms for underdetermined MIMO systems," in *Proceedings of the IEEE SPAWC 2011*, June 2011, pp. 371-375.
- [56] K. K. Wong and A. Paulraj, "Near maximum-likelihood detection with reduced-complexity for multiple-input single-output antenna systems," in *Proc. Asilomar Conf. on Signals, Systems, and Computers*, Nov. 2004.
- [57] F. Khan, *LTE for 4G Mobile Broadband: Air Interface Technologies and Performance*, Cambridge University Press, 2009.
- [58] 3GPP TS 36.211, "Physical channels and modulation (Release 11)," July 2013.

- [59] M. Sawahashi, *et al.*, "Coordinated multipoint transmission/reception techniques for LTE-Advanced," *IEEE Wireless Commun. Mag.*, vol. 17, no. 3, pp. 26-34, Apr. 2010.
- [60] R. Irmer, *et al.*, "Coordinated multipoint: concepts, performance, and field trial results," *IEEE Commun. Mag.*, vol. 49, no. 2, pp. 102–111, Feb. 2011.
- [61] 3GPP TR 36.819, "Coordinated multi-point operation for LTE physical layer aspects (Release 11)," Dec. 2011.
- [62] M. Hong, R. Sun, H. Baligh, and Z.-Q. Luo, "Joint base station clustering and beamformer design for partial coordinated transmission in heterogeneous networks," *IEEE J. Sel. Areas Commun.*, vol. 31, no. 2, pp. 226-240, Feb. 2013.
- [63] Y.-F. Liu, Y.-H. Dai, and Z.-Q. Luo, "Max-min fairness linear transceiver design for a multi-user MIMO interference channel," *IEEE Trans. Signal Process.*, vol. 61, no. 9, pp. 2413-2423, May 2013.
- [64] D. Gesbert, S. Hanly, H. Huang, S. S. Shitz, O. Simeone, and W. Yu, "Multi-cell MIMO cooperative networks: a new look at interference," *IEEE J. Sel. Areas Commun.*, vol. 28, no. 9, pp. 1380-1408, Dec. 2010.
- [65] M. R. McKay, I. B. Collings, and A. M. Tulino, "Achievable sum rate of MIMO MMSE receivers: A general analytic framework," *IEEE Trans. Inf. Theory*, vol. 56, no. 1, pp. 396-410, Jan. 2010.
- [66] R. Uehara and Y. Uno. "Efficient algorithms for the longest path problem," in *15th Annual International Symposium on Algorithms and Computation (ISAAC 2004)*, 2004, pp. 871-883.

簡歷

姓 名：黃 崇 榮

性 別：男

出生年月日：民國 57 年 5 月 13 日

籍 貫：臺灣省桃園縣

學 歷：臺灣工業技術學院電子工程技術系學士 (78/9 ~ 80/6)

交通大學電信研究所碩士 (81/9 ~ 83/6)

交通大學電信研究所博士班 (96/9 ~)

經 歷：合勤科技資深工程師 (83/7 ~ 88/11)

勁取科技資深工程師、經理、資深經理、協理 (88/11 ~ 98/3)

論文題目：高效率之球型解碼演算法及其應用

Publication List

Journal Paper

- [J1] C.-J. Huang, G.-H. Chung, W.-H. Chung and T.-S. Lee, "An efficient codebook search algorithm for LTE-A uplink coordinated multipoint systems," submitted to *IEEE Wireless Comm. Letters* for publication.
- [J2] C.-J. Huang, W.-H. Chung and T.-S. Lee, "A geometry based efficient decoder for underdetermined MIMO systems," submitted to *IEEE Trans. Vehicular Technolog* for publication.
- [J3] C.-J. Huang, G.-H. Chung, W.-H. Chung and T.-S. Lee, "Two-stage interference alignment aided transceiver design for LTE-A uplink coordinated multiple systems," submitted to *IEEE Trans. Vehicular Technology* for publication.
- [J4] 黃崇榮, 李大嵩, "前瞻長程演進系統之多載波聚合技術," 新電子 8 月 2013.
- [J5] C.-J. Huang, C.-W. Dai, T.-Y. Tsai, Wei-Ho Chung and T.-S. Lee, "A closed-form phase-comparison ML DOA estimator for automotive radar with one single snapshot," *IEICE Electronics Express*, Vol. 10 (2013), No. 7, 20130086.
- [J6] C.-J. Huang, C.-S. Sung, and T.-S. Lee, "A Near-ML complex K -Best sphere decoder with efficient search design for MIMO systems," *EURASIP Journal on Advances in Signal Processing*, vol. 2010, Article ID 892120, 18 pages, 2010. doi:10.1155/2010/892120.
- [J7] 黃崇榮 "無線音訊廣播標準, 相關技術及未來展望" 電子月刊. Vol. 121, pp. 160-166.

Conference Paper

- [C1] C.-S. Lee, M.-C. Lee, C.-J. Huang and T.-S. Lee, "Sectorization with beam pattern design through 3D beamforming techniques," APSIPA ASC 2013, 29 Oct. – 1 Nov., 2013, Kaohsiung, Taiwan.
- [C2] C.-J. Huang, G.-H. Chung, W.-H. Chung, and T.-S. Lee, "Efficient interference alignment aided transceiver design for LTE-A uplink coordinated multipoint systems," *IEEE PIMRC 2013*, 8-11 September, London, UK.

- [C3] C.-J. Huang, W.-C. Chang, and T.-S. Lee, "Codebook based interference alignment in uplink coordinated multipoint systems," in *Proceeding of the IEEE ISPACS 2012*, Nov., 2012. pp. 816-821.
- [C4] C.-J. Huang, C.-W. Dai, T.-Y. Tsai and T.-S. Lee, "FMCW MIMO transceiver for middle-range over-the-horizon radar," in *Proceedings of the IEEE ICSPCC 2011*, June 2012, pp. 20-25.
- [C5] C.-J. Huang, C.-Y. Wu, and T.-S. Lee, "Geometry based efficient decoding algorithms for underdetermined MIMO systems," in *Proceedings of the IEEE SPAWC 2011*, June 2011, pp. 371-375.
- [C6] C.-J. Huang, C.-S. Sung, and T.-S. Lee, "A near-ML complex K -Best sphere decoder with efficient search design for MIMO systems," in *Proceedings of the IEEE ISPACS 2010*, 2010, pp. 1-4.
- [C7] T.-Y. Dai, T.-S. Lee and C.-R. Hwang, "Novel beamspace neural network approach to mobile unit localization," in *Proceedings of the IEEE Asia-Pacific Conference on Circuits and Systems*, 1994, pp. 18-23.
- [C8] T.-Y. Dai, T.-S. Lee and C.-R. Hwang, "Localization of vehicles in a multipath environment via beamspace vorrelation level neural processing," in *Proceedings of the ISCOM94*, 1994, pp. 12-17.

Patents

- [P1] T.-Y. Tsai, C.-J. Huang, and T.-S. Lee, "Method and apparatus for analyzing the correctness of detected angle of target," under internal review.
- [P2] 蔡宗育, 黃崇榮, 李大嵩, "用於分析目標物角度估計之正確性之方法與裝置," 校內審查中。
- [P3] 黃崇榮, 戴家威, 蔡宗育, 李大嵩, "移動參數估計方法、角度估計方法及判斷方法," 中華人民共和國專利, 申請中, 2012.
- [P4] C.-J. Huang, C.-W. Dai, T.-Y. Tsai and T.-S. Lee, "Motion parameter estimating method, angle estimating method and determination method," U.S.A. patent pending, 2012.(43274-US-PA).
- [P5] 黃崇榮, 戴家威, 蔡宗育, 李大嵩, "移動參數估計方法、角度估計方法及判斷方法," 中國發明專利, 申請中(申請號: 101127474), 2012.
- [P6] 黃崇榮, 吳智湧, 李大嵩, "基於幾何欠定多輸入多輸出系統之解碼裝置," 中華

民國專利, 申請中, 2010.

[P7] C.-J. Huang, C.-Y. Wu, and T.-S. Lee, “Geometrical approach based decoding apparatus for underdetermined MIMO systems,” U.S.A. patent pending, 2011.

[P8] 黃崇榮, 宋志晟, 李大嵩, “用於多輸入多輸出系統之複數 K -Best 球體解碼裝置,” 中華民國專利, 申請中, 2009 年.

[P9] C.-J. Huang, C.-S. Sung, and T.-S. Lee, “A complex K -Best decoding apparatus for MIMO systems,” U.S.A. patent prosecution highway..

[P10] C.-J. Huang and T.-S. Kao, “Method of calculating equal error protection profile,” United States Patent, Patent Number: US7613269, Mar.3, 2009.

[P11] 黃崇榮, 高再生, “均等錯誤保護參數的計算方法,” 中華民國發明專利, 編號: I315144, 中華民國 96 年 11 月 16 日.

Provisonal Patents

[P1] C.-J. Huang, G.-H. Chung, W.-H. Chung and T.-S. Lee, “An efficient codebook search algorithm for LTE-A uplink coordinated multipoint systems,” provisional with MTK index.

[P2] C.-S. Lee, M.-C. Lee, C.-J Huang and T.-S. Lee, “Sectorization with beam pattern design through 3D beamforming techniques,” provisional with MTK index.

[P3] C.-J. Huang, G.-H. Chung, W.-H. Chung, and T.-S. Lee, “Efficient interference alignment aided transceiver design for LTE-A uplink coordinated multipoint systems,” provisional with MTK index.

[P4] C.-J. Huang, W.-C. Chang, and T.-S. Lee, “Apparatus and method of codebook extension for MIMO communications,” provisional with MTK index.

[P5] C.-J. Huang, S.-T. Liang, and T.-S. Lee, “Transmit diversity scheme for PUCCH in LTE/LTE-A systems,” provisional with MTK index, CTO-12-005PUS.